ASPECTS OF
A TIDAL POWER SCHEME
IN THE WYRE ESTUARY

REPORT SUBMITTED

AS PART REQUIREMENT FOR

MSc DEGREE IN CIVIL ENGINEERING

AT DELFT UNIVERSITY OF TECHNOLOGY

S. Delfgaauw

NOVEMBER 1991

TU Delft

Delft University of Technology

BINNIE & PARTNERS

PREFACE

This report is the result of the work carried out during a seven month training period at Binnie & Partners in the United Kingdom. It forms the completion of my Master's Degree study in Civil Engineering at Delft University, the Netherlands.

I would like to thank all staff of the Hydraulics Department of B & P for the great working atmosphere they created. Their comments during the long tea-breaks were most of the time both useful and interesting.

I am particularly grateful to Peter Clark (MA, MSc, DIC, MICE), head of the department and also a member of my board of examiners. Despite an enormous working pressure, he always managed to find some time to discuss technical topics not always involving my project.

Furthermore, I would like to thank Dr. Richard Young (Bsc, PhD, MICE), project manager of the Wyre Tidal Power project. His experience on Tidal Power has helped me a lot.

Last but not least I want to thank ir. Kees Bezuyen for bringing me in contact with B & P and for the time and effort he spent to help me with my project. His advice, mostly over the phone, has had a great influence on my report.

Steven Delfgaauw
Redhill, November 1991

CONTENTS Page

1.	**SUMMARY**		3
2.	**INTRODUCTION**		3
	2.1	Tidal Power Generally	3
	2.2	Previous Studies	7
	2.3	The Wyre	7
		2.3.1 Estuary Data	7
		2.3.2 Selection of the Wyre	7
		2.3.3 The Wyre Scheme	9
	2.4	Objectives of the Study	9
3.	**ENERGY MODELLING**		12
	3.1	Introduction	12
		3.1.1 Scope of Studies	12
		3.1.2 Sites Examined	12
		3.1.3 Models Used	12
	3.2	Model Description	13
		3.2.1 0-D Model	13
		3.2.2 1-D Model	14
	3.3	Turbine and Sluice Characteristics	19
		3.3.1 Sluices	19
		3.3.2 Turbines	21
	3.4	Computer Modelling	21
		3.4.1 Turbine Optimisation	22
		3.4.2 Sluice Optimisation	25
		3.4.3 Annual Energy Output	28
		3.4.4 Further Optimisation Studies	32
	3.5	Differences between 0-D and 1-D Results	34

4. CAISSON DESIGN 37

4.1 Introduction 37
4.2 Location 37
4.3 Topography Data 37
4.4 Design Criteria 39

4.4.1 Wind and Wave Criteria 39
4.4.2 Tide and Water Level Criteria 40
4.4.3 Soil Parameters 40

4.5 Global Dimensions 41

4.5.1 Turbine Section 41
4.5.2 Sluice Section 42

4.6 Turbine and Sluice Configuration 42

5. STEEL CAISSON DESIGN 50

5.1 Introduction 50

5.1.1 Objectives 50
5.1.2 Restrictions 50

5.2 Design Method 52

5.2.1 Global Stability 52
5.2.2 Program Description 52
5.2.3 Schematisation 56
5.2.4 Frame Loading Cases 58
5.2.5 Panel Loading Cases 58

5.3 Results 59

6. GLOBAL STABILITY 62

6.1 Introduction 62
6.2 Loading Cases 62
6.3 Horizontal Loadings on Caisson 65
6.4 Vertical Loadings on Caisson 67
6.5 Results 67
6.6 3-Dimensional Stability 69

7. TRANSPORT AND PLACING 71

7.1 Introduction 71
7.2 Construction Sequence 71
7.3 Transport 71
7.4 Placing of the Caissons 77

7.4.1 General 77
7.4.2 Model Description 79
7.4.3 Friction in Gap and Sluices 82
7.4.4 One Caisson in Place 84
7.4.5 Placing of Second Caisson 84
7.4.6 Both Caisson in Place 93

7.5 Bottom Protection 95

APPENDICES

1. Wave Heigth Calculations

2. Frame Calculations

3. Panel Calculations

4. Wave Force Calculations

5. Stability and Draft Calculations

6. Closure Model Description

LIST OF FIGURES

		Page
2.1a	Ebb Generating Scheme	4
2.1b	Double Basin Scheme	4
2.2	Water Levels at Different Tidal Power Schemes	5
2.3	Location of the Wyre Estuary	8
2.4	Plan of the Wyre Estuary showing Barrage Locations and 1-D Model Sections	11
3.1	Tidal Curves Used in Power Output Studies	15
3.2	Surface Area vs. Elevation	16
3.3	Graph of Backwater Effects at the Seaward Side of The Barrage	16
3.4	The Fishpass	17
3.5	Turbine Characteristics	20
3.6	Energy Output for Different Turbine Arrangements; Central Site	23
3.7	Energy Output for Different Turbine Arrangements; Northern Site	24
3.8	Levels in the Estuary during two Tidal Cycles	26
3.9	Graph of Energy Output v Sluicing Capacity; A.B.P. Scheme	27
3.10	Graph of Energy Output per Tidal Cycle vs. Tidal Range	29
3.11	Graph of Energy Output against Design Head; Spring Tide	30
3.12	Occurances of Tidal Ranges and Energy Output per Tidal Range per Year; A.B.P. Scheme	30
3.13	Graph of Annual Energy Output vs. Installed Capacity	31
3.14	Graph of Water Surface During a Tidal Cycle; A.B.P. Scheme	36
4.1	Geotechnical Sections at Barrage Locations	38
4.2	Ideal Turbine Dimensions	42
4.3	Layout Turbine Section of Wyre Caisson	43
4.4	Turbine - Sluice Configurations	45
4.5	General Arrangements of Turbine - Sluice Caisson	48
4.6	General Arrangements of Barrage	49
5.1	General Arrangements of Steel Caisson	50
5.2	Comparison of Steel and Concrete Plate	53
5.3	Types of Panels Used by Bagpus	54
5.4	Loads on Panels	54
5.5	Caisson Representation in Strap	57
5.6	X1-X2 Frames with Typical Loadings	57
5.7	X2-X3 Frames	57
6.1	Load Cases for Stability of Turbine - Sluice Caisson	64
6.2	Loads and Bearing Pressures during Extreme Flood	68
6.3	3-D Stability; Friction Distribution and Resulting Forces	68

7.1	Barrage Installation Sequence	72
7.2	Plan of Caisson during Transport	74
7.3	Pressure and Centre Points	74
7.4	Head Losses in Gap	79
7.5	Inlet Loss Coefficients	79
7.6	Surface Area; Modelled and Real	80
7.7	Cross Area of Gap	80
7.8	Velocities and Levels with 1 Caisson in Place; Spring Tide	85
7.9	Velocities and Levels with 1 Caisson in Place; Neap Tide	85
7.10	Maximum Velocity vs. Tidal Range	86
7.11	Plan of Caisson showing Head Ribs	87
7.12	Placing Actions	87
7.13a	Closure at Low Water during a Neap Tide; Concrete Caisson	90
7.13b	Closure at High Water during a Neap Tide; Concrete Caisson	90
7.14a	Closure at Low Water during a Neap Tide; Steel Caisson	91
7.14b	Closure at Low Water during a Spring Tide; Steel Caisson	91
7.15	Levels and Discharge after Closure	94
7.16	Scour Protection around Caisson	96

A1.1	Dimensionless Depth at Breaking versus Breaker Steepness
A1.2	Friction Loss over a Bottom of Constant Depth
A1.3	Forecast Curves for Shallow-water Waves
A2.1	Frame Numbering
A2.2	Moment and Force Definition
A3.1	Panels in Caisson
A3.2	Sluice pier Schematisation
A3.3	Schematisation for Walls with Ballast Loads
A3.4	Lanels in Conning Tower
A4.1	Definition of Terms; Nonbreaking Wave Forces
A4.2	Nonbreaking Wave Forces
A4.3	Nonbreaking Wave Moments
A5.1	Definition of Axis for Stability Calculations

1. SUMMARY

In 1987 a study of small estuaries around the coast of the United Kingdom was undertaken by Binnie & Partners for the Department of Energy. The Wyre was identified as one of the most promising sites for the construction of a small tidal power scheme.

The Wyre Estuary is located in Lancashire on the north west coast of England. The estuary fulfils the main requirements for a tidal energy scheme in that it has a high tidal range and a mouth which is relatively narrow in relation to its surface area.

The main features of the estuary are as follows :

- Mean spring tidal range : 8.2 m
- Mean neap tidal range : 4.4 m
- Surface area at +4.0 mOD : 7.5 km^2
- Highest astronomical tide : 5.4 mOD
- 50 year surge tide level : 6.3 mOD
- Mean fresh water flow in river : 6.5 m^3/s
- Length of tidal river : 21 km

During 1990 a preliminary feasibility study of a tidal energy scheme in the Wyre estuary has been carried out by Binnie & Partners and T.H. Technology, a subsidery of the commercial organisation, Trafalgar House.

The scheme was optimised by the utilisation of hydro-dynamic models with the objective to maximise the annual energy output. Two potential barrage sites were examined :

- The Pandoro or North site, located 300 m downstream of Fleetwood Docks

- The A.B.P. or Centre site, located 100 m upstream of Fleetwood Docks

The outcome of these studies were that the North scheme would generate more energy. However, the Centre site was more favourable considering the existing infrastructure. The preferred arrangement for a tidal barrage on this location comprises :

- 4 No 6.0 m diameter turbines, peak power 14.96 MW each
- 12 channel sluices with radial gates, 9 m wide
- 2 fish passes

This scheme would generate an annual energy output of 117.2 GWh.

The turbines, sluices and fish passes would be incorporated in two caissons. These would be constructed off-site, and towed to the location where they would be sunk onto the prepared sill to form the closure of the estuary.

A steel caisson with concrete floor was designed at T.H. Technology. The caisson was designed as a gravity structure : its stability depends on its own weight. Therefore ballast chambers were included in the caisson. The stability was checked for several loading cases during both the installation and operating phase.

The behaviour of this caisson during transport and placing was compared with that of a concrete caisson. A spreadsheet model was developed in order to predict the effects of the closure on the velocities in the estuary. It was concluded that although the closure of the estuary is possible with both both types of caissons, the closure with a steel caisson would have considerable advantages.

2. INTRODUCTION

2.1 Tidal Power Generally

The principal of tidal power is to generate energy by using a tidal wave moving into an estuary. The possible energy output of a scheme depends mainly on two aspects:

- the amplitude of the tidal wave
- the surface area of the estuary

This will be explained by describing the operating process of the most efficient system, the **ebb generating scheme**. This scheme consists of a barrage containing the following structures (see Figure 2.1a and 2.2a):

- sluices
- turbine caissons

With the incoming tide the water enters the estuary through the opened gates of the sluices. The sluices close after the sea level has reached the highest level of the tidal cycle. The waterlevel in the estuary will be almost the same as the sealevel, depending on the sluice capacity : number, type and size of sluices. After this moment, the sealevel will go down, which results in a head difference between estuary and sea. Once this head has reached a certain range, the generating will start. Turbining will continue until the head difference has reached a minimum. In a 12.4 h tidal cycle, usually 5 hours can be utilised for for generation.

The power output during turbining and total energy output are derived from the following formulas:

$$- P = n * p * g * Q * H$$

$$- E = n * p * g * \int Q * H * dt$$

In which :

n = efficiency factor [-]
p = density of water [kg/m^3]
g = acceleration of gravity [m/s^2]
Q = discharge through turbines [m^3/s]
H = head difference between estuary and sea [m]

The tidal range determines the head difference, while the tidal range and the surface area of the estuary determine the amount of water stored in the basin, i.e. the potential energy. The turbine capacity determines the discharge and the change in head during turbining.

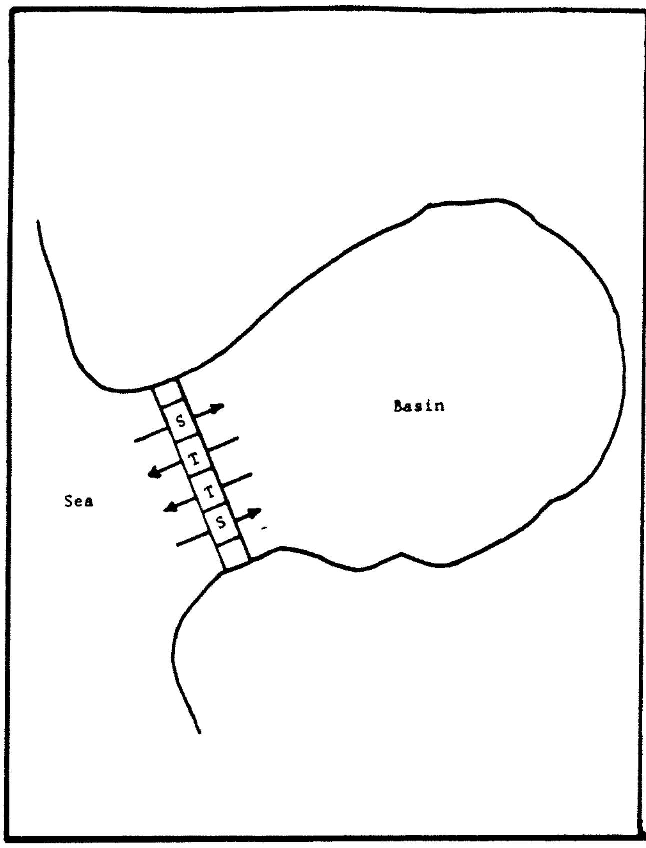

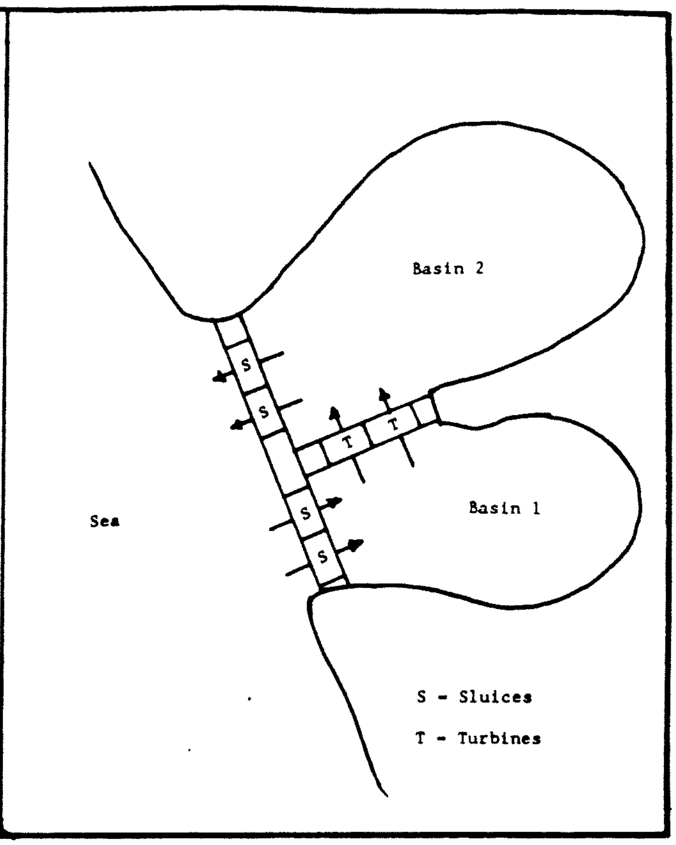

Fig 2.1a Ebb Generating Scheme

Fig 2.1b Double Basin Scheme

Two effects can increase the tidal range in an estuary:

- Resonance : if the ratio of tidal wave length and estuary length is equal to 2n (n = 1, 2, 3, ...) resonance can increase the tidal range by a factor of 2-3.

- Funneling effects : when the estuary is narrowing in the upstream direction the levels are pushed up.

The power output can be increased by the use of the turbines as pumps. Immediately after high water the seawater is pumped into the basin against a small head difference, so the required energy will be small. This extra volume of water is turbined against a large head later in the cycle, so the investment in energy is gained back. Recent studies have proven an increase of energy output by pumping of 15%. The extra cost of the turbines is relatively small.

The principle of the **flood generating system** (Figure 2.2b) is the same, except that generating will occur from sea to estuary, during flood. The basin levels will be constantly lower than before and the tidal range in the estuary will be smaller as well.

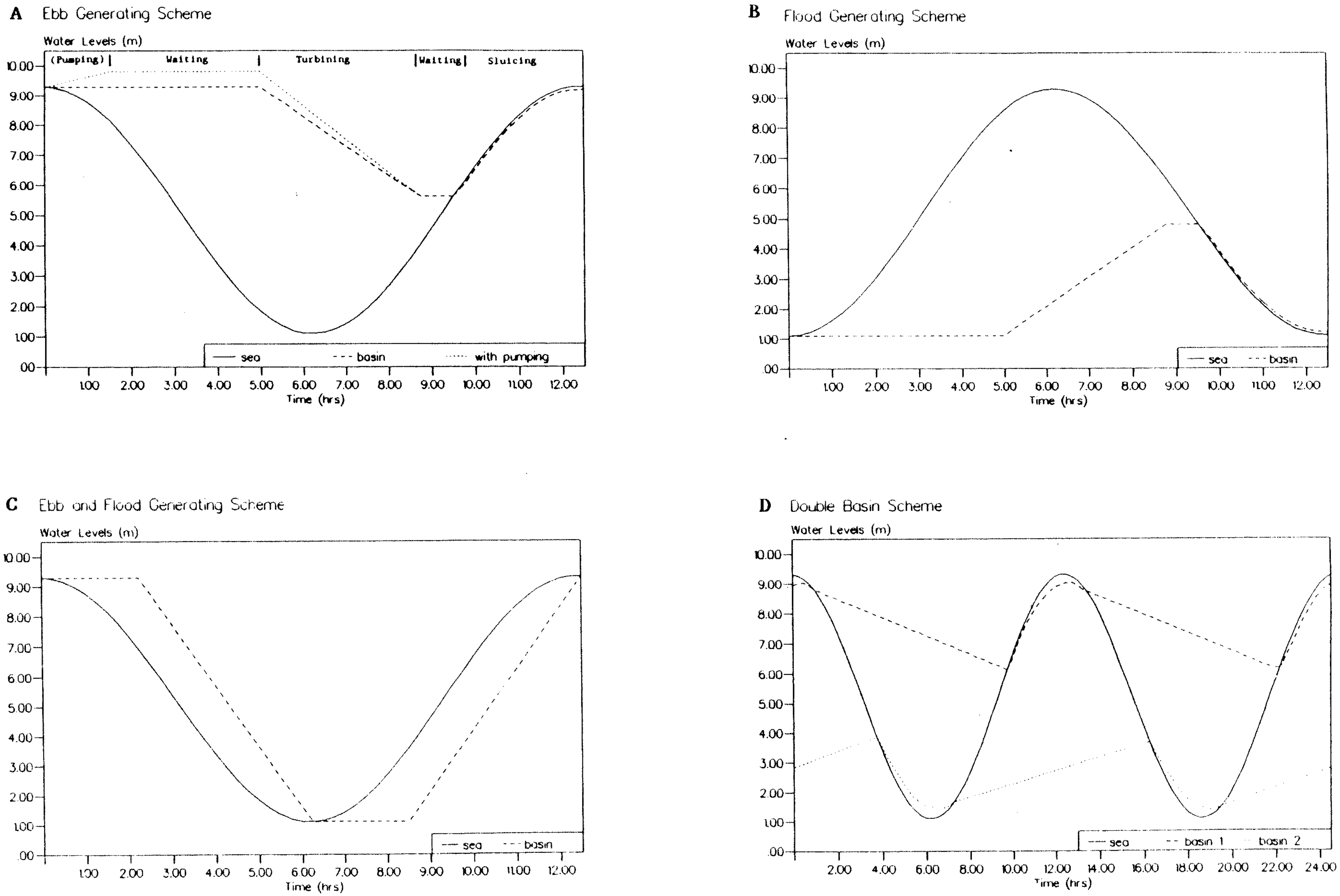

Fig 2.2 Water Levels at Different Tidal Power Schemes

The systems described above both have the disadvantage that the generating period is less than 40% of the tidal period. By the development of an **ebb and flood generating system** (see Figure 2.2c) the energy production time can be increased to 70%. However, the head differences will be considerably smaller and studies have shown that the energy output will be lower. Because of the high cost of the turbine system it is not likely to be an economical alternative.

A system that can generate energy continuously is the **double basin scheme**, shown in Figure 2.1b and 2.2d. The water will flow permanently from basin 1 to basin 2. When the sealevel is higher than basin 1, sluices a will be opened to allow the water to flow into the basin. When the sealevel is lower than basin 2, sluices b will be opened in order to empty this basin. The head difference between the two basins is not constant, neither is the energy production which can vary with a factor of 2 during a tidal cycle and with a factor of 5 during a lunar month. The total energy production will be lower than the production of an ebb generating scheme. Another disadvantage is that the barrage length will be much higher and that the number of sluices required is twice as high as at the other schemes.

Tidal power has been identified as one of the more promising sources of clean, renewable energy. However, the building and operating of a tidal power scheme has a severe influence on several environmental aspects near the location. Some of them will be described below.

- The operation of an ebb-generating scheme results in a change in water levels. Especially the estuary levels will be affected : the lower levels are considerably higher than in the situation without the barrage. The decrease of the intertidal zone in the estuary will affect the population of wildlife, particularly birds, who normally live there and find their food in this zone.

- The barrage reduces the fish migration in the estuary. This problem can be solved by including fish passes in the barrage.

- The sediment movement in the estuary changes dramatically. This is due to the change of velocity currents throughout the estuary.

- The higher water levels in the estuary are beneficial to ships. However, the necessity of a lock in the barrage will reduce this benefit.

- The higher basin levels benefit the recreation in the estuary.

2.2 Previous Studies

Over the past fourteen years the feasibility of tidal power generation has been extensively studied. Binnie & Partners were involved in the hydraulic modelling of several possible tidal power schemes on the west coast of England and Wales. These include schemes in the rivers Severn, Loughor and Conwy.

2.3 The Wyre

2.3.1 Estuary Data

The estuary of the river Wyre is located at the west coast of England (see Figure 2.3) in the County of Lancashire mid way between the seaside town of Blackpool and Morecambe Bay. The tidal limit of the river is generally at Cartford Bridge, some 18 km from the mouth of Fleetwood, although the effect of particularly high tides is felt some 8 km further upstream at St Michael's on Wyre (see Figure 2.4). The river is about 50m wide at Cartford Bridge and broadens fairly uniformly as far as north of Thornton where it is about 700m wide. It remains at about this width for some 4.5 km to Fleetwood where it narrows to about 500m immediately before reaching the sea.

The low water channel is relatively narrow, being rarely more than 100m wide except for the last 2 km before the mouth. The intertidal zone consist largely of mudflats and saltings with some sandy material being found towards the mouth of the river. Seaward of the river mouth the coast is fringed by sandbanks which are exposed for a distance of about 3 km from the shore at low water. Within this area the low water channel takes a fairly direct route just west of north through the sandbanks to deep water.

A major feature of the estuary is the port at Fleetwood, comprising two docks and a roll-on-roll-off ferry terminal. The once large deep-sea fishing fleet has shrunk considerably so that the docks now contain many more pleasure than commercial craft. In order to provide a route to the sea the low water channel is dredged and mainained at a level of -4.5 mOD, over a width of 150m.

2.3.2 Selection of the Wyre

The Wyre is one of the most promising estuaries to be identified, because :

- the tidal range is large
- the estuary has a relatively narrow mouth in proportion to its area
- the construction of a barrage would result in the rise of low water levels in the estuary, which would benefit tourist and leisure industries

Fig 2.3 Location of the Wyre Estuary

The estuary has been extensively studied by organisations with interest in the region. Therefore a substantial amount of information, such as estuary topography and bird population, has already been collected by those organisations.

2.3.3 The Wyre Scheme

The barrage would comprise the construction of a barrage across the mouth of the estuary at either of the two sites identified on Figure 2.4.

The barrage would include :

- Turbines
- Sluices and fishpasses
- Embankment
- A navigation lock
- Possibly a road crossing
- Control buildings, visitor centre, etc.

2.4 Objectives of the Study

The work for this thesis has been carried out at Binnie and Partners, who are acting as a consultant on hydraulic modelling and power generation to a commercial organisation, Trafalgar House. The latter are investigating the potential of the site with a view to investment in tidal power. Much of the engineering studies of the scheme have been carried out by Trafalgar House Technology, a subsidery of the main company. Most of the structural aspects of this study was undertaken under the direction of T.H.T.. All other aspects have been carried out in the B & P offices.

The objectives of this study are to undertake an investigation into the engineering and construction aspects of a tidal power scheme in the mouth of the river Wyre. The study will contain the following aspects:

- identification of the optimum barrage location

- optimisation of the arrangements in terms of sluices and turbines

- the global design of the caisson and more specific of a steel caisson

- the closure of the estuary

- transport of the caisson

The first aspect of this thesis is about the hydro-dynamic studies carried out in order to identify the potential energy output of the scheme and the required turbine and sluice capacity. The studies have been carried out for two potential sites.

Subsequently, the global design of the sluice and turbine caissons is highlighted: the seizing of turbine tubes, sluices, ballast chambers. The design in concrete was carried out by T.H. Technology; this thesis concentrates on the design of a steel caisson.

Using the dimensions and weights of the caissons calculated before, an investigation has been done into the problems and possibilities concerning the placing of the caissons in the estuary mouth and the transport of the caissons from the construction site to the Wyre Estuary.

Other aspects of the barrage, such as the embankment, navigation lock and road crossing will not be discussed in this thesis.

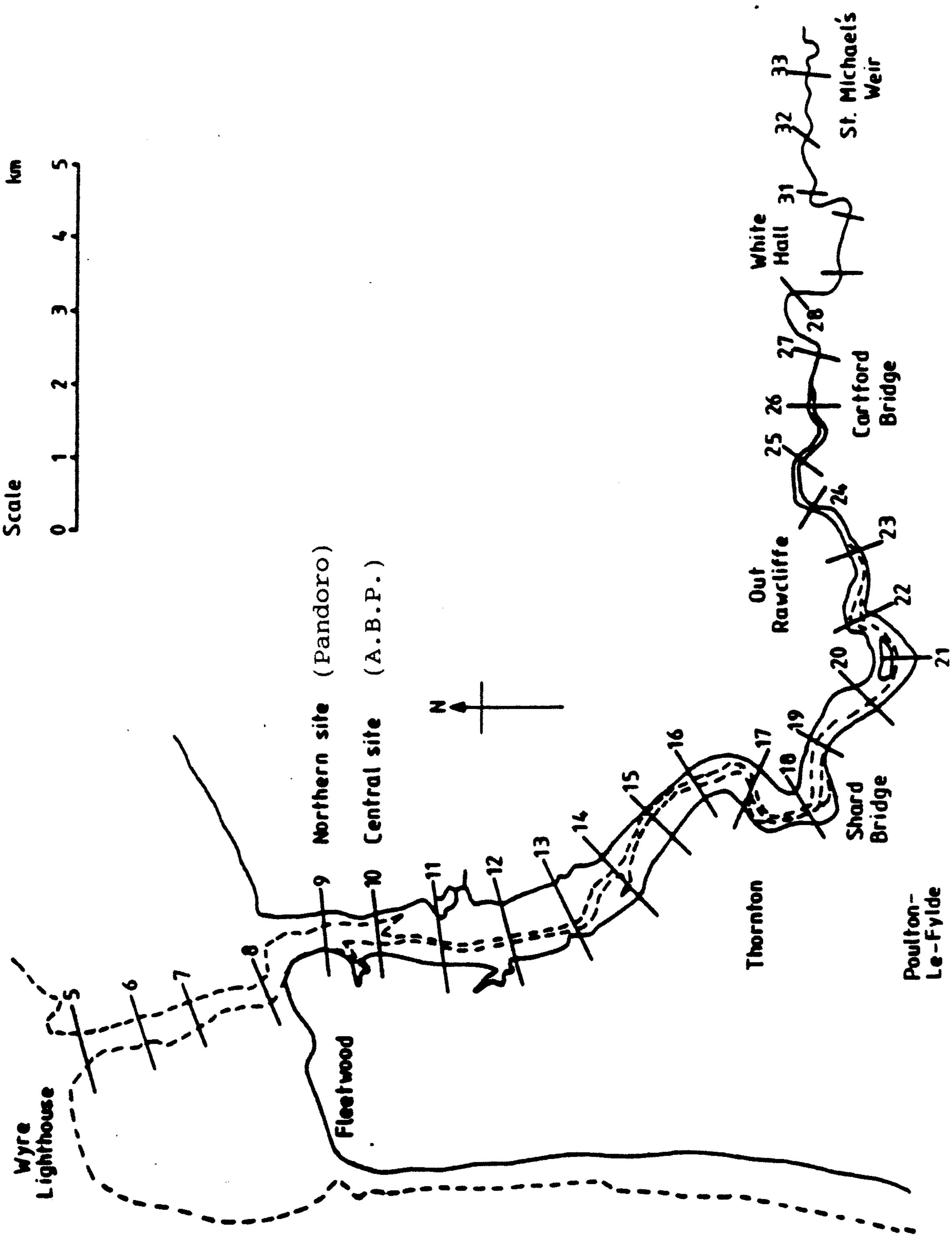

PLAN OF THE WYRE ESTUARY SHOWING BARRAGE LOCATIONS AND 1-D MODEL SECTIONS

Fig 2.4

3. ENERGY MODELLING

3.1 Introduction

3.1.1 Scope of Studies

The main purpose of energy modelling is to predict the energy output of the Wyre scheme. In this chapter it is described how the scheme was optimised by the utilisation of hydro-dynamic models.

Hydraulic model studies were undertaken for two purposes:

- To determine the amount of energy the scheme can produce as a function of the combination of sluices and turbines included in the barrage.

- To determine the effect the scheme will have on water levels and flows in the estuary, and from this the sediment transport and water quality.

This chapter describes the way the energy output was determined and the optimisation of the scheme. Water quality and the effects on the estuary will not be discussed in this thesis.

The schemes were optimised by maximising the annual energy output.

Once the optimum turbine-sluice configuration was selected, several runs have been done in order to examine the effect of varying the design head of the turbines.

Futhermore, the effect of pumping has been examined.

3.1.2 Sites Examined

In this study two principal sites for the barrage have been examined. One location was near a proposed marina village development by A.B.P., called the A.B.P. or Centre site. It is located 100 m upstream of Fleetwood docks. The other site, near the Pandoro ro-ro facility is called Pandoro or North site. It is located 300 m downstream of Fleetwood docks (see Figure 2.3).

3.1.3 Models Used

For this study two hydraulic models have been used; a Flat Estuary Model (0-D model) and a one-dimensional model (1-D model). This relatively simple flat estuary model needs less computional power than the one dimensional model and is therefore used to obtain an optimum configuration of number and size of sluices, which required a great number of runs.

After these initial runs the more complex one-dimensional model was used to check the optimising results and to obtain a more detailed estimation of a smaller number of configurations.

3.2 Model Description

3.2.1 0-D Model

In the Flat Estuary Model, or 0-D model, the barrage is presented by the open sea at one side and the enclosed basin at the other side. Water levels at sea side follow a tidal cycle. The flow through the barrage is determined by hydraulic characteristics of the turbines and sluices, by the barrage operating rules and the difference in water level across it.

Only two water levels are used : one immediately upstream of the barrage and one immediately downstream of the barrage.

In this model backwater effects downstream of the barrage are taken into account. These effects are due to friction; the contribution of inertia is negligible. With a known topography at seaside the backwater elevation is calculated for a range of discharges and water levels. These data are stored in a look-up table, which is used by the Flat Estuary Model.

All hydro-dynamic effects in the basin are ignored. The water levels throughout the whole estuary are assumed to react instantaneously to any flow, so that the water surface is flat at all times. Because of these assumptions the Flat Estuary Model tends to overestimate the power output (see section 3.6).

Data required are:

1) sea-levels as a function of time (Fig 3.1)
2) turbine characteristics
3) sluice characteristics
4) relation between elevation and surface area in basin (Fig 3.2)
5) river discharge (median discharge: 6.5 m^3/s)
6) look-up table

SUB 1) The sea-levels at neap and spring tide are derived from the Admiralty Time Tables for Fleetwood in 1983. For the mean tide a sinusoidal relation was used with an average range and mean level.

SUB 2) The turbine characteristics are obtained by using a spreadsheet based on Escher- Wyss characteristic curves.

SUB 3) The sluice characteristics are determined by discharge coefficients for submerged sluices.

SUB 4) Throughout the whole estuary width - elevation relationships were measured. A topography programm calculated the surface area as a function of elevation at each section. With these data the surface area - elevation relationship was determined.

SUB 5) For the energy study the median river discharge was used : 6.5 m^3/s.

SUB 6) The lookup-table was created by running a backwater calculating programm. A graph of the backwater elevation for the A.B.P. site is shown in Figure 3.3. The backwater elevation is plotted as a function of the total discharge through the turbines, for four low sea levels. In reality the sea levels will be in this range during the stage of generation. Example : if the sea level is -2.0 mOD and the total discarge through the turbines is 1250 m^3 then the backwater elevetion will be 0.4 m. So the water level immediately downstream of the barrage is : -2.0 + 0.4 = -1.6 mOD.

The Flat Estuary Model has two versions. "Opti" optimises the combination of the head difference at which the pumping stops and the head difference at which the generating starts. "Tidal" provides water-levels for a particular combination.

3.2.2 1-D Model

The one-dimensional model used in this study was used for earlier studies of tidal power schemes in Severn, Loughor and Conwy estuaries. The estuary is divided into several boxes and uses hydrodynamic equations of motion to determine the discharge, velocity and water level variations along the estuary as the tide at the mouth varies. Only longitudinal variations are considered to be significant. It is assumed that lateral and vertical variations are small in the relatively long and narrow Wyre Estuary. The results will be adequate for this preliminary study.

The Wyre Estuary is represented by 33 cross-sections from the open sea beyond the Wyre Lighthouse to the tidal limit at the weir at St Michaels-on-Wyre, as shown in Figure 2.4. The topography data are obtained from I.C.I., a chemical company that carried out environmental studies in the estuary several years ago.

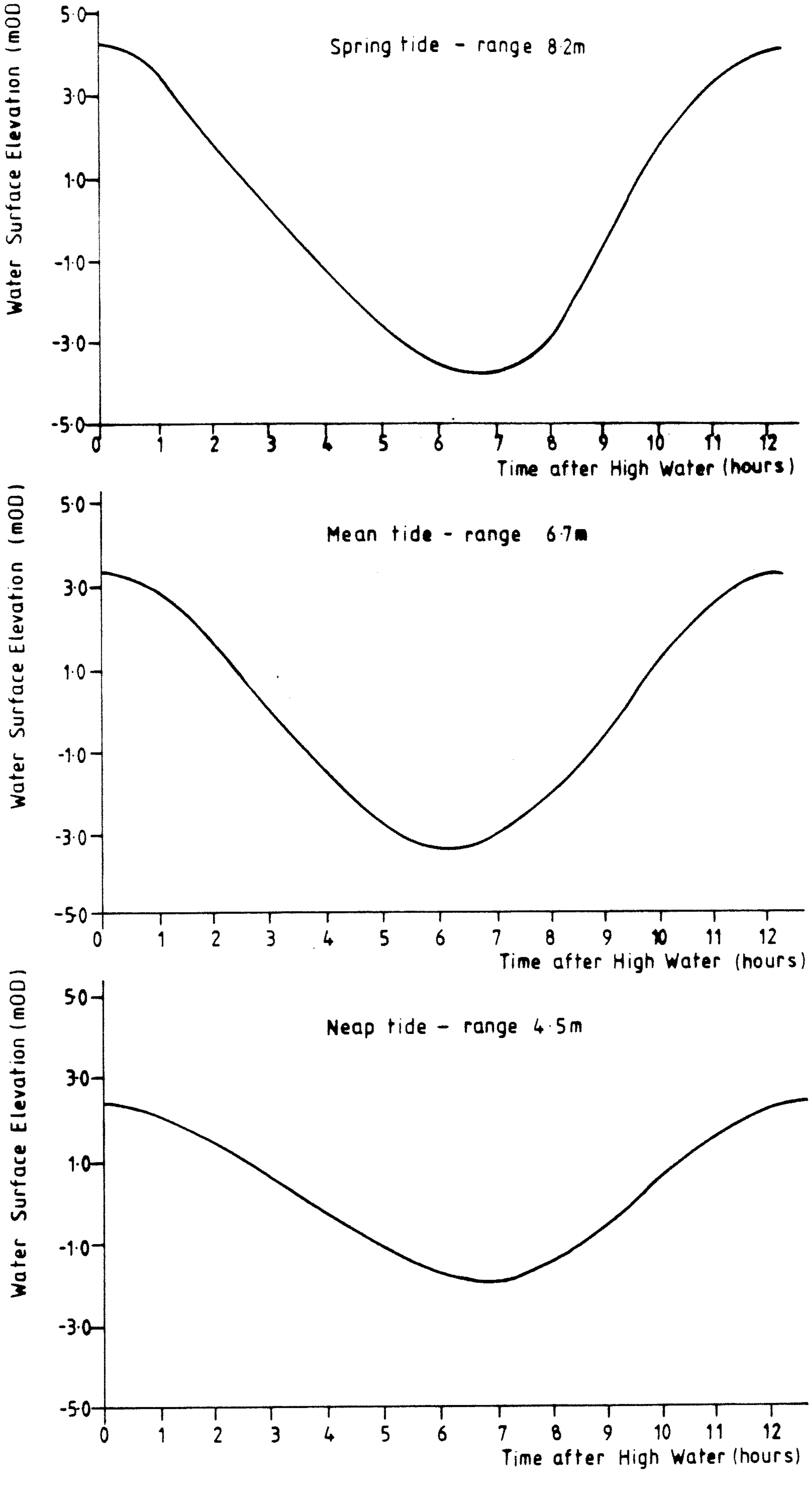

TIDAL CURVES USED IN POWER OUTPUT STUDIES Fig 3.1

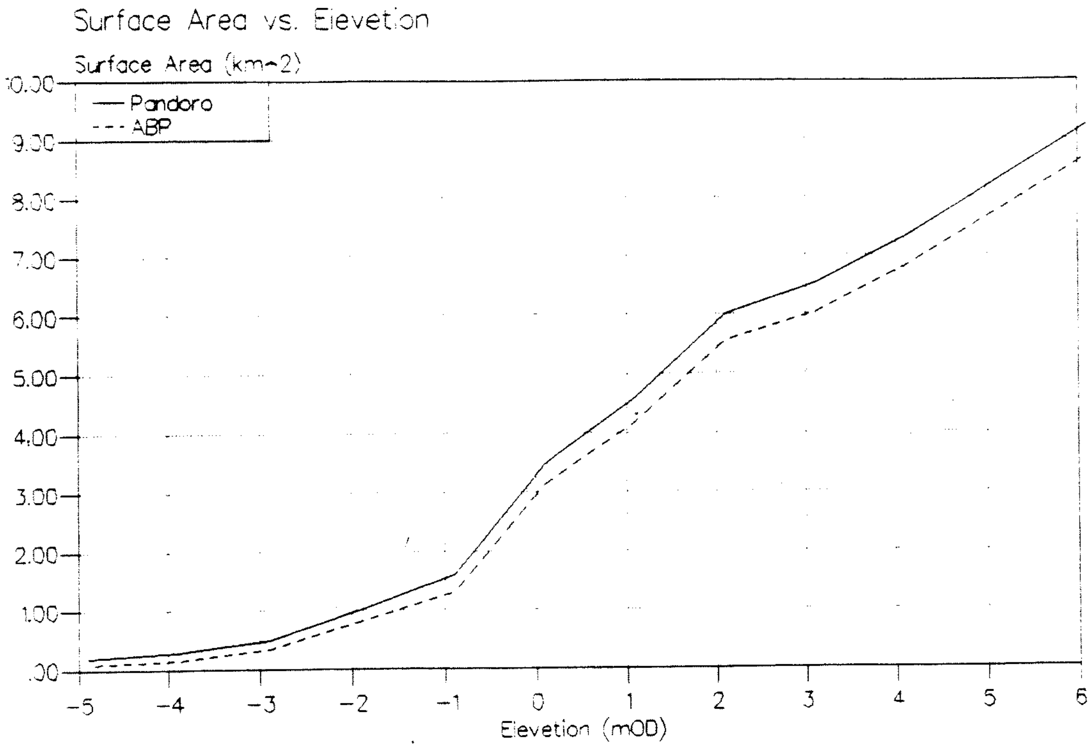
Surface Area vs. Elevetion
Surface Area (km^2)
Pandoro
ABP
10.00
9.00
8.00
7.00
6.00
5.00
4.00
3.00
2.00
1.00
.00
-5
-4
-3
-2
-1
0
1
2
3
4
5
6
Elevetion (mOD)

Fig 3.2

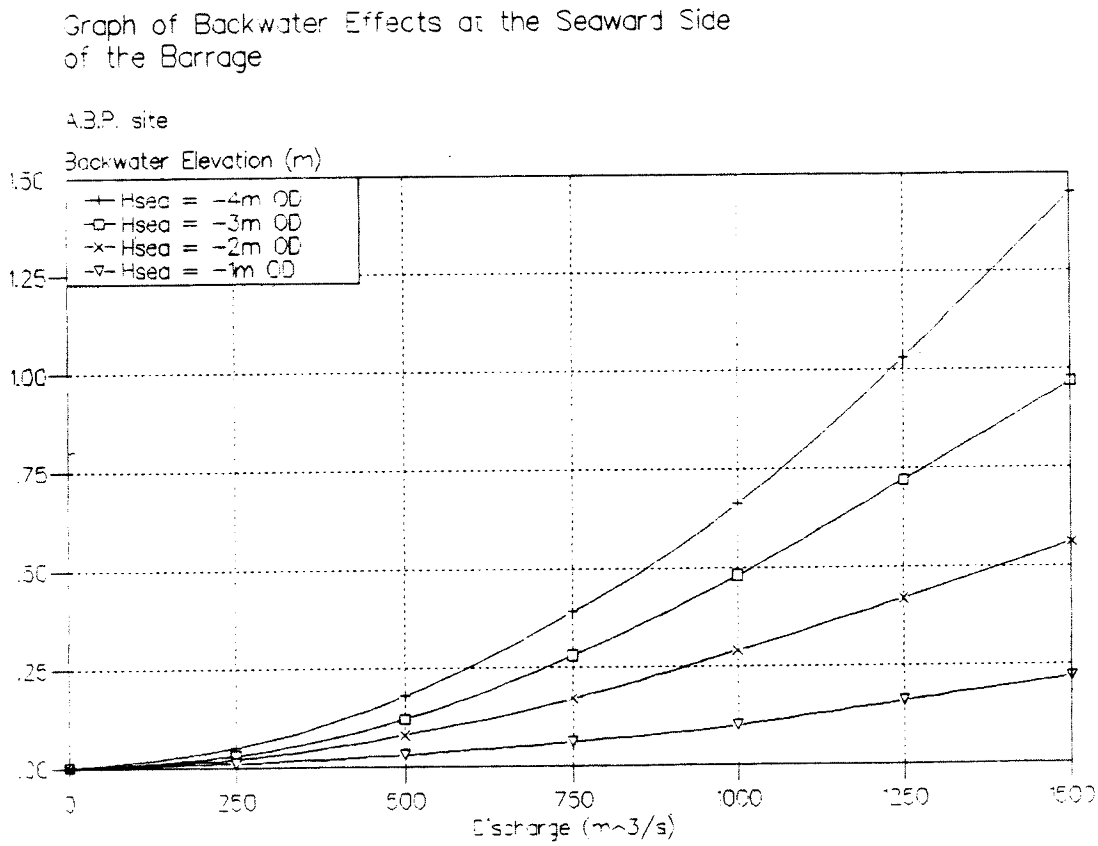
Graph of Backwater Effects at the Seaward Side of the Barrage
A.B.P. site
Backwater Elevation (m)
Hsea = -4m OD
Hsea = -3m OD
Hsea = -2m OD
Hsea = -1m OD
1.50
1.25
1.00
.75
.50
.25
.00
0
250
500
750
1000
1250
1500
Discharge (m^3/s)

Fig 3.3

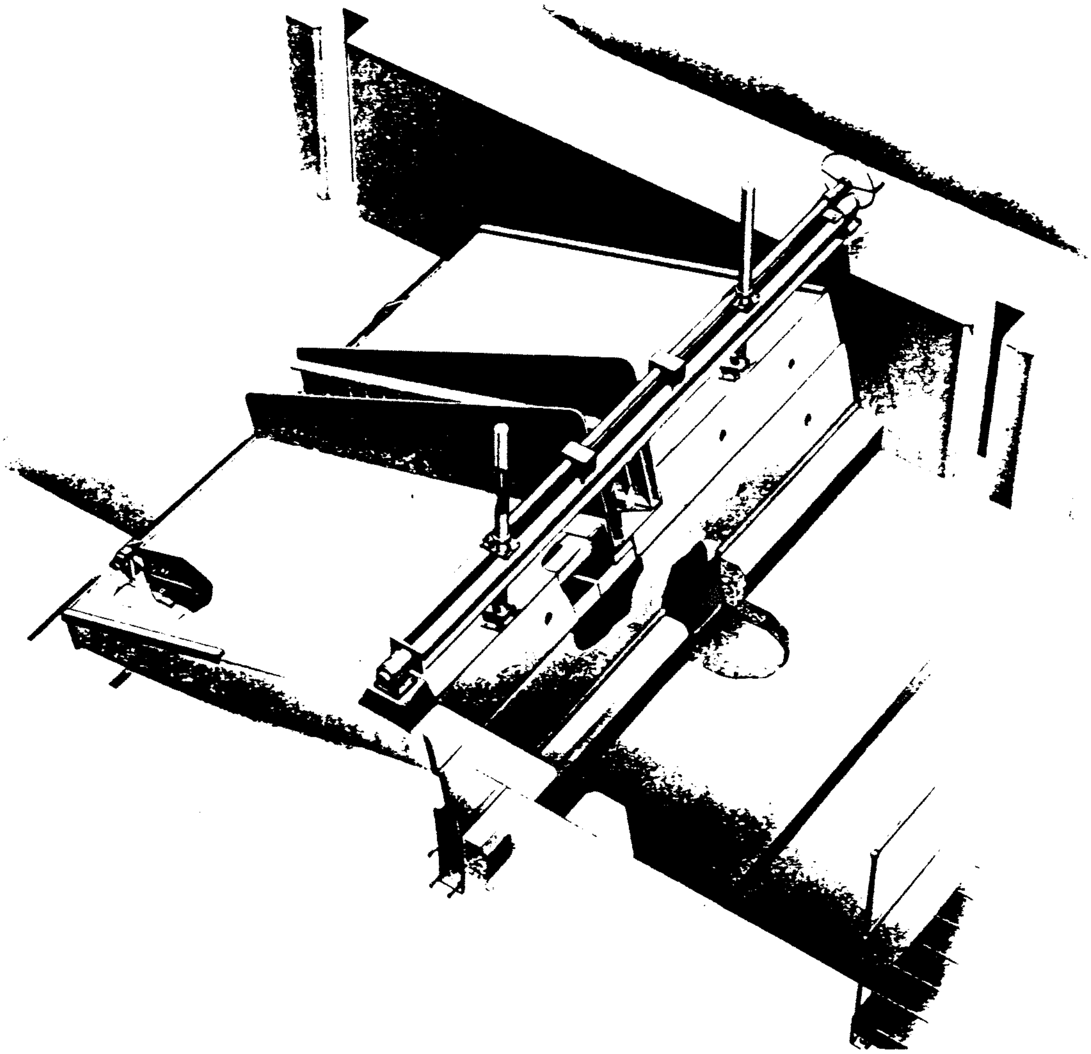

THE FISHWAY GATE -

The Fishway Gate is a unique design of tilting gate which contains an integral fish pass. It permits upstream water levels to be controlled while providing an easy ascent for migratory fish, all within a single mechanism.

The main advantages are:

1. Considerably lower capital cost than a conventional gate and separate pass.
2. Requires simple, economic foundations.
3. Can be fully automated or manually operated.
4. Overshot blockage-free profile gives slow increase in discharge.
5. Provides pass at natural congregation point.
6. Can pass all species of migratory fish upstream.
7. Can be ascended at very low flows.
8. Utilizes hydrostatic pressure to assist in raising, therefore power requirements are low.
9. Can be descended by canoe.

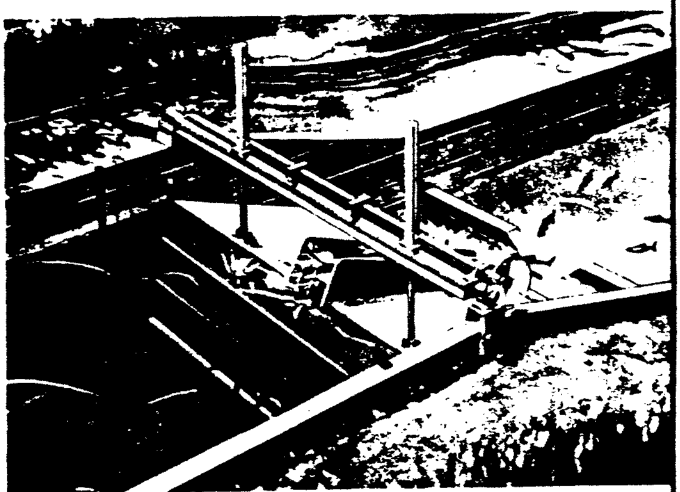

Fig 3.4 The Fishpass

3.3 Turbine and Sluice Characteristics

3.3.1 Sluices

When the barrage is operating normally, water would flow from the sea to the basin through both the sluices and the fish passes, the discharge being controlled by their hydraulic characteristics. In this barrage the sluices have radial gates. Radial gate discharge equations were used in the 1-D model. However, the flat estuary model is not capable of using the characteristics of radial gates. Therefore, submerged sluices were used in this model. For the actual sluice optimisation the 1-D model was used.

The submerged sluices converge from the inlet over a short length to the point where the gates are sited, this being the section of minimum cross-sectional area. Thereafter the passages diverge to the outlet. The convergent and divergent angles are selected to avoid flow separation so limiting head losses. The head-loss coefficients are listed in Table 3.1. The discharge equation through the sluices is :

$$-H = \frac{C * Q^2}{2g * A^2}$$

in which :

- C = Head Loss Coefficient (-)
- Q = Discharge (m^3/s)
- g = Acceleration of Gravity (m/s^2)
- A = Area of the Throat (m^2)

Flow direction	Head Loss Coefficient
Seaward	2.4
Landward	1.6

Table 3.1

The fish passes would also be capable of discharging in both directions. They are assumed to operate as broad-crested weirs when the gate is in its fully open condition, with the same characteristics in each direction (see Figure 3.4, source : Boving Newton Chambers Ltd brochure).

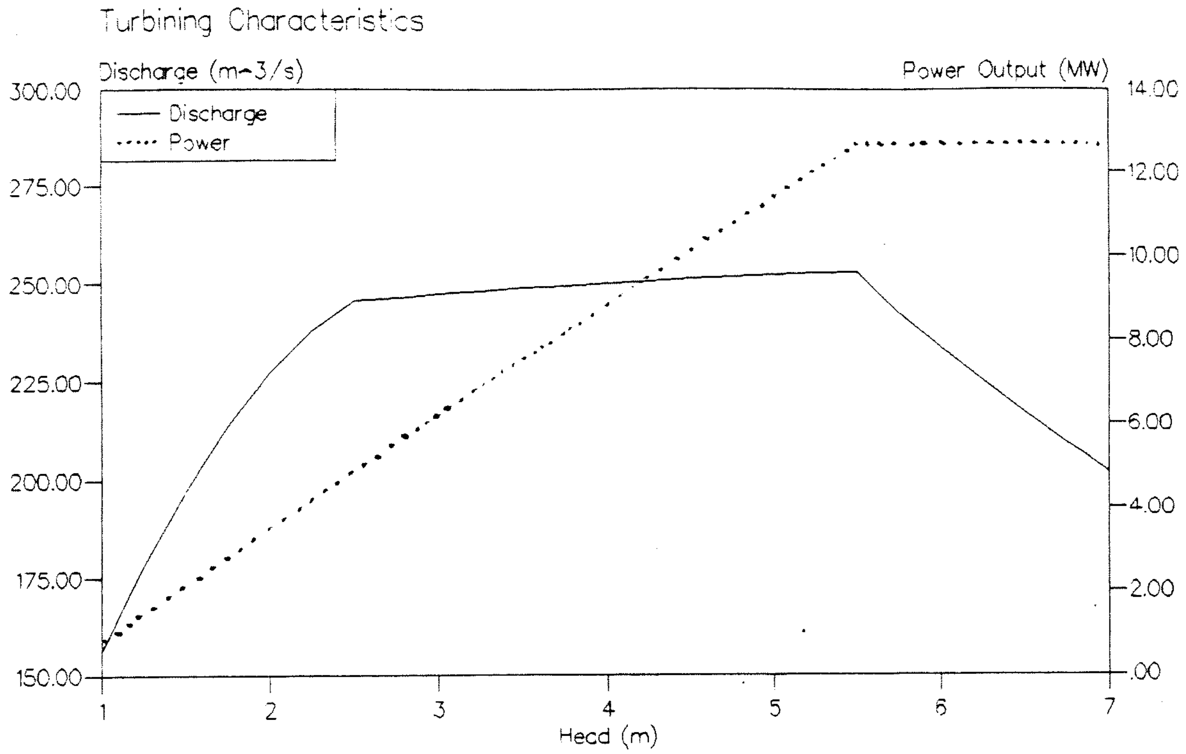

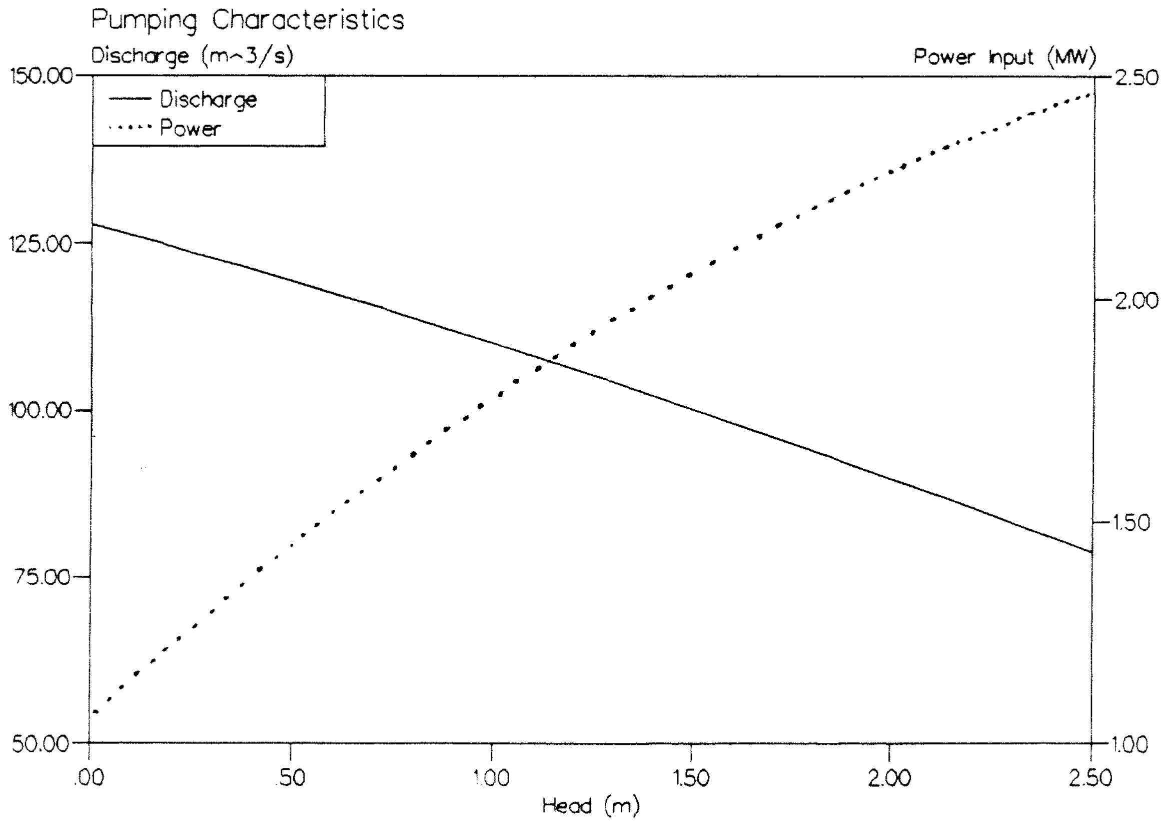

Turbine Diameter : 6.0 m
Rotation Speed : 58.82 rpm
Axis Level : -3.4 mOD

Fig 3.5 Turbine Characteristics

3.3.2 Turbines

Turbine characteristics have been derived from data based on Escher-Wyss curves. This data is in the form of families of curves relating operating efficiencies to specific discharges and heads. The curves relate to a specific inlet and draft tube geometry.

For practical reasons the axis level of the turbine was located at 0.75 * turbine diameter below Mean Low Water at Spring tide (MLWS). From the Escher-Wyss curves polynomial relationships between head across the turbine and discharge and power output were derived for each size of turbine, and for several design heads. The speed of rotation was maximized under the limitation that no cavitation would occur.

The generator capacity, with the turbine size and operating speed, defines the maximum output of the turbine and the design operating head; the least head at which the tubine will produce the maximum output. At heads greater than this the turbine is throttled back to reduce the discharge and so maintain the same output. Typical turbine and pumping relationships are shown in Figure 3.5.

3.4 Computer Modelling

For this study two models were used. The objective of 0-D modelling was to determine a relation between several barrage arrangements and power output, both at the A.B.P. and Pandoro sites (Figure 2.3).

This was done by examining the following variables during the optimising process:

- size of turbines
- number of turbines
- operating conditions
- design head

The one dimensional model was used to obtain more detailed results of the power output and to optimise the number of radial gates in the barrage.

Pumping was included in both models.

3.4.1 Turbine Optimisation

The speed of the turbines (n) was determined by calculating the maximum speed at which no cavitation occurs.

At first the design head for all turbines was taken at 6.5m, this being 80 percent of the mean spring tidal range. The design head defines the maximum output of the turbine and hence the size of the associated generator. At heads greater than the design head the turbine is throttled back to reduce the flow and maintain a constant turbine speed, and thus a constant output.

The turbine characteristics have been obtained by running a spreadsheet based on Eścher-Wyss curves. The main characteristics are given in Table 3.2.

Turbine Diameter (m)	Axis Level (mOD)	Speed of Rotation (rpm)	Peak Power (MW)
4.0	-6.8	83.33	6.28
5.0	-7.6	68.18	10.03
6.0	-8.3	58.82	14.96
7.0	-9.1	51.72	20.88

Table 3.2 : Turbine Characteristics

The first series of flat estuary runs examined the effect of varying the number and diameter of turbines while keeping the sluice area fixed at 12 numbers of 40 m^2. This sluice area was considered not to constrain the flow into the basin. Reversed turbining, sluicing through the turbines, was included in these calculations. Various configurations of turbines with a diameter of 4, 5, 6 and 7 m were run at spring, mean and neap tide. The results have been plotted in Figure 3.6 and 3.7 : it shows the energy output per tidal cycle as a function of the total installed capacity of the turbines. For example : On a spring tide, 10 turbines with a diameter of 4m (installed capacity 10 * 6.28 = 62.8 MW) produce an energy output of 243 MWh per tidal cycle. Curves have been plotted through these points in order to to determine a relationship between the installed capacity and the energy output per tidal cycle for each tidal range.

The maximum amount of energy is obtained if the turbine is operated at the design head, because the high efficiency factor at this head. This can only be reached when the installed capacity of the turbines is large enough to turbine all the water in the short time that the sealevel is at its lowest point. However, by increasing the installed capacity the discharges increase and as a result of that the backwater effects in the estuary become more significant.

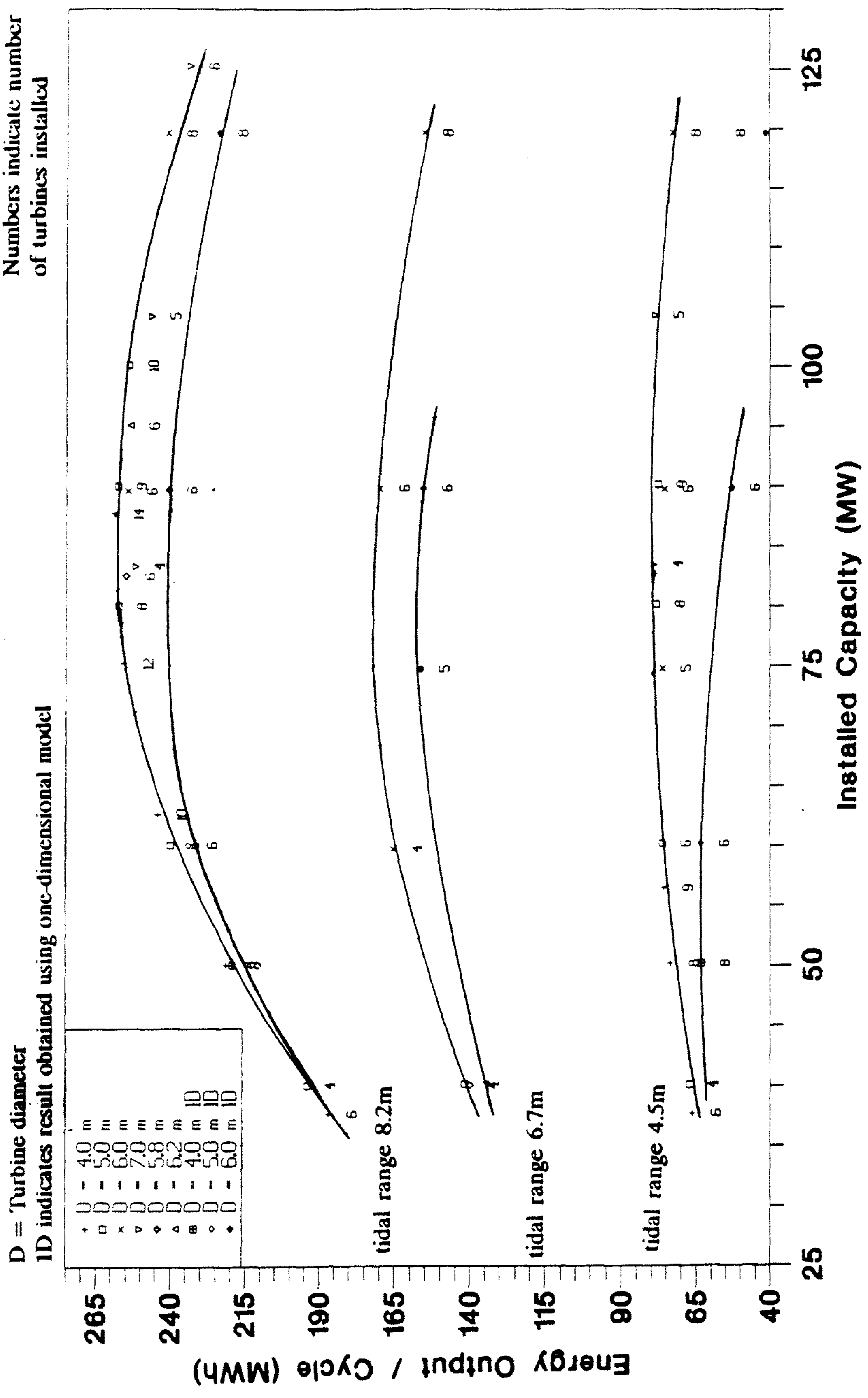

ENERGY OUTPUTS FOR DIFFERENT TURBINE ARRANGEMENTS; CENTRAL SITE

Fig 3.6

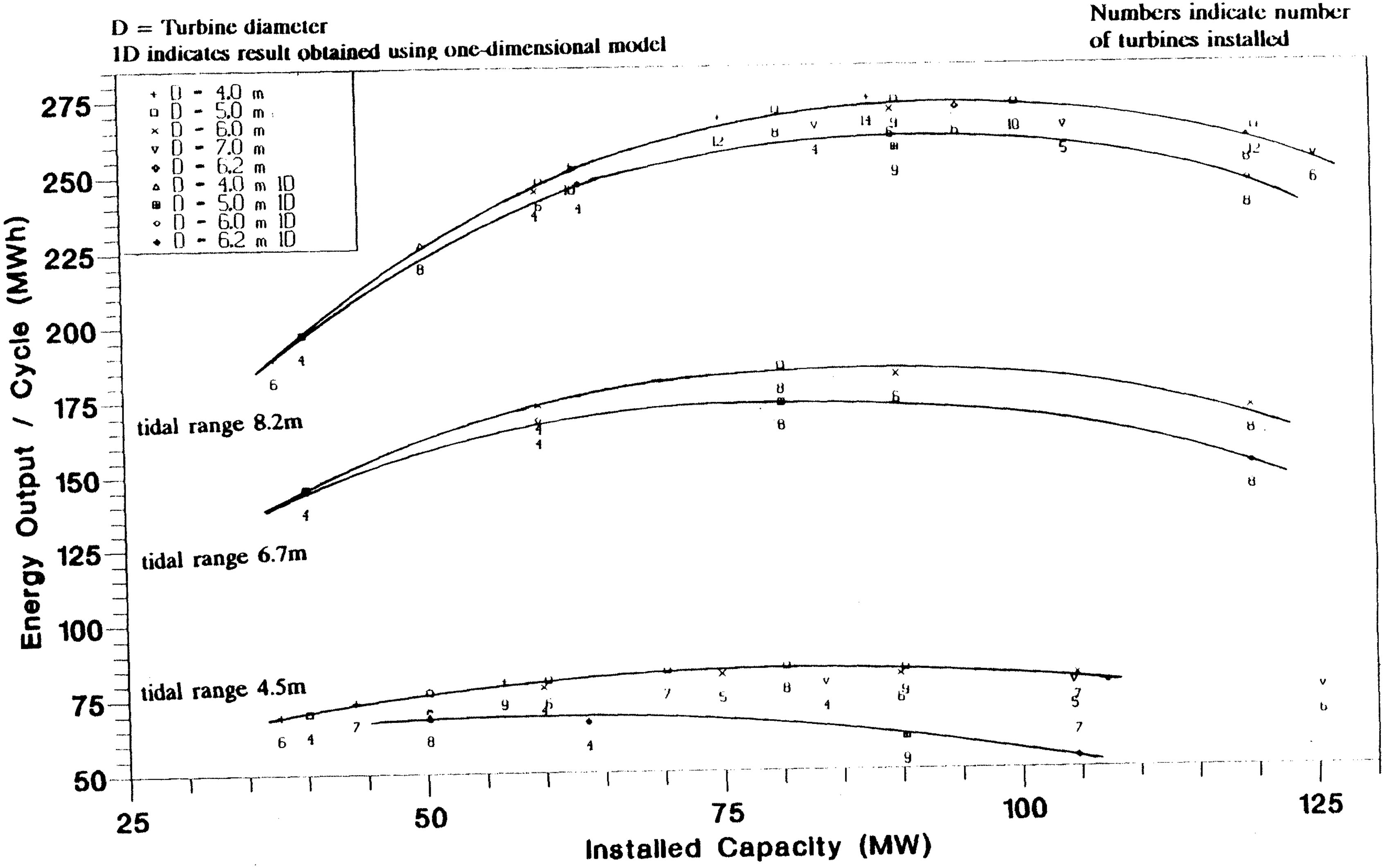

ENERGY OUTPUT FOR DIFFERENT TURBINE ARRANGEMENTS;
NORTHERN SITE

Fig 3.7

Figure 3.6 shows these effects: after passing the 85 MW mark of the installed capacity at a spring tide the energy output starts to decrease as a result of headlosses due to backwater effects.

At mean and neap tides the stored water in the basin is less. In that case the required capacity to turbine all the water at the highest head difference is less. As a result of that the optimum output occurs at a smaller installed capacity.

During a neap tide the lowest sea levels are higher than during a spring tide. This results in lower backwater effects. This explains the flatter curves at these tides.

The results for different turbine diameters are almost the same for a certain installed capacity. This indicates that the power output depends on the installed capacity, rather than on the size of the turbines.

The same figures show the one dimensional results. The sluice area comprises 14 radial gates and 2 fish passes. A new curve was plotted using the one dimensional output and the shape of the flat estuary (or 0-D) curve. The output is lower and the optimum is reached at a smaller installed capacity. The difference with the flat estuary results increases at a higher installed capacity, because the hydro-dynamic effects become more important. This will be explained in section 3.5.

Figure 3.8 shows the water-levels in the estuary during two tidal cycles. The levels immediately downstream of the barrage show the importance of the backwater effects, resulting in a decrease of energy output. Dredging on the seaward side of the barrage could decrease the backwater effects, and therefore increase the energy output.

3.4.2 Sluice Optimisation

The output of a given barrage depends not only on the turbine capacity but also on the ability to fill the basin subsequently. Several one dimensional runs examined the effect of decreasing and increasing the sluice capacity while keeping the number and size of the turbines fixed. For the A.B.P. scheme four numbers of 6.0 m diameter turbines were used, for Pandoro four 6.2 m diameter turbines. The results for the A.B.P. scheme, both with and without reversed turbining, are shown in Figure 3.9.

Reversed turbining allows water to flow through the turbines during the filling of the basin and therefore reduces the number of sluices required. However, the rotation of the blades as the turbines free-wheel can cause considerable damage to fish swimming upstream through the draft tubes.

Levels in the Estuary
during two Tidal Cycles

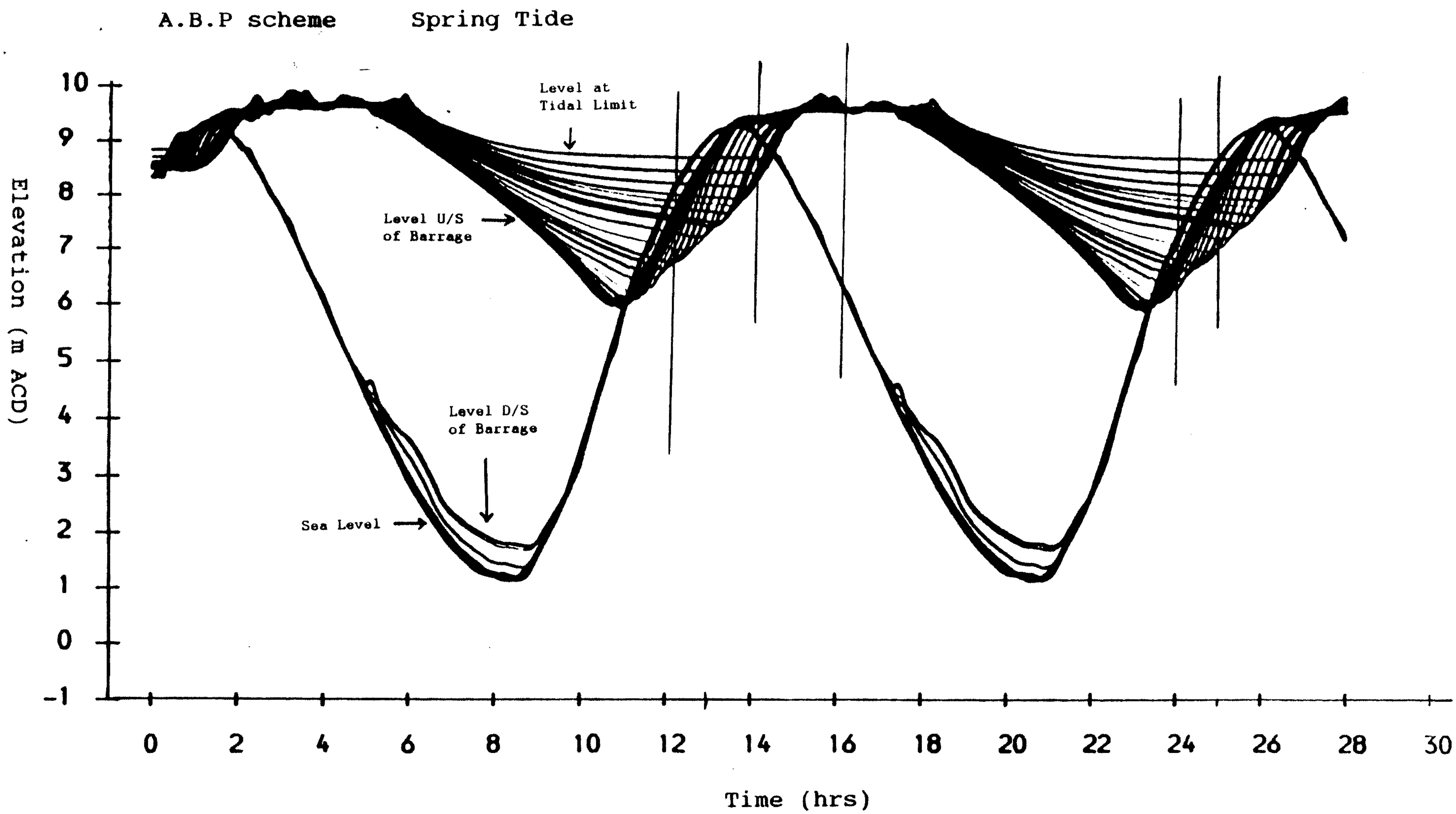

Note : ACD = Above Chart Datum
Chart Datum is 4.9m above Ordnance Datum

Fig 3.8

Graph of Energy Output v Sluicing Capacity
A.B.P. scheme
Spring Tide

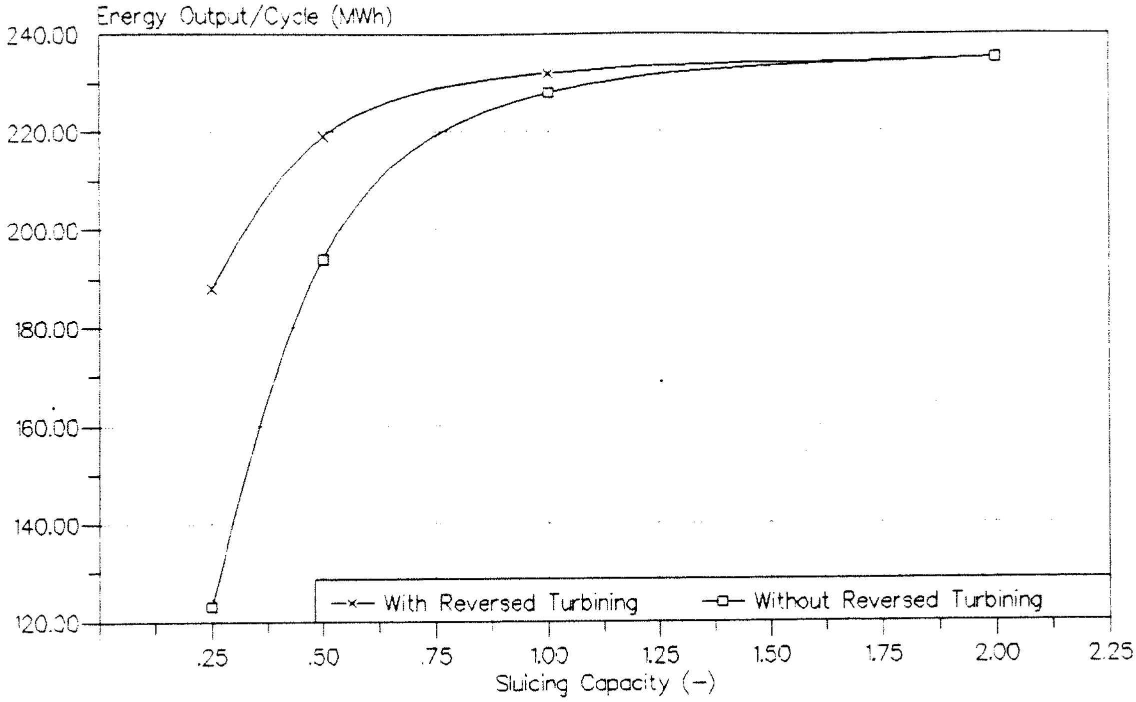

Sluicing Capacity = 1 means 14 radial gates and 2 fishpasses

Neap Tide

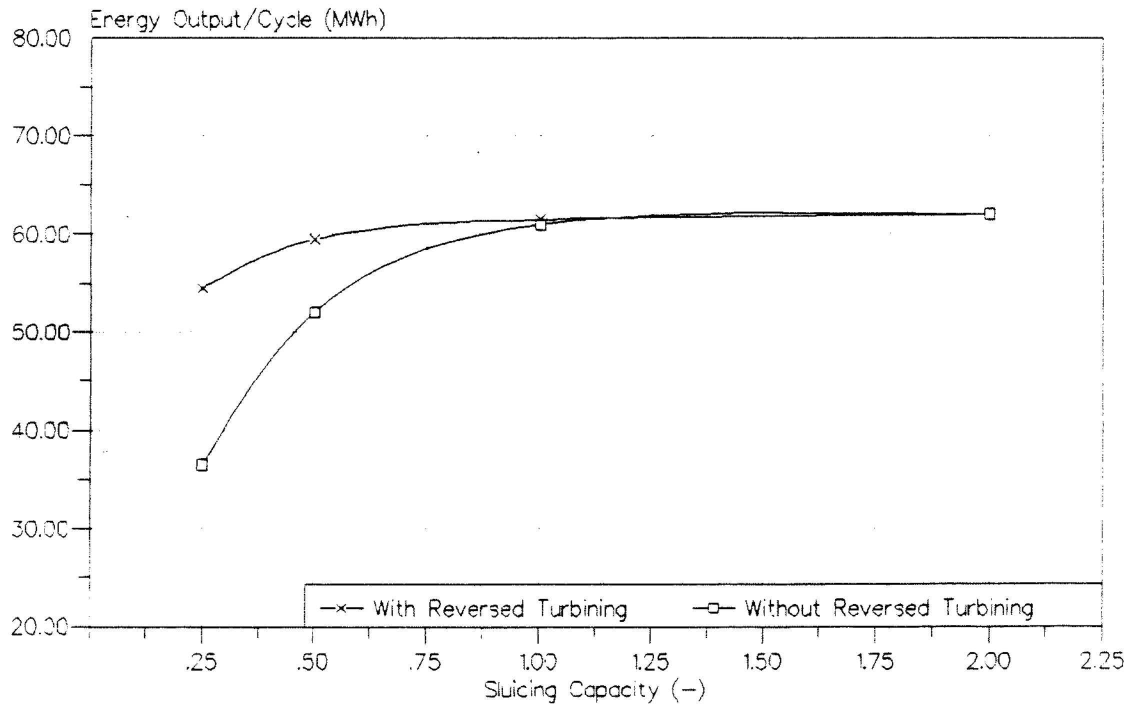

Fig 3.9

Becauce the cill of all sluices and fish passes is at the same level (-2.0 mOD), the sluicing capacity was considered to be a function of the width of all sluices.

If we consider the original sluice configuration of 14 radial gates and 2 fishpasses (sluicing capacity = 1.00), it is clear that this capacity is sufficient on a neap tide (see Figure 3.9). At spring tide, the filling of the basin is somewhat constrained, and therefore the energy output is not at a maximum. However, if reversed turbining is included, the energy loss compared to a configuration with a double capacity, is marginal (approx. 1.5 %).

It was decided to reduce the amount of sluices to twelve (sluicing capacity = 0.87). The energy loss on a spring tide is about 2 %. One annual output calculation with reversed turbining was carried out for twelve sluices and two fish passes. The result was that the annual energy output reduced by one percent compared to the original amount of fourteen sluices.

3.4.3 Annual Energy Output

The energy outputs at neap, mean and spring tide derived from Figure 3.6 and 3.7 are used to obtain a relation between energy output per tidal cycle and tidal range at different installed capacities. Since the energy output is known for three tidal ranges, this relation is assumed to be quadratic. These curves are shown in Figure 3.10. The histogram of tidal ranges of Fleetwood in 1983, an average year concerning the distribution of tides, is shown in Figure 3.12. The annual energy output is obtained by applying the following formula:

$$* \qquad Ea = \sum_{R=3}^{10} Er * Nr$$

in which :
- Ea = Annual Energy Output (MWh)
- Er = Energy Output per Tidal Range (MWh)
- Nr = Number of Occurances of Tidal Range per Year (-)
- R = Tidal Range (m)

The annual energy output was determined for four installed turbine capacities. The numeric results are listed in Table 3.3. A graph was created by drawing a line through these points (Figure 3.13). At the Pandoro site the maximum annual energy output of 129 GWh occurs at an installed capacity of 90 MW. At the A.B.P. site the maximum annual output is 120 GWh at an installed capacity of 75 MW. The output figures calculated in Table 3.3 include the basic efficiencies of generation (the turbine efficiency derived from the characteristic curves for the turbines, and the generator efficiency, taken as 95%).

Graph of Energy Output per Tidal Cycle
vs. Tidal Range

A.B.P. scheme

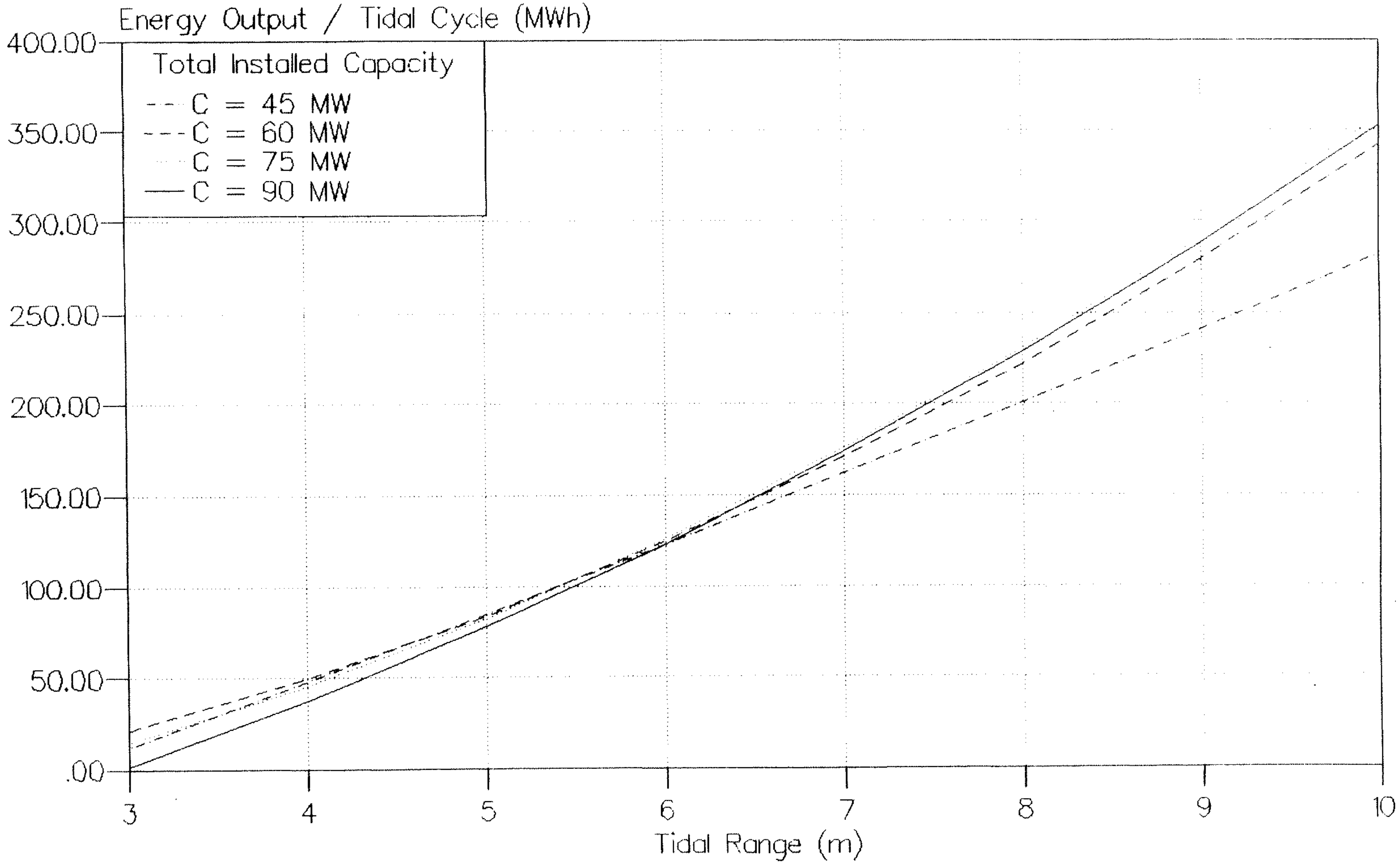

Fig 3.10

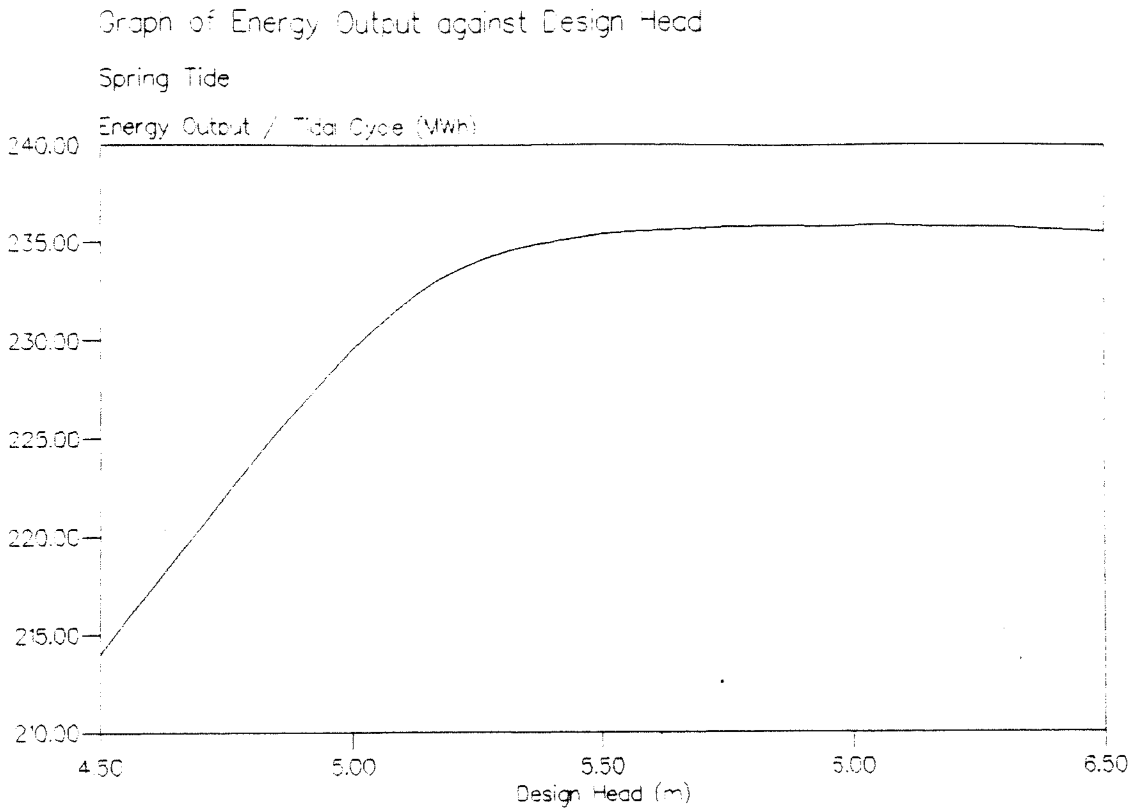

Fig 3.11

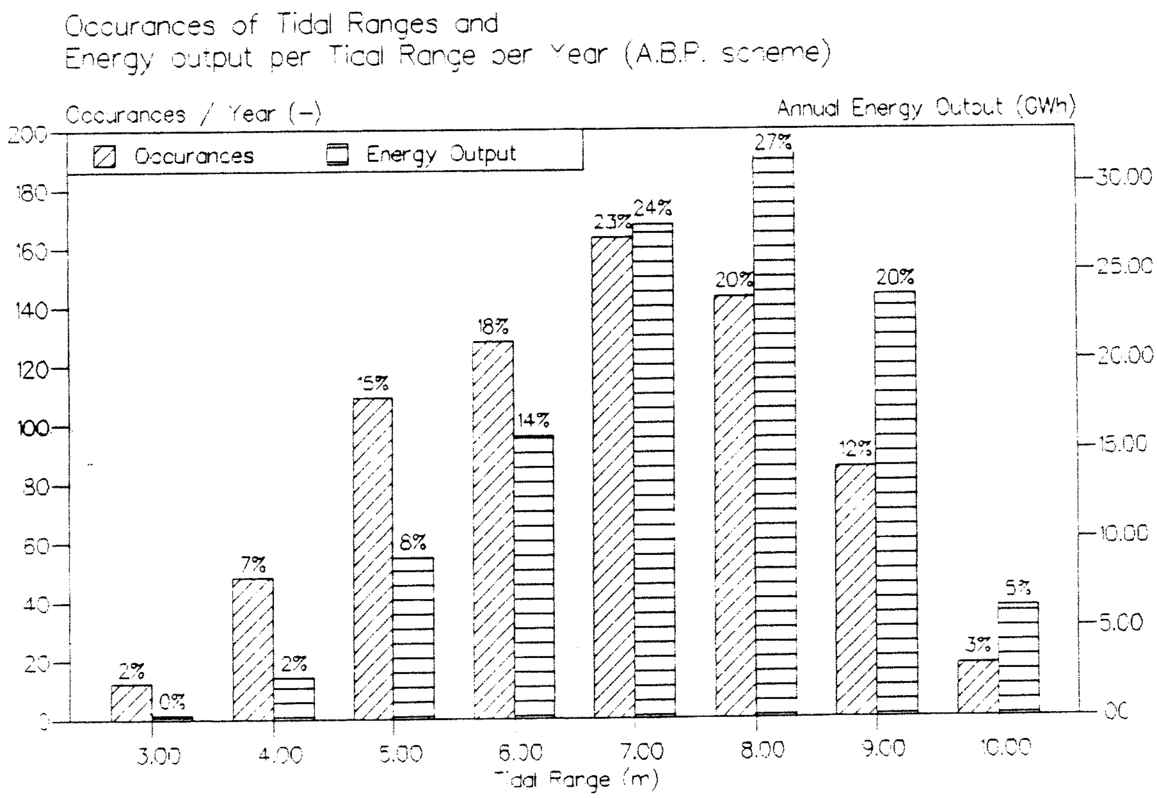

Fig 3.12

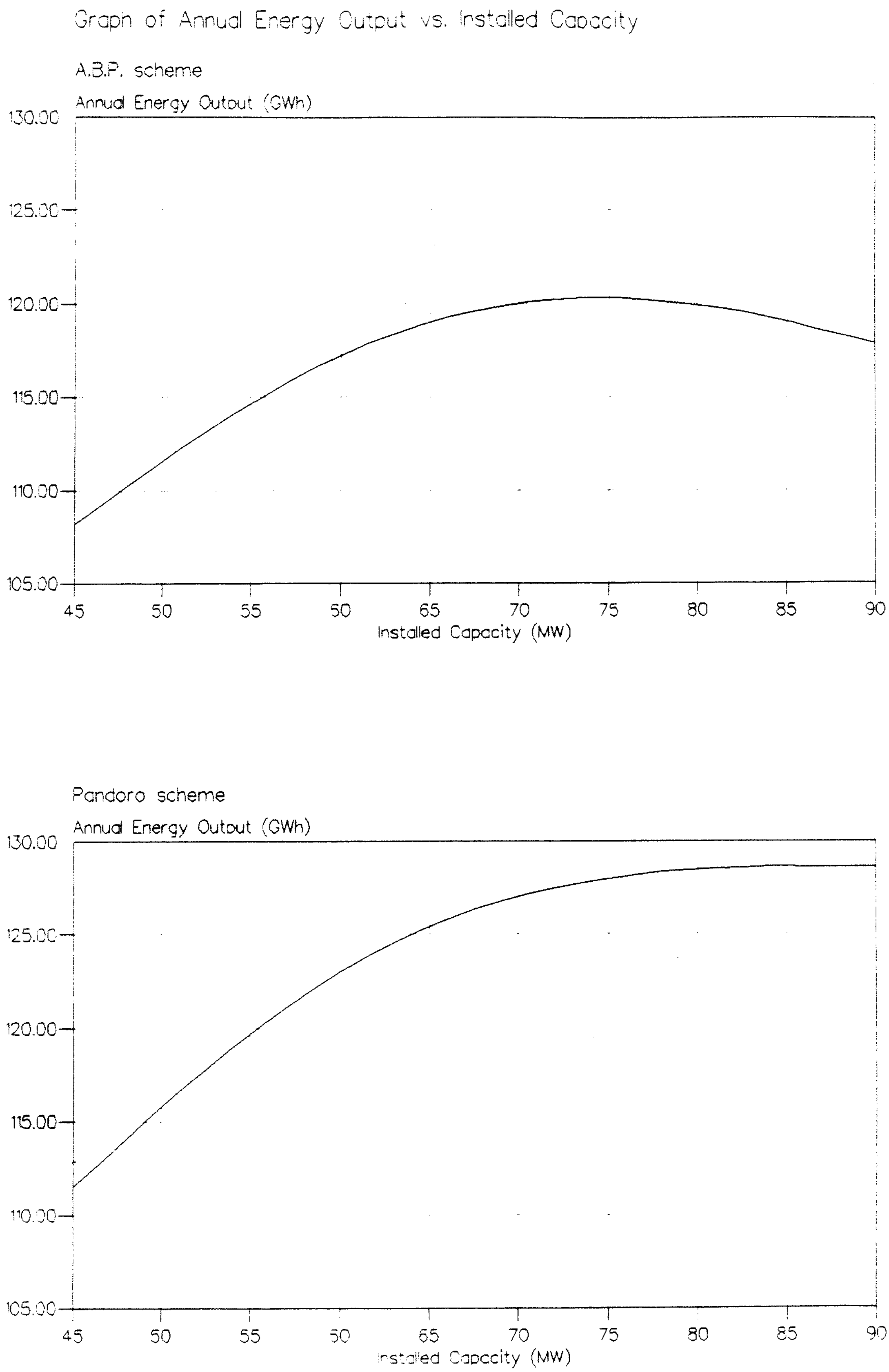
Graph of Annual Energy Output vs. Installed Capacity
A.B.P. scheme
Annual Energy Output (GWh)
130.00
125.00
120.00
115.00
110.00
105.00
45
50
55
60
65
70
75
80
85
90
Installed Capacity (MW)
Pandoro scheme
Annual Energy Output (GWh)
130.00
125.00
120.00
115.00
110.00
105.00
45
50
55
60
65
70
75
80
85
90
Installed Capacity (MW)

Fig 3.13

Installed Capacity (MW)	Annual Output (GWh)	
	A.B.P	Pandoro
45	108.2	111.2
60	117.1	123.0
75	120.4	128.3
90	117.9	129.0

Table 3.3 : Annual Energy Output

In Figure 3.12, the tidal range histogram, the distribution of the annual energy output per tidal range is shown. This illustrates the importance of the spring tides (range greater than 7.5 m) : occurring only for 35 percent of the year they provide 52 percent of the annual energy.

3.4.4 Further Optimisation Studies

Further optimisation studies included the examination of pumping and varying the design head of the turbines.

The principle of pumping in a tidal barrage is to pump sea water into the basin immediately after high water, while the head difference over the barrage is still small (smaller than 0.5 m). During the generation period, this extra volume of water is turbined against a larger head difference (5-6 m).

The effect of pumping was examined by runs with the 0-D model. Table 3.4 shows the results for the optimised A.B.P. scheme. These results are nett results : the energy loss due to pumping has been subtracted from the gross output.

	Energy output / Tidal Cycle (MWh)	
Tide	Pumping	No Pumping
Spring	235.6	226.1
Mean	165.6	153.5
Neap	73.9	64.5
	Annual Energy Output (GWh)	
	123.2	114.8

Table 3.4 : Energy Output (A.B.P. scheme)

Pumping increases the annual energy output by 7 percent.

The turbine design head was optimised by examining a number of runs with design heads of 4.5, 5.0, 5.5 and 6.0 m. Figure 3.11 shows that reducing the design head from 6.0 to 5.5 m does not affect the spring tide output significantly. Decreasing the design head results means that the turbine is less efficient at heads greater than the design head, but more efficient at smaller heads. In this case the gains weigh up to the losses, so the installed capacity can be reduced without loss of energy.

The best arrangement was not considered to be the one with the highest energy output. Other criteria, such as the total costs of the scheme and energy prices, have to be taken in account. Once these are known, the scheme can be optimised. In this preliminary stage, three considerations were taken into account :

- The total installed capacity of the turbines was chosen just below the capacity that would deliver the highest annual output.
- In view of the general lay-out of the barrage a total number of four turbines would be favourable.
- It was decided that twelve sluices would be sufficient, because the annual loss of energy compared to the original number of fourteen sluices is only in the order of one percent.

The final recommendations for both schemes are listed in Table 3.5.

SITE	Central (A.B.P.)	Northern (Pandoro)
TURBINES		
Number	4	4
Diameter (m)	6.00	6.20
Speed (rpm)	58.82	56.60
Peak power/turbine (MW)	14.96	15.89
Entrance area (m^2)	141.75	151.40
Exit area (m^2)	116.50	124.50
Bed Level (mOD)	-16.00	-16.00
Axis Level (mOD)	-8.30	-8.45
Design head (m)	5.50	5.50
SLUICES		
Number	12	12
Cill level (mOD)	-2.0	-2.0
Channel width (m)	9.0	9.0
FISH PASSES		
Number	2	2
Cill level (mOD)	-2.0	-2.0
Channel width (m)	4.0	4.0

Table 3.5 : Preferred Arrangements for Schemes Examined

These configurations of turbines and sluices result in the following annual energy outputs (pumping is included):

- A.B.P. : 117.2 GWh
- Pandoro : 125.0 GWh

3.5 Differences between 0-D and 1-D Results

The Figures 3.5 and 3.6 show the differences between the one dimensional results and the flat estuary results :

- The 0-D output is higher at any installed capacity, regardless of the tidal range.

- The difference becomes more evident at high installed capacities.

These differences are mainly due to negligence in the 0-D model of :

- Inertia downstream of the barrage.

- Both inertia and friction in the basin.

The Flat Estuary Model uses a backwater analysis for the seaward side of the estuary, which improves the accuracy of the energy output estimation considerably. The basin surface level is assumed to remain flat at all times.

Figure 3.14 shows the water levels in the basin at several stages of a tidal cycle. The main effects concerning the energy output are :

- During turbining the water level in the basin near the barrage drops much more than at the end of the basin. This results in a lower head across the turbines and thus in a decrease in energy output.

- During pumping the waterlevel near the barrage is higher than at the end of the basin. Therefore the pumping has to occur against a bigger head difference and costs more energy.

- During sluicing the waterlevel near the barrage is higher than the average level. Therefore less water will be stored in the basin.

The Flat Estuary Model neglects all these effects and will therefore calculate a higher energy output.

The difference between the energy output for the two locations, Pandoro and A.B.P., is caused by the fact that Pandoro is closer to the sea. Therefore the enclosed basin will be larger. This means that more energy can be generated. Another benefit is that the water that is turbined can flow much more easily to the sea. The backwater effects will be less at this location. Therefore the calculated energy output at the Pandoro site is higher than at the A.B.P. site.

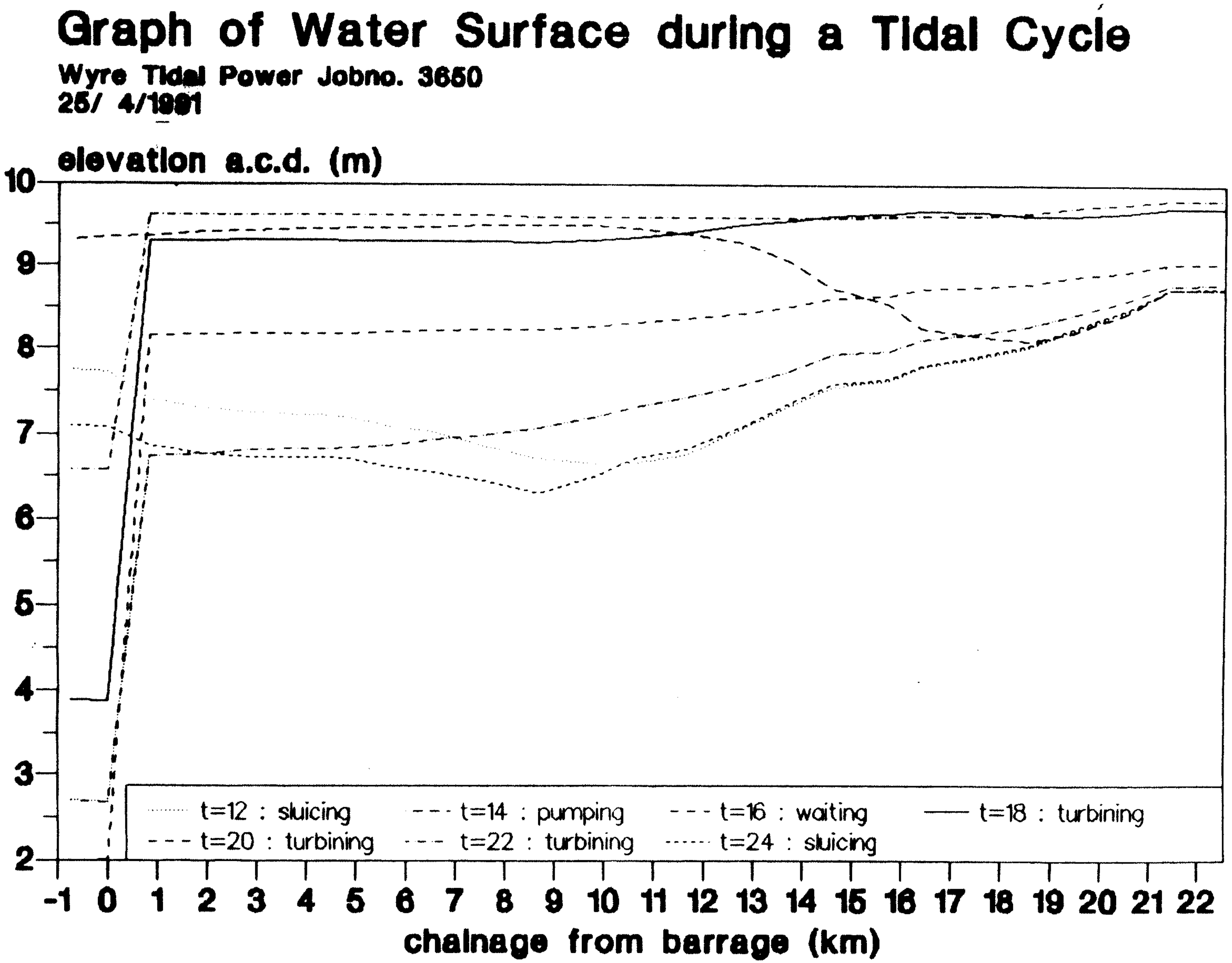
Graph of Water Surface during a Tidal Cycle
Wyre Tidal Power Jobno. 3650
25/ 4/1991
elevation a.c.d. (m)
10
9
8
7
6
5
4
3
2
t=12 : sluicing
t=14 : pumping
t=16 : waiting
t=18 : turbining
t=20 : turbining
t=22 : turbining
t=24 : sluicing
-1 0 1 2 3 4 5 6 7 8 9 10 11 12 13 14 15 16 17 18 19 20 21 22
chainage from barrage (km)

Fig 3.14

4. CAISSON DESIGN

4.1 Introduction

In this chapter the design of the sluice and turbine structures is discussed. It was decided to place the turbines and sluices in caissons. These would be constructed in a dock elsewhere and floated into the estuary at the appropriate time. The hydraulic aspects of transport and placing are discussed in Chapter 7.

In this chapter it is described how the number and the general lay-out of these caissons was determined. Also, the main criteria concerning the design, such as turbine dimensions, water levels, wave heights and soil parameters, are described. A more detailed design of a steel caisson is presented in Chapter 5.

The caisson is a gravity structure : it needs sufficient own weight in order to remain stable in all loading conditions. The calculation of this own weight (including ballast material) is described in Chapter 5. A final check on stability is carried out in Chapter 6.

The work presented in the chapters 4, 5 and 6 was carried out at T.H.T.. All the design of the concrete caisson was carried out by T.H.T.

4.2 Location

In Chapter 3 two principal sites were examined : the North or Pandoro site and the Centre or A.B.P. site. Although a barrage at the North site would provide more energy output, the centre site is more promising concerning existing infrastructure (roads, port).

The choice between the potential sites will probably be made on a political level, i.e. not simply on engineering or cost grounds. At the time this was written, the decision had not been made yet. Arbitrarily, it was decided to concentrate on the A.B.P. or Centre site.

4.3 Topography Data

A cross section of the estuary at the Centre site is shown in Figure 4.1. In absence of detailed geotechnical studies across the width of the river at the barrage site, the following assumptions have been made :

- Between -5 and -8 mOD : Alluvial and marine deposits
- Between -8 and -28 mOD : Glacial deposits (gravelley/cobbley clay)
- Below -28 mOD : Mudstone

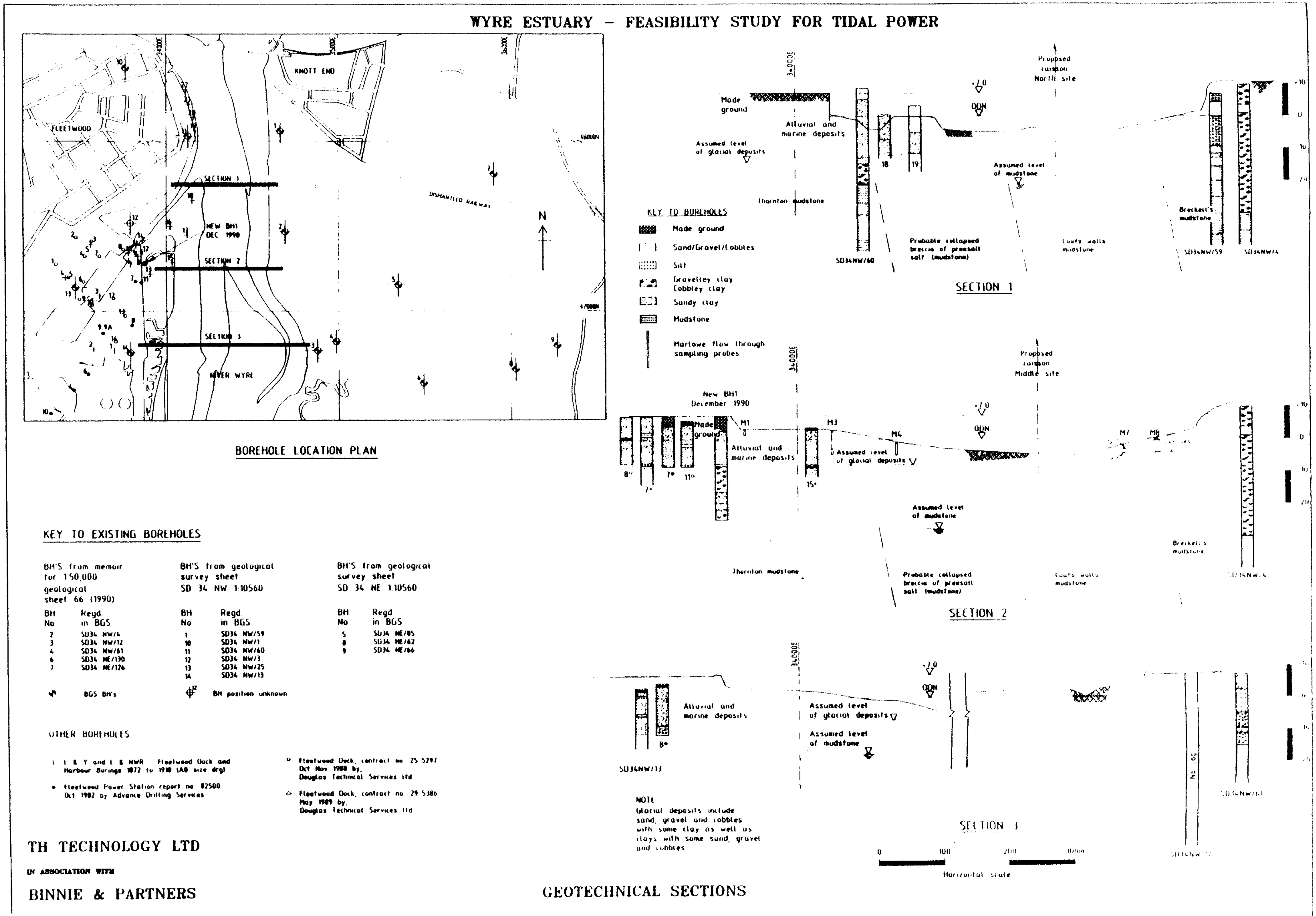

Fig 4.1 Geotechnical Sections at Barrage Locations

4.4 Design Criteria

4.4.1 Wind and Wave Criteria

Wind Speeds

Wind speeds in the area near the Wyre Estuary have been derived from data published in References 1 and 2 as follows:

Average Annual 21 m/s average hourly annual maximum
1 in 10 years 27 m/s maximum hourly wind speed
1 in 50 years 34 m/s hourly mean all year

Wave Heights

With the barrage located at the Centre site the effective fetch to the basin side of the barrage is about 3.8 km. The wave heights and periods that result from these wind speeds are shown in Table 4.1.

	Wind Speed (m/s)	Significant Wave Height (m)	Wave Period (s)
Average annual	21	0.9	2.8
1 in 10 years	27	1.2	3.2
1 in 50 years	34	1.5	3.5

Table 4.1 : Significant Wave Height and Period

The 1 in 50 years extreme wave height in Moorecambe Bay is 14 m, corresponding to a significant wave height of about 7 m. These deep water waves will be affected by the topography of the seabed as they approach the shore. North of the estuary, sandbanks are present for about 3 km. At M.H.W.S., the depth on these tidal flats will be only 5.7 m. All waves higher than 4.5 m will break on these flats (see Appendix 1). Since only high waves break, it is assumed that the significant wave height equals the maximum wave height. While moving over the tidal flats, the wave height will be further reduced to about 2.5 m, due to friction losses. Taking into account shoaling, defraction and refraction, the maximum wave height at the barrage is estimated to be 2.0 m. For a detailed calculation see Appendix 1.

Wave Characteristics	Basin side	Sea side
Significant Height (m)	1.5	2.0
Period (s)	3.5	10.0

Table 4.2 : Wave Characteristics at Barrage

A return period of 50 years has been taken as the design wave condition at the barrage. The design values are summarized in Table 4.2. The seaward side conditions are conservative as they are assumed to coincide with the 1 in 50 years high water level. Lower water levels reduce the maximum wave height. The likelihood of 50 year wave and 50 year high water events occuring together will have a return period considerably greater than 50 years.

4.4.2 Tide and Water Level Criteria

The highest and lowest astronomical tide levels at Fleetwood Docks are (Reference 3):

HAT +5.4 mOD Newlyn[1)]
LAT -4.9 mOD Newlyn

Extreme high water levels generally result from the superposition of a positive surge (caused by meteorological conditions) on a high astronomical tidal level. The high water level with a return period of 50 years is estimated as 2 m over Mean High Water Spring Tide in Morecambe Bay. Mean High Water Spring Tide is +4.3 mODN, so the high water level with a return period of 50 years is +6.3 mODN. By adding a 1m surge (estimated) the Extreme High Water level becomes +7.3 mOD Newlyn.

The water levels at the basin side will be changed considerably by the barrage. The resulting loading cases will be discussed in Chapter 6.

4.4.3 Soil Parameters

The bearing capacity calculations of the glacial deposits under the barrage has been assessed on the following basis:

- the material behaves in a drained manner (effective stress analysis)

- the underlying mudstones are at least as strong as the glacial deposits

From three tests conducted on samples from a borehole at the barrage location average lower bound values have been assessed:

- effective friction angle, ϕ' : 28°
- effective cohesion, c' : 30 kN/m^2
- saturated density : 21 kN/m^3

1) Relative to Ordnance Datum Newlyn

From these parameters the nett allowable bearing pressure has been calculated by T.H.T. at approx. 280 kN/m^2, with a factor of safety of 3.0, depending on the ratio of horizontal and vertical load and effective width and length of the loaded area.

4.5 Global Dimensions

4.5.1 Turbine section

In chapter 3 it was concluded that the barrage should comprise four turbines with a diameter of 6.0 m. Studies undertaken to a potential tidal power scheme in the Severn estuary (Reference 4) have pointed out that the ideal dimensions for a draft tube are:

1) Centerline of the turbine at least 0.75 * turbine diameter below Mean Low Water at Spring tide (MLWS), so that the turbine is almost at any time submerged.

2)

Inlet Area	: 1.75D * 2.25D	
Outlet Area	: 1.75D * 1.85D	
Overall Length	: 7.5D	(see Figure 4.2)

These parameters are valid for a bulb turbine. The turbines in this barrage will be of the pit type. Therefore the dimensions have been changed slightly:

Inlet Area	: 2.40D * 2.00D	
Outlet Area	: 1.85D Circulair	
Overall Lentgh	: 8.0D	(see Figure 4.3)

Because the size of the conning tower in the inlet tube is larger than the bulb, the inlet area and length is increased. For practical reasons (the size of the proposed construction dock) the outlet length has been reduced to 24m. Detailed studies should assess what the resulting energy losses will be.

Assuming a floor and roof thickness of respectively 1.5m and 1.0m results in a sill level of the turbine caisson of approx. -16.5 mOD, while the top of the roof is at -2.0 mOD.

The top level of the barrage (eventually the level of the road crossing) is at +7.2 mOD, 0.5 m above the 1:50 year highest sea level. When this sea level occurs, the waves are allowed to topple over the barrage.

The Pit type turbine requires two vertical shafts to enable access to runner blades and generator/alternator. In case of damage or maintenance these parts can be lifted out of the draft tube. The shaft will reach to a height of +7.2 mOD, which is the height at which the road is positioned.

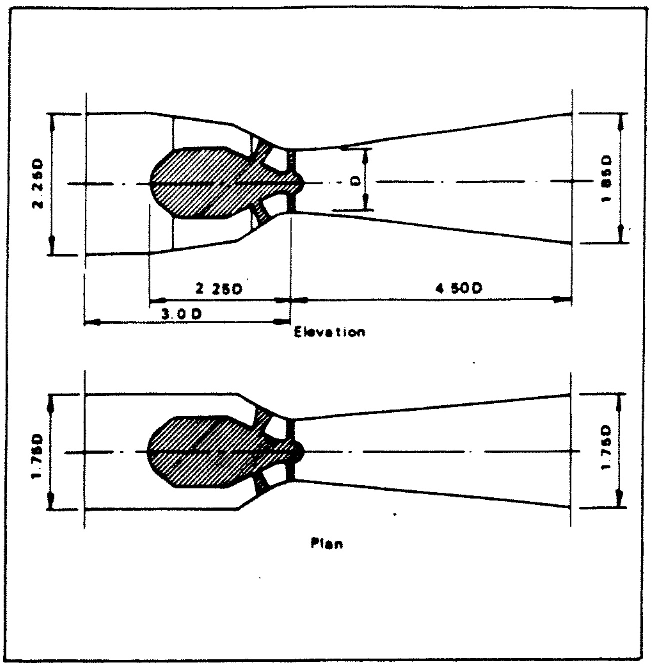

Fig 4.2 Ideal Turbine Dimensions

Generally the two shafts are part of a "conning tower". This tower, as it is an obstacle in the inlet tube, is circular at the basin side, so that energy losses are reduced to a minimum.

4.5.2 Sluice section

In Chapter 3, energy modelling, it was concluded that 14 sluices with a width of 9 m and 2 fish passes, width 5.6 m, both at a sill level of -2.0 mOD would be the optimum arrangement. However, it is also possible to use another arrangement with the same sluicing capacity.

In this scheme, the gaps between the conning towers are used as sluices, the conning towers act as sluice piers. Therefore, the conning towers are shaped circular at the seaward side, to avoid eddies at the outlet of the tube. Five sluices are located above the turbines, the sill level will be at -2.0 mOD. These sluices will have radial gates. The other sluices could be submerged.

4.6 Turbine and Sluice configuration

As stated before, the barrage must comprise 4 turbines with a diameter of 6.0 m and 14 sluices with a width of 9m at a sill level of -2.0 mOD, or an equivalent of that.

The caissons are gravity structures : their own weight must be sufficient to meet safety factors against sliding, overturning and floatation. Since both sluices and the tube of a turbine are relatively buoyant (especially when they are dewatered), they need to be connected to a heavy section. This will normally be a section containing

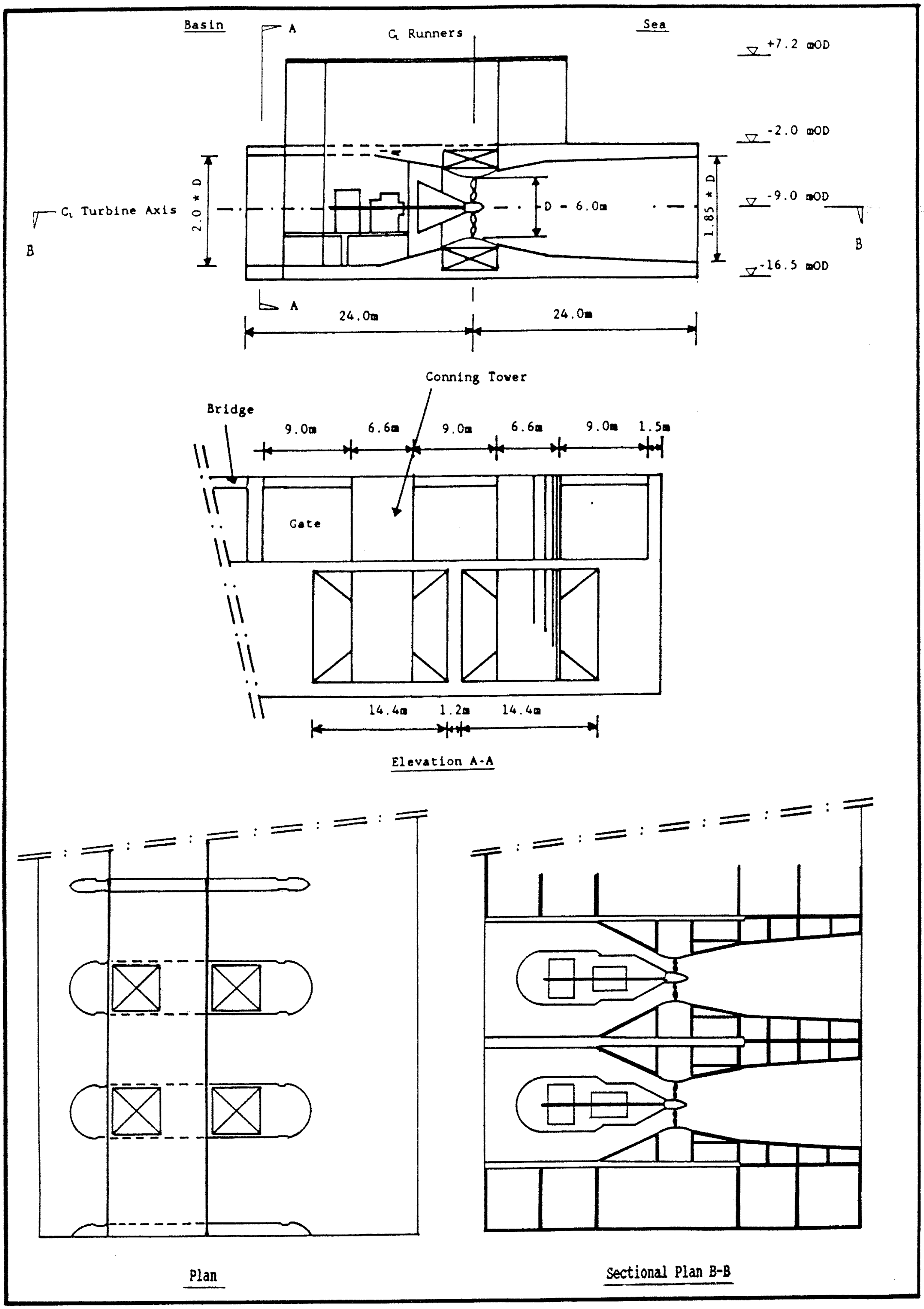

Fig 4.3 Layout Turbine Section of Wyre Caisson

several chambers to be filled with ballast (sand, hydraulic fill). There are numerous possible combinations for a turbine/sluice/ballast caisson. The following criteria play a role in the choice between those combinations.

1) Volume
2) Symmetry
3) Construction/Placing
4) Type of gates
5) Maximum draft
6) Location of turbines

SUB 1) The amount of concrete or steel, an important cost aspect, is mainly determined by the volume of the caisson. This weight determines the floating draft. In order to meet the factors of safety regarding stability, the volume of ballast should be adequate.

SUB 2) The disadvantage of a non-symmetrical configuration is that 3-dimensional stability problems are introduced. Further, a non-symmetrical caisson will probably need ballasting during transport, in order to keep the caisson level. This will increase the floating draft of the structure.

SUB 3) The simplicity of a structure is an important cost factor. Unequal sill levels for different caissons require complex construction techniques, e.g. cofferdams or sheet piles, in order to close the gaps under the caissons. These solutions are expensive and hard to realise, considering that the sill of the turbine caisson is 16.8m below the mean sea level.

SUB 4) The use of the area above the turbines as sluices means that the size of the sluice gate is determined. The other sluices could be of a different size or type. However, this also means that an additional spare gate is required.

SUB 5) The floating draft is an important feature for both the transport and placing stages of the caissons. It is determined by the weight and bottom surface area of the caisson. Seperating the sluice from the turbine caissons results in a greater draft for the turbine caisson, because the sluice caisson is relatively light before ballasting.

SUB 6) Preferably, all turbines should be placed beside each other. This is because the required bottom level near the turbines is the lowest. Separating the turbines will increase the amount of dredged material.

The alternative caisson configurations that have been selected are shown in Figure 4.4.

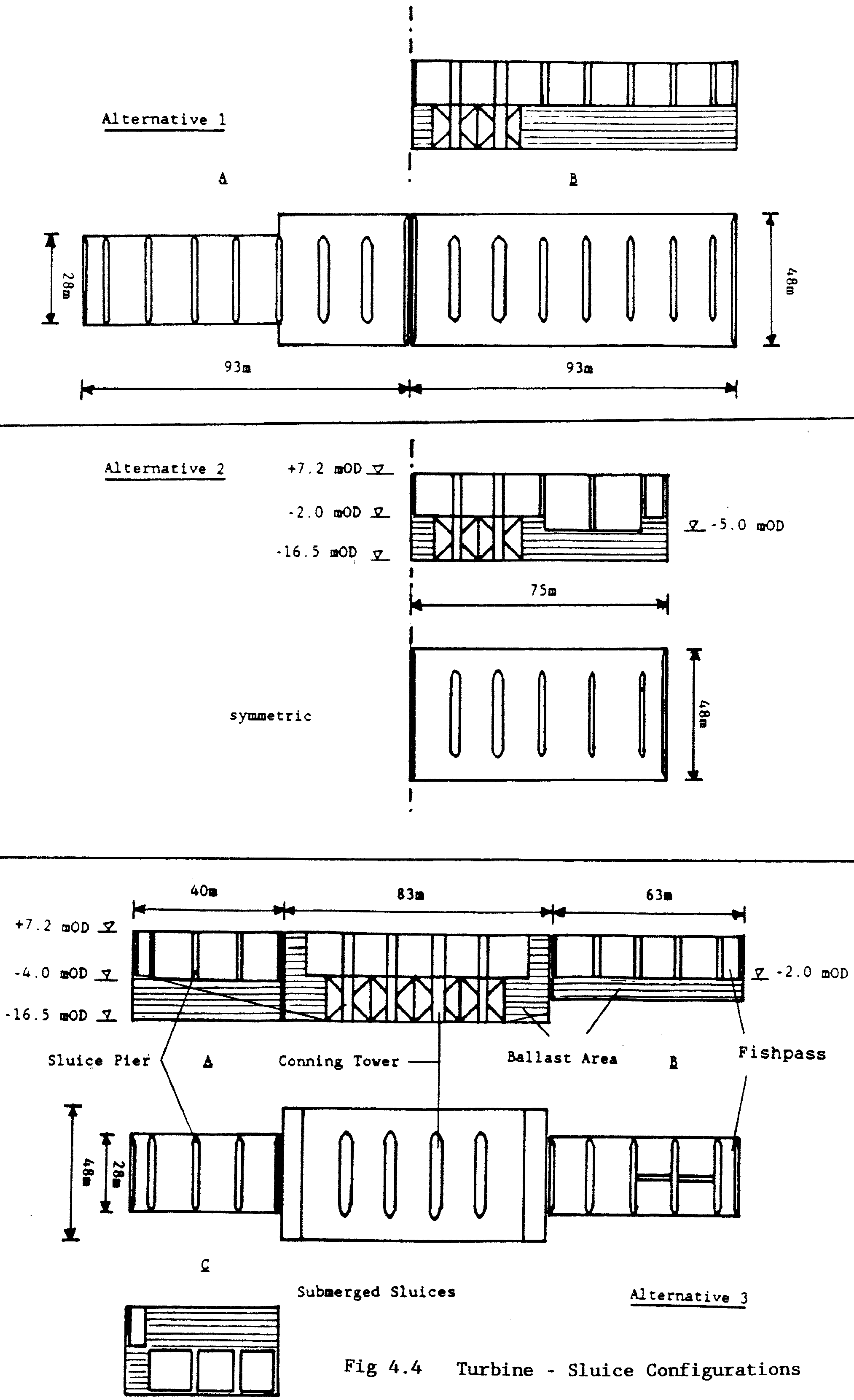

Fig 4.4 Turbine - Sluice Configurations

Alternative 1B is the first caisson that has been designed by T.H. Technology. It comprises two 6m diameter turbines, seven 9m wide sluices and a fishpass. The other caisson is mirror-symmetric. This is the most simple design with the caisson shaped as a box. The total width is 48m, and the length would be 93m. This simplicity will result in a low cost/volume ratio. The gates are radial gates and have all equal sizes.

This alternative was checked against overall stability and found to be stable for all loading cases. The obtained factors of safety were substantially higher than design values. Therefore it was tried to cut down on the costs by decreasing the caisson volume.

Alternative 1A shows that the width of the sluice part of the caisson is decreased. The caisson shape is more complex. This shape is not favourable for the transport stage.

The solution T.H. finally selected is **alternative 2**. Four small sluices have been replaced by two larger ones with a similar capacity. The overall length is decreased to 75m. A stability check showed that with these dimensions the factors of safety were just adequate.

Other possibilities are described under **alternative 3** :

* 1 caisson containing 4 turbines and 5 sluices
* 2 caissons containing sluices

A) The sluices differ from the ones in the turbine caisson. The sill level can be determined by calculating the amount of ballast needed for stability.

B) The sluices are as in the turbine caisson. The bottom level of the caisson is determined by :

- stability conditions
- maximum slope to overcome difference in base level between turbine and sluice caisson. If the bottom level is higher than possible with a slope, then a permanent sheet pile construction is required.

C) Submerged sluices: amount of ballast as in A). No slope is possible along front and back, so sheet piles are needed to overcome the height difference. Fully submerged sluices have a better sluicing capacity, so they can be smaller.

The main advantage of the alternative 3 solutions is that they are symmetric. A disadvantage is that the turbine caisson is relatively heavy during transport and consequently will have a greater draft.

In this preliminary stage of the study, the advantages and disadvantages are hard to quantify. Table 4.3 summarizes the (dis)advantages of the alternative solutions (+ is positive, 0 is indifferent, - is negative).

ALTERNATIVE	1A	1B	2	3A	3B	3C
CRITERIA						
1	0	-	0	0	0	0
2	-	0	0	+	+	+
3	0	0	0	+	0	-
4	+	+	0	0	+	-
5	+	+	+	-	-	-
6	-	-	-	+	+	+

Table 4.3 : Qualitative Comparison of Alternatives

A real judgement can only be made when the relevance of each criterion is quantified. Although alternative 3A looks the most promising, T.H. Technology chose to design a concrete variant of 2. Drawings of the concrete caisson are shown in Figure 4.5. To make a comparison possible, a steel caisson with the same dimensions as alternative 2 has been designed. This will be discussed in Chapter 5.

Figure 4.6 shows the general arrangement of the barrage, including the two sluice/turbine caissons, the dams and the shipping lock.

REFERENCES

1. Environmental Parameters in UK Continental Shelf
Noble Denton 1984.

2. Floods and Resevoir Safety
ICE 1978.

3. Associated British Ports
Fleetwood Docks Tide Tables 1990.

4. Tidal Power from the Severn Estuary, Volume II
The Severn Barrage Committee, 1979.

WYRE ESTUARY - FEASIBILITY STUDY FOR TIDAL POWER

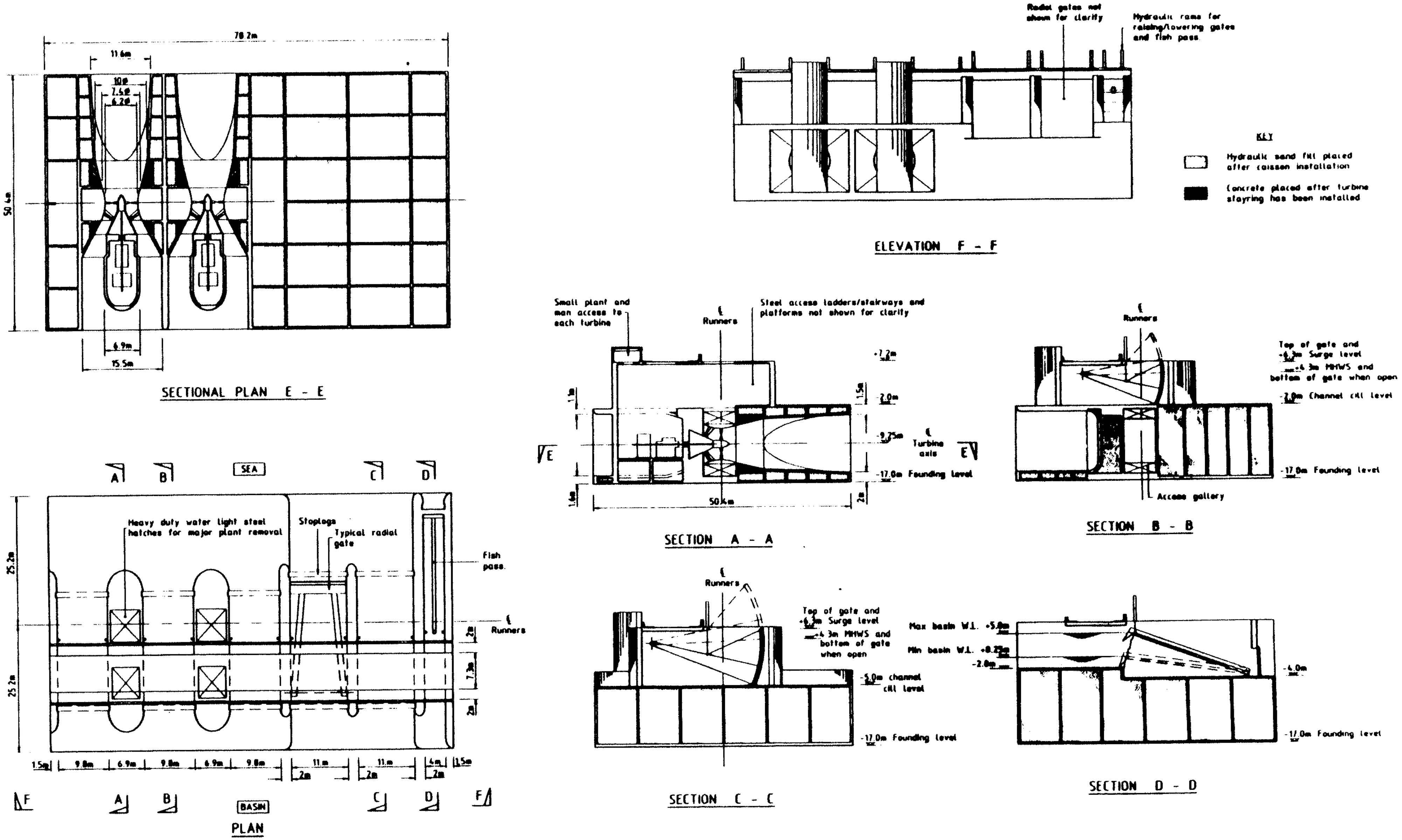

TH TECHNOLOGY LTD

IN ASSOCIATION WITH

BINNIE & PARTNERS

GENERAL ARRANGEMENT OF TURBINE - SLUICE CASSION

Fig 4.5

WYRE ESTUARY - FEASIBILITY STUDY FOR TIDAL POWER

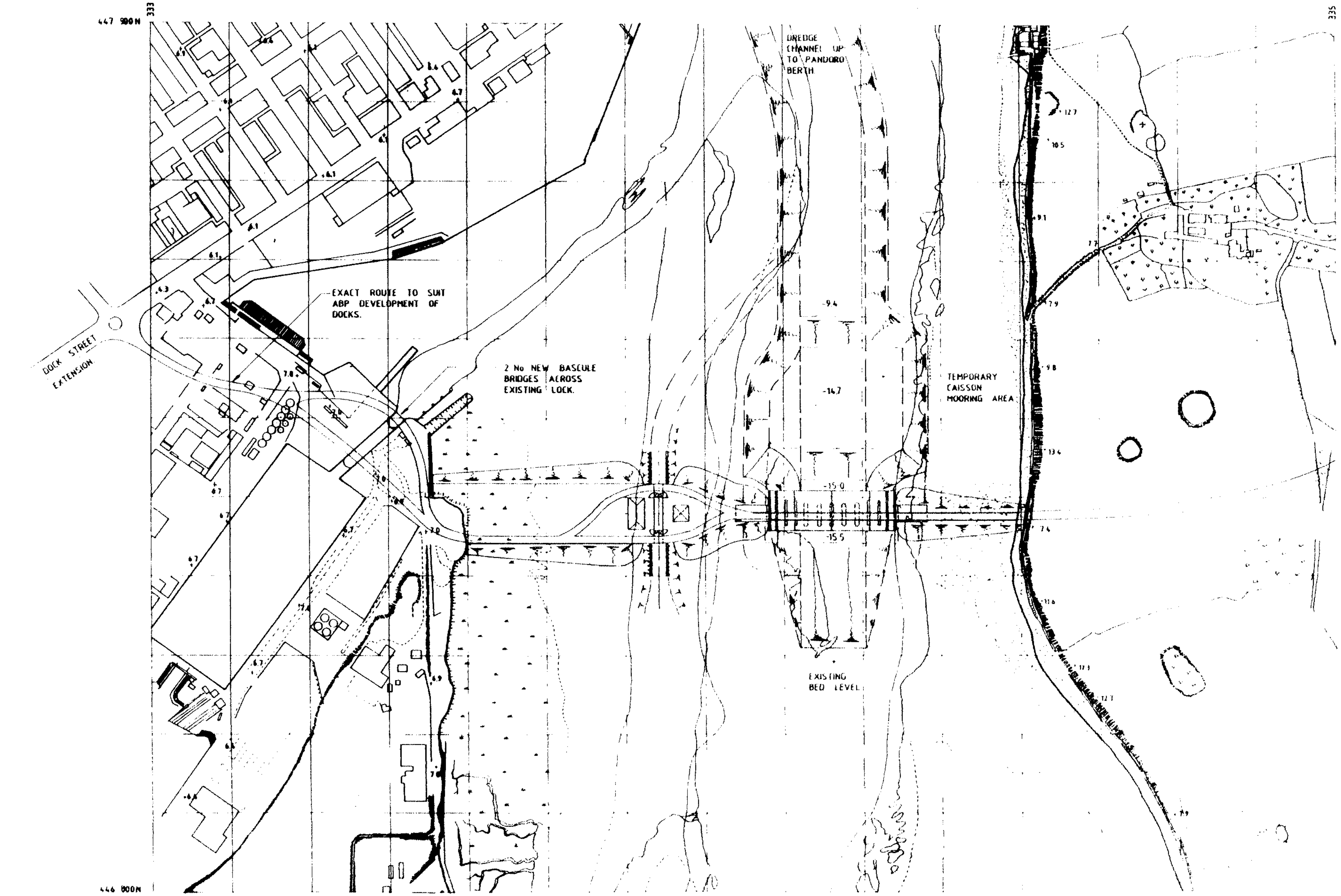

T H TECHNOLOGY Ltd.
IN ASSOCIATION WITH
BINNIE & PARTNERS

GENERAL ARRANGEMENT OF BARRAGE

DRAWING No.

Fig 4.6

5. STEEL CAISSON DESIGN

5.1 Introduction

5.1.1 Objectives

The objective of the work discussed in this chapter is the design of a steel caisson, under the restrictions of the global dimensions as stated in chapter 3. A drawing of the steel caisson is shown in Figure 5.1. An effort has been made to use the advantages of steel compared to concrete, such as the high strength - weight ratio, so that the steel weight is minimized. This will reduce the floating draft of the structure, which can have considerable advantages during transport and placing of the caisson.

Not the entire caisson will be made of steel. Because the high local loads of the foundation it was decided to apply concrete for the floor. This will also improve the stiffness of the structure. Also, this extra weight will reduce the otherwise large metacentric height of the caisson, which will improve the dynamic stability (see chapter 7). The rest of the caisson (walls, draft tube, conning towers etc.) will be made of steel. The whole steel/concrete caisson will be constructed off-site. After the placing, the ballast chambers will be filled with ballast material (sand).

In order to assist with the structural analysis, two computer programs, "Bagpus" and "Strap" have been utilised.

5.1.2 Restrictions

1) All beams and plates are designed according to the British Standards 449: part 2 1969.

2) Structural Steel will be of Grade 50.

3) No excact data about the tolerance between the runner blades and the draft tubes have been obtained. Therefore, the following assumptions have been made :

   * In the entire caisson, no deflection larger than 12 mm may occur.

   * Around the runner blades, the maximum deflection is 5mm.

4) The general dimensions of the caisson are as alternative 3 in Chapter 4.

5) The caisson must meet all safety factors for stability (see Chapter 6)

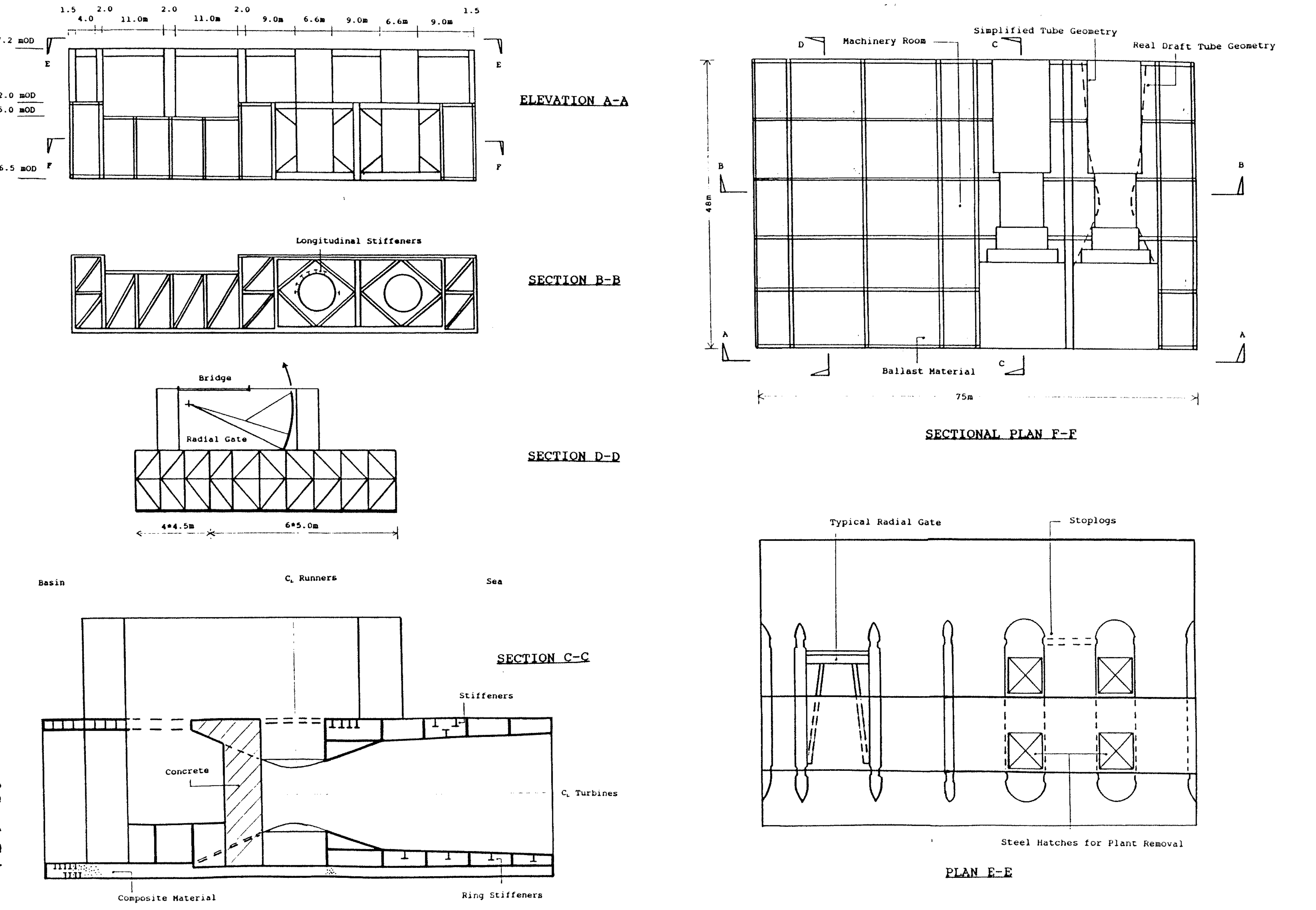

Fig 5.1 General Arrangements of Steel Caisson

5.2 Design Method

5.2.1 Global Stability

The caisson is a gravity structure, i.e. its stability depends on its own weight. This means that all voids in the caisson, e.g. around the draft tubes, inside the sluice piers, in the ballast chambers, will be filled with ballast material. In order to forecast the stability of the caisson, a comparison is made with a concrete caisson with dimensions equal to this one. This concrete caisson was designed by T.H. Technology and and optimised during several design cycles with the purpose of minimising the caisson weight while still meeting the safety factors for stability. The steel caisson needs approximately the same dead weight for stability reasons.

Basicly, the concrete caisson consists of the following materials :

- Structural Concrete :	14500 m^3	or	354.000 kN
- Steel (Turbine assembly, gates, etc.) :	260 m^3	or	20.000 kN
- Ballast :	20000 m^3	or	490.000 kN

The weight of the structural concrete in the concrete caisson is 41 % of the total weight. For the steel caisson, the structural concrete will be replaced by structural steel and ballast. We can estimate the amount of required steel by comparing a concrete plate and a steel panel : the panel weight is 80 percent of the structural steel weight. Figure 5.2 shows two panels, one made of reinforced concrete and one made of grade 50 steel. Both panels have the same critical bending moments. From this example it was estimated that the weight of structural steel will be 5 times less than the weight of structural concrete. So 1 m^3 of structural concrete can be replaced by 0.2 m^3 of structural steel. In order to obtain an adequate dead weight, 65 percent of the volume, 0.8 m^3, is replaced by ballast material. The total weight of the steel and ballast is : 0.2 * 78.5 + 0.65 * 0.8 * 18 = 25.0 kN. The weight of 1 m^3 of reinforced concrete is 24.5 kN. So the total weight of a steel caisson will not be much different from the concrete caisson. Consequently : if the concrete caisson is stable, then the steel caisson should be stable too.

5.2.2 Program Description

Bagpus is a computer program developed by the Steel Construction Institute in order to assist with the design of steel tidal barrage caissons. The caisson will be built up out of flat stiffened steel panels. There are three construction types (see Figure 5.3, obtained from Reference 1) :

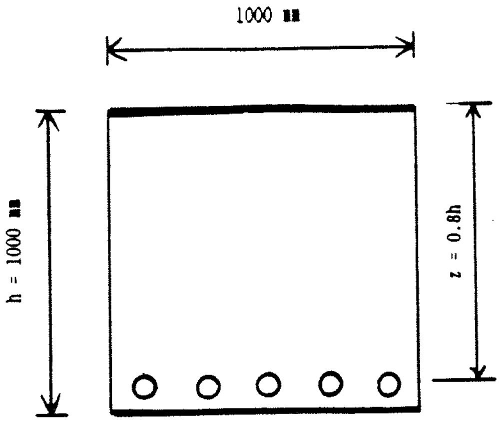

Concrete Plate

$M_u = A_s * z * f_s / 1.7$

with :

A_s = Steel Area of Section (mm^2)

$= w_0 * A_c$

A_c = Concrete Area of Section (mm^2)

$= 1000 * 1000\ mm^2$

w_0 = percentage of reinforcement (-)

$= 1.3 * 10^{-2}$

f_s = allowable tensile stress (N/mm^2)

$= 400\ N/mm^2$

z = effective height (mm)

$= 0.8 * h$

h = total height of plate

= 1000mm

Substitution of variables gives :

$M_u = 2448$ KN/m

Weight = 1.0 * 24.5 = 24.5 kN/m^2

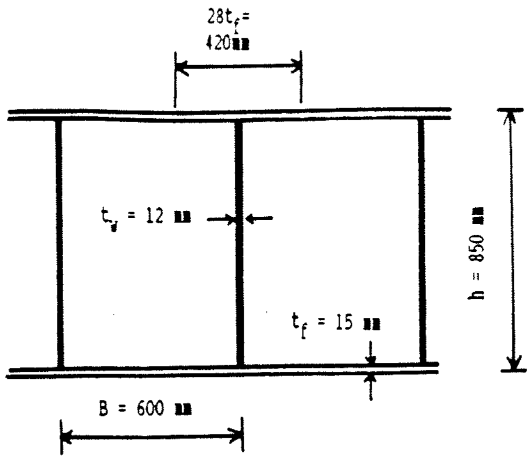

Steel Panel

$Mu = p_{bc} * 2 * I / h * 1000/B$

with :

p_{bc} = Allowable Stress in Bending (N/mm^2)

$= 230\ N/mm^2$

I = Moment of Inertia (mm^4)

$= 1/12 * t_w * (h-2t_f)^3$

$+2 * 28 * t_f^2 * ((h-t_f)/2)^2$

t_f = Flange Thickness (mm)

= 15 mm

t_w = Web Thickness (mm)

= 12 mm

h = Total Height of Panel (mm)

= 850 mm

Substitution of variables gives :

M_u = 2470 KNm/m

Weight $= (2 * 1000 t_f + (h-2t_f) * t_w * 1000/B)$

$* 78.5 * 10^{-6}$

= 3.64 kN/m^2 Consider 25 % extra steel for buckling : 4.55 kN/m^2

$$\frac{\text{Steel Weight}}{\text{Concrete Weight}} = \frac{4.55}{24.5} = \frac{1}{5}$$

Fig 5.2 Comparison of Steel and Concrete Plate

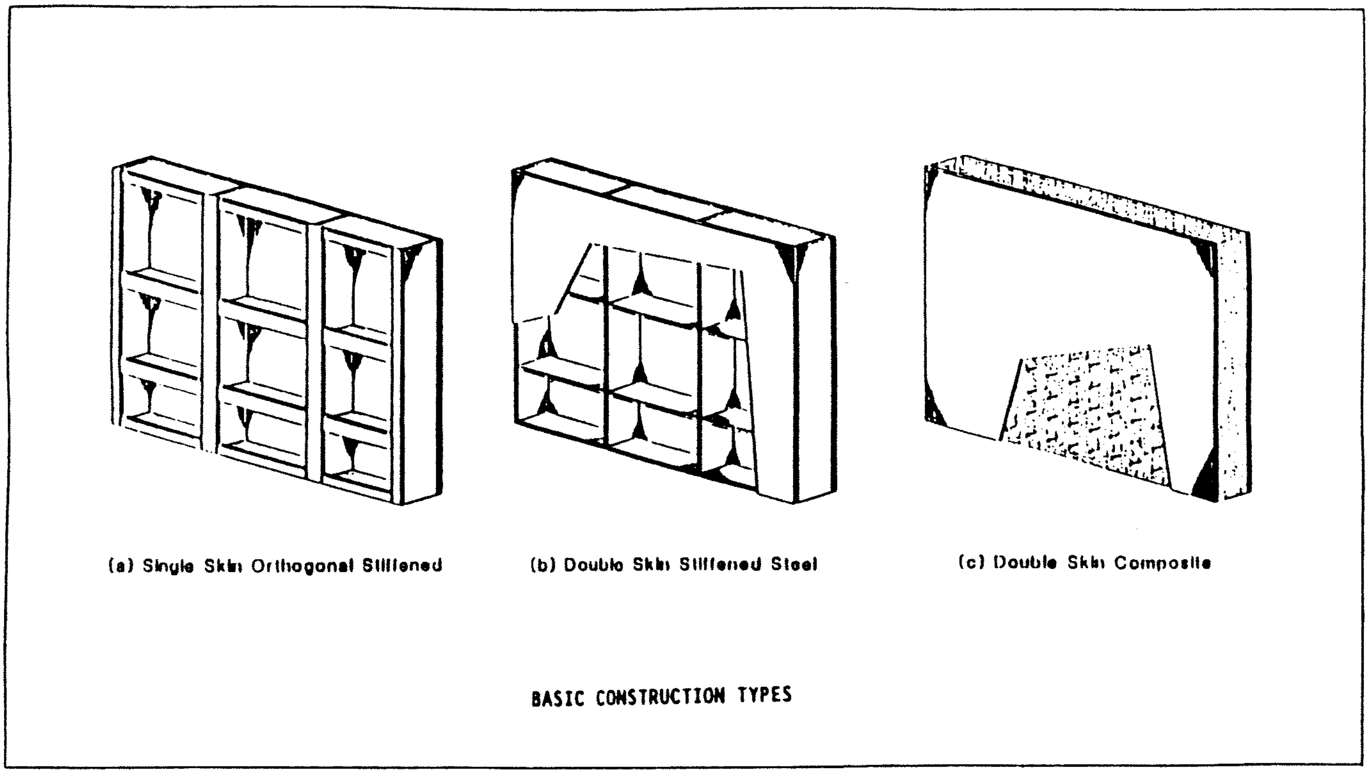

Fig 5.3 Types of Panels Used by Bagpus

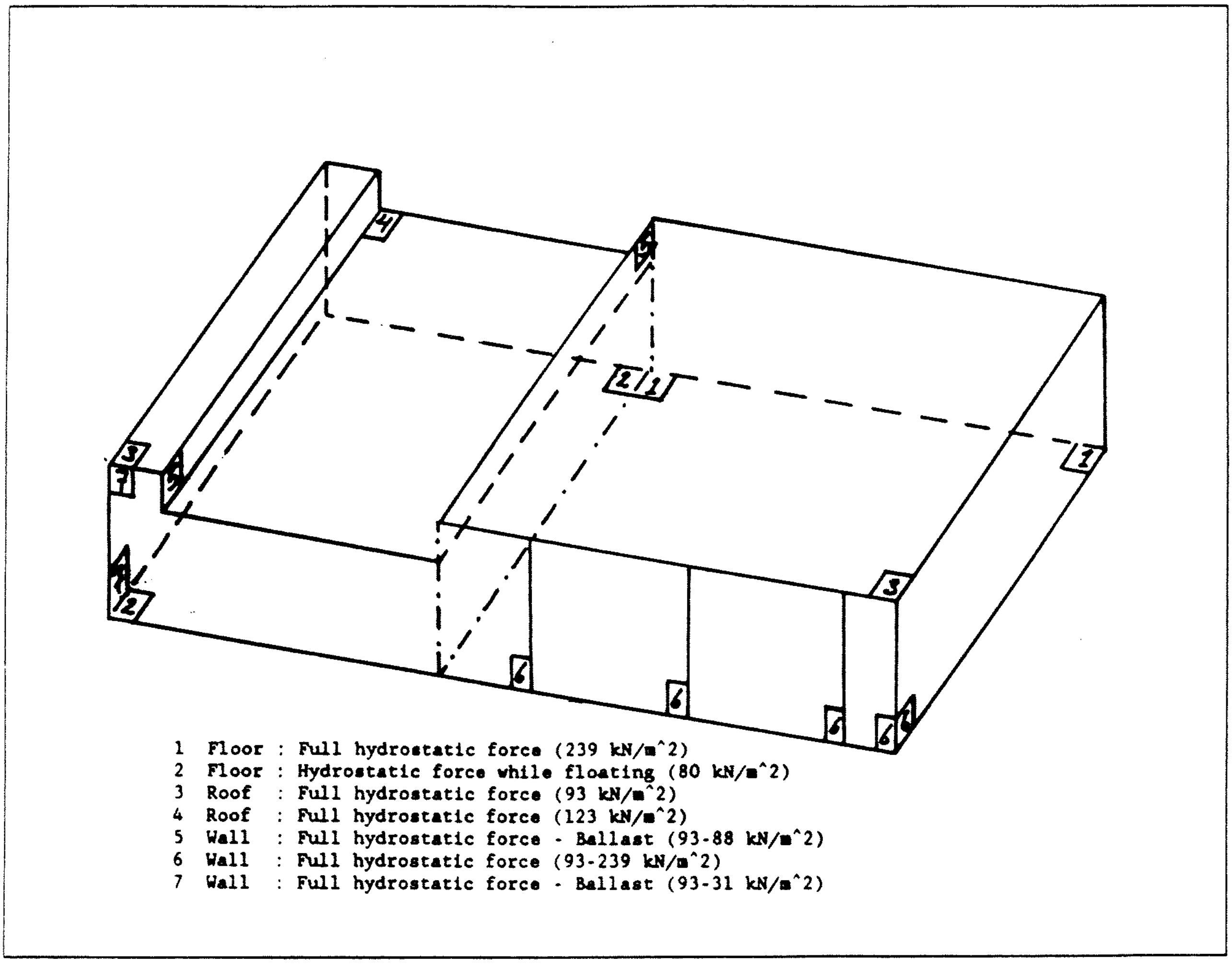

Fig 5.4 Loads on Panels

1) Single skin steel plate with flat bar and/or 'T' section stiffeners welded to one side.

2) Twin skin steel plates with flat plate stiffeners between.

3) Twin skin steel plates with concrete infill.

Once the construction type is chosen, the program can optimise the panel to minimise costs or weight by varying aspects such as plate thickness and number of stiffeners.

The program contains subroutines for the design of draft tube, cranes, bridges, etc.

Once all panels have been designed, it is possible to carry out a global stability check for the caisson.

Regarding the accuracy of the design with Bagpus, two remarks must be made:

1) The program tends to overestimate the dimensions of some panels, because:

   - All panels are supposed to be supported on two sides, while in reality some panels will be supported on three or four sides.

   - In a more advanced design the draft tube and walls would be combined, instead of both being designed for the full hydrostatic load.

2) Cumulative plate stresses due to addition of in-plane stresses from out-of-plane effects are neglected.

This means that Bagpus will not give results about :

- overall bending and shear
- global deflections

Because deflections are thought to be a severe problem for a steel caisson, it was decided not to use Bagpus for the overall caisson design. Instead, a framework was modelled in order to predict global deflections. Bagpus was used only for the panel and draft tube design.

5.2.2 Schematisation

A 3-dimensional frame, built up out of Universal Beams, was set up, to represent the caisson under global loadings (see Figure 5.5, note that this figure is taken from a different angle than all other figures). Only the part below -2.0 mOD is represented in the model: conning towers and sluice piers are designed separately. The frame has to cater for global bending and shear, and deflections as a function of those. The main loadings in the members of the frame are axial loadings. A 3-dimensional structures analysis program, "Strap", was used for the calculations.

The framework consists of

- 10 frames in the X1-X2 plane

- 11 frames in the X2-X3 plane

A typical X1-X2 frame is shown in Figure 5.6. The distance between the frames varies. The frames under the large sluices have a reduced height compared to the other frames. The conning towers are represented by frames with less length.

The X2-X3 frames only consist of horizontal members connecting the X1-X2 frames. In the middle of the caisson, where the draft tube size is reduced, diagonal members have been added in order to increase the stiffness in the X2-X3 plane (see Figure 5.7).

Innitially, all members were assumed to be of UB 900. In an iterative process the members were seized according to the actual stresses. Some members were adjusted in order to decrease the global deflections of the frame. These calculations were repeated until both the deflections (see restriction 3) and the stresses were acceptable.

The frame was plated with panels where necessary, to carry the loads into the frame. The panels are mainly loaded by out-plane bending and shear. Panels were designed by using "Bagpus" (Appendix 3). All panels have been assumed to be single skin panels, except the floor (twin skin filled with concrete) and roof (twin skin with stiffeners).

The floor of the caisson has been designed with twin skin plates filled with concrete (see Figure 5.3c)in order to increase the stiffness. This is needed because the bottom loading will not be completely uniform due to difficulties in levelling the bed protection material. This may result in high local stresses. In more detailed studies studies it needs to be decided wether to use these composite panels, or to apply a reinforced concrete floor.

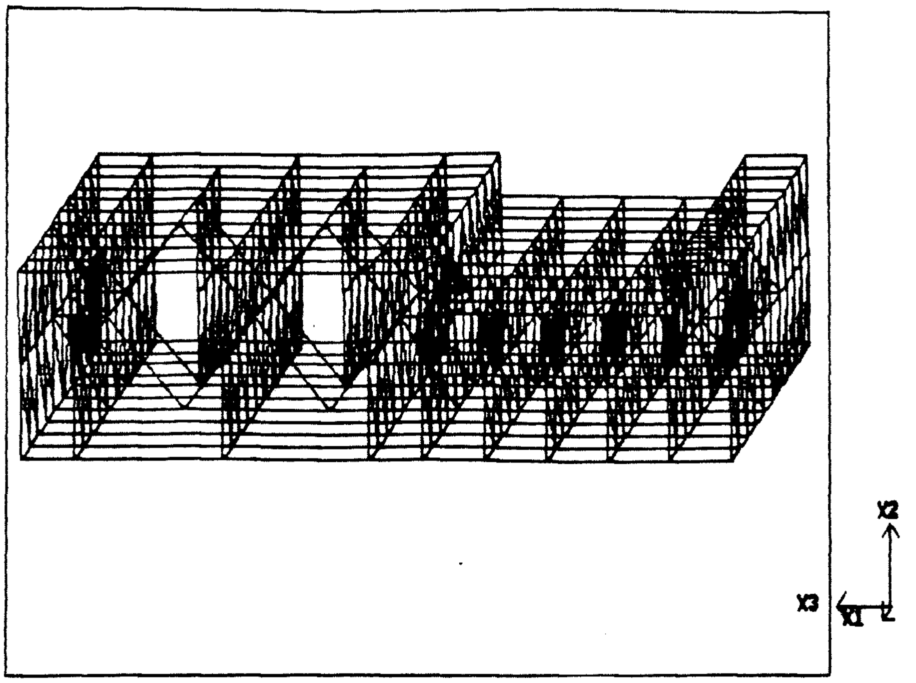

Fig 5.5 Caisson Representation in Strap

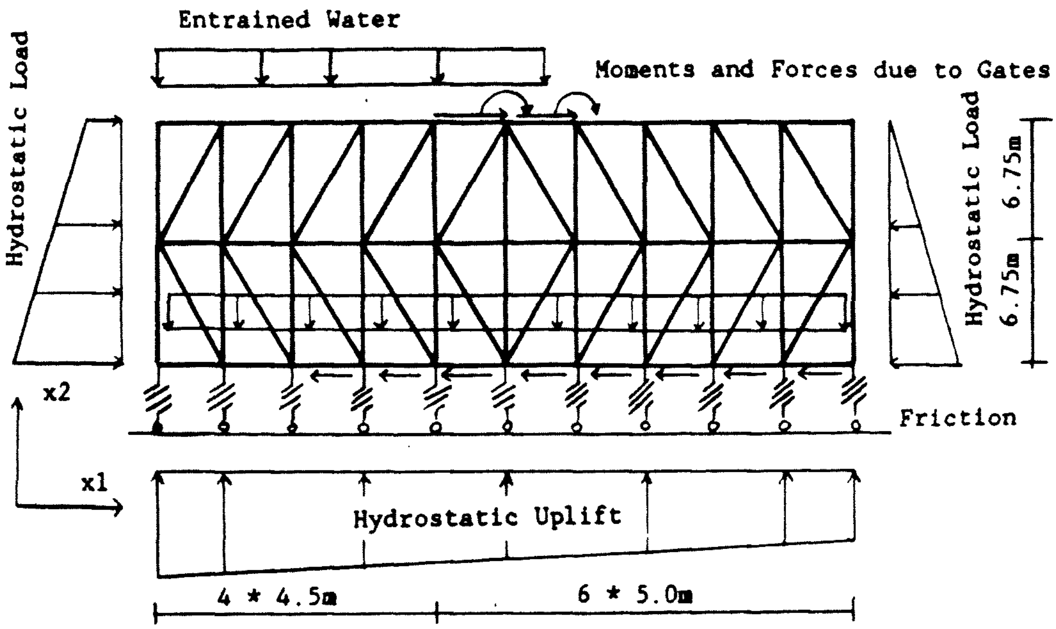

Fig 5.6 X1-X2 Frames with Typical Loadings

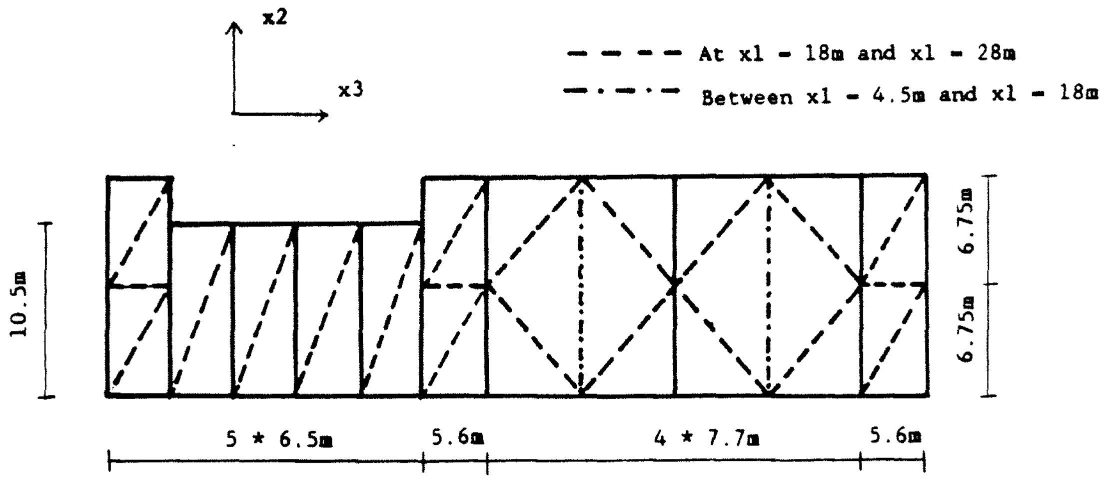

Fig 5.7 X2-X3 Frames

In the model the bearing pressures are modelled as springs under the stiff points, i.e. the caisson walls.

The draught tube is a highly complex structure. For this calculation the tube was simplified by representing it by four cylinders with varying diameters. Bagpus contains a subroutine that calculates structural solutions for several combinations of plate thicknesses and longitudinal and circumferential stiffeners (Appendix 3).

5.2.3 Frame Loading Cases

It is not possible to input global loadings in Strap: each member has to be loaded separately. In section 6.2 all loading cases concerning global stability are described. For the structural analysis, the number of loading cases for the frame is restricted to two :

1) Extreme Flood

2) Maximum Head at Start of Generation

SUB 1) This loading case means that the water levels are at a maximum : the sea level is at +6.7 mOD, while the basin level is at +5.0 mOD. This condition will result in the highest global bending and compression of the structure, and therefore the highest axial forces in the horizontal and vertical members.

SUB 2) The difference between basin (+5.0 mOD) and sea level (-2.0 mOD) is at a maximum. This will introduce high global shear in the structure. This results in high axial forces in the diagonals.

5.2.4 Panel Loading Cases

For the panels the loadings are divided in four parts:

1) Full hydrostatic load

2) Full hydrostatic load - Ballast

3) Floating hydrostatic load

4) Wave Loads

SUB 1) The maximum water level is +7.2 mOD. Since the draft tube has to be dewatered from time to time, the panels around the draft tube need to be designed on this full hydrostatic load.

SUB 2) In the ballast area, the full hydrostatic load is reduced by the hydraulic fill inside the caisson. The horizontal pressure of the sand is assumed to be neutral (K0) (appendix 4.3).

SUB 3) This is the hydrostatic load during the transport of the caisson. The floating draft is assumed to be 7 m. This loading case can be more significant than the permanent loading case. For example, in the floor under the ballast chambers the upward hydrostatic loads almost equal the downward ballast loads, which means that the net load is virtually zero. The loading in the transporting phase is approximately 70 kN/m^2.

SUB 4) The wave loads act in the splash zone, which is approximately in between 2.0 mOD and the top of the barrage at +7.2 mOD.

A summary of loads is shown in Figure 5.4.

5.3 Results

The Strap output was analyzed by the following procedure:

X1-X2 frames were divided into groups of equal loadings. Of each group the diagonal, horizontal and vertical member with the highest stresses was selected and designed as a U.B. A list of axial, shear and bending stresses of each of those members is given in Appendix 2. Figure 5.7 gives the typical results for a X1-X2 frame. The calculated weight of each frame is listed in Appendix 2. In some beams, e.g. the vertical beams at the outside, the stresses are too high for one single U.B. For simplicity reasons these members were seized as more than one U.B. In reality, these beams will be trusses.

Only the diagonals in the X2-X3 frames were sized. Twenty percent was added to the total weight, because the floating loading case could introduce higher stresses into these members. This has not been checked, but in the floating condition the caisson is relatively heavy at the sides (draft tubes + turbine assembly at one side, ballast at the other side). The horizontal members are replaced by the main beams in the panels.

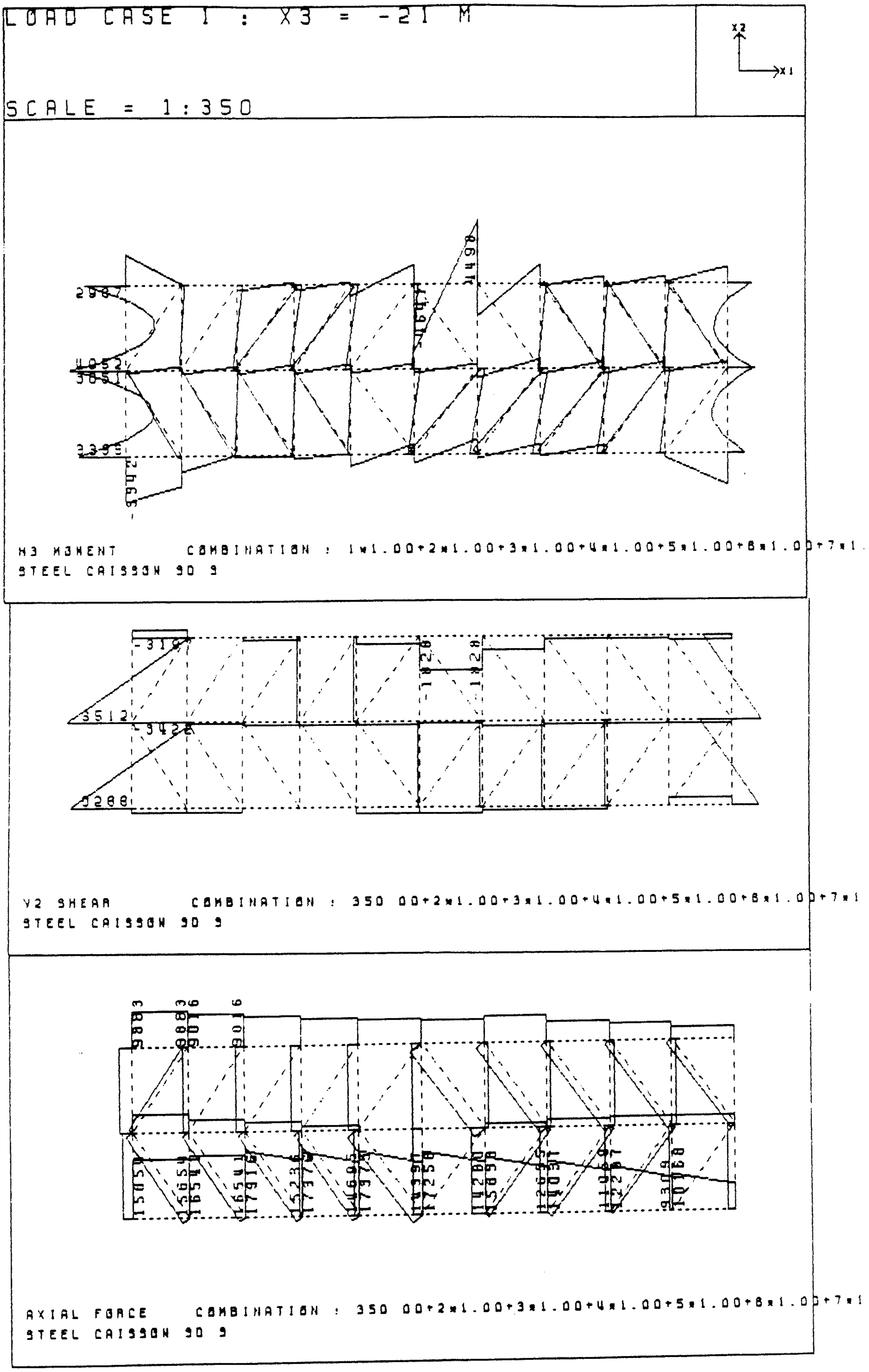

Fig 5.6 Typical Moments, Shear and Axial Force

Sluice piers and upper part of the conning towers are designed as panels, the results are listed with the other panels in Appendix 3.

In Appendix 5 all parts of the caisson are listed with their weights and centres of gravity. Table 5.1 shows the main features.

	Weight (kN)
Frame	6826
Plates	58556
Floor	78672
Venturies	5960
Sluice piers	8630
Conning towers	9480

Table 5.1 : Weights of Caisson Sections

The weight of the frame is only 4 percent of the total weight. It can be concluded that the local loadings are more important than the global ones.
For a detailed design more loading cases should be considered. This will not change the total weight of the caisson significantly, since the total frame weight is relatively small.

REFERENCE

1. Bagpus Manual
   The Steel Construction Institute, 1990

6. GLOBAL STABILITY

6.1 Introduction

The objective of this part of the study is to determine the stability of the steel caisson during its final operating stage. Innitially, the stability is considered in a 2-dimensional way. Several extreme conditions have been obtained from the hydro-dynamic studies and, additionally, wave loads have been calculated. The caisson dimensions and weight are derived from the work presented in chapter 4 and 5. Finally, 3-dimensional stability problems are discussed.

The stabilty during transport and placing is discussed in chapter 7.

6.2 Loading Cases

In respect to the global stability of the caisson several loading cases can be summarized. The loads are basically hydrostatic; the water levels are derived from the hydro-dynamic studies (1-D model). Wave heights and periods are described in section 4.2.1. The factors of safety of each loading case are calculated for 4 stability failure mechanisms: sliding, overturning, floatation and too high bearing pressures. In all cases the most excentric of the turbines is dewatered, in order to achieve a worst loading case.

The loading cases are divided into 4 categories:

1) Normal
2) Abnormal
3) Extreme
4) Temporary

SUB 1) The worst loading cases occur during a high spring tide. There are two critical phases.

1A) At the start of generation basin levels are high (+5.0 mOD), sea levels are at -2.0 mOD. A seaward wind generates internal waves in the basin with a height of 1.5 m.

1B) Three hours later (still in the generation stage) both sea and basin level are lower. The sea level has dropped to -4.0 mOD, the basin level dropped to +3.5 mOD. The head difference has thus increased. These low water levels combined with a large head difference result in high bearing pressures at the sea side of the caisson.

SUB 2) Load case **2A** and **2B** conditions are similar to the ones described above. However an accidental rapid shutdown of the turbines is included in the load cases. This causes a surge at both sides of the caisson :

- In the basin the water will still be flowing towards the barrage, which results in an elevation of the basin level near the barrage. The elevation is estimated to be 1 m.

- On the seaward side the backwater elevation due to generation will no longer exist. This results in a decrease of the sea level of 1 m (estimated).

Another abnormal situation (load case **2C**) is the power failure at high water (just before turbining) with the result that no turbining or sluicing is possible. Three hours after high water the basin surface will still be at a maximum level (+5.0 mOD) and the sea level will have dropped to -4.0 mOD.

SUB 3) This condition includes an extreme tidal flood with an occurrence of 1 : 50 years. All sluices are opened, like in a normal situation. A landward wind generates offshore waves, that despite loss of energy due to shoaling and friction, still have a significant wave height of 2.0 m (for wave height calculation, see appendix 1). The seaside water levels are +6.7 mOD. The basin levels are controled by the sluices. If it is necessary to protect the "hinterland" from flooding, it is possible to close the gates in time. The levels in the estuary would be restricted to +5.0 mOD. This situation would be a worst case for overturning. If, for any reason, the gates are not closed in time, the stability of the caisson will not be affected in a negative way. The higher basin levels will increase the f.o.s. for sliding and overturning, and the f.o.s. for floatation will be approximately the same (the increase in uplift force equals the increase of the downward force of the entrained water in the sluices).

SUB 4) During the installation of the caisson there are two critical phases. At first the caisson will be sunk by ballasting with water. At this stage, the caisson will still be moored to berthing dolphins and/or tugboats. Then hydraulic fill is added to the ballast rooms. The commissioning of the turbines requires that both tubes are dewatered. The centre of gravity of the structure will be substantially out of the geometric centre of the base, which can cause 3-dimensional stability problems. These stability problems will be discussed seperately in chapter 7.

The loading cases are summarized in Figure 6.1.

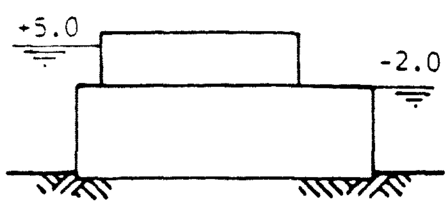

LOAD CASE 1A OPERATING CONDITION
MAX.HEAD DIFFERENCE AT START OF GENERATION

1.1m Waves on basin side
1 No draught tube or sluice passage dewatered

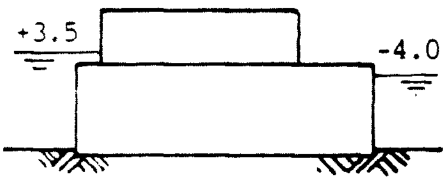

LOAD CASE 1B OPERATING CONDITION
MAX.HEAD DIFFERENCE DURING GENERATION

1.1m Waves on basin side
1 No draught tube or sluice passage dewatered

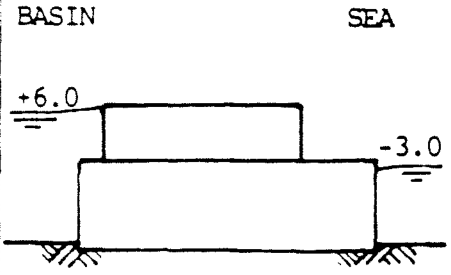

LOAD CASE 2A ABNORMAL CONDITION
ACCIDENTAL RAPID SHUTDOWN AT START OF GENERATION

1.1m Waves on basin side
1 No draught tube or sluice passage dewatered
±1m surge

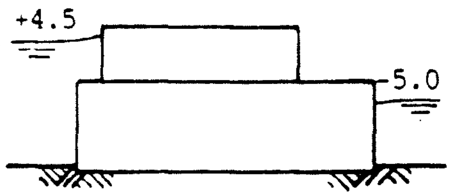

LOAD CASE 2B ABNORMAL CONDITION
ACCIDENTAL RAPID SHUTDOWN DURING GENERATION

1.1m Waves on basin side
1 No draught tube or sluice passage dewatered
±1m surge

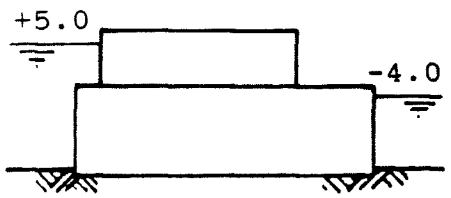

LOAD CASE 2C ABNORMAL CONDITION
POWER FAILURE

1.1m Waves on basin side
1 No draught tube or sluice passage dewatered

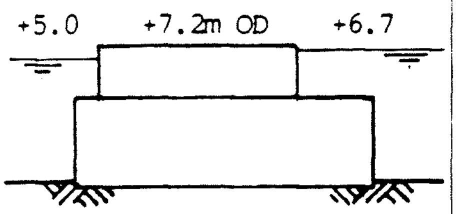

LOAD CASE 3 EXTREME CONDITION
EXTREME FLOOD

2m Waves on seaward side
1 No draught tube or sluice passage dewatered

Levels Above Ordnance Datum

WYRE BARRAGE

LOAD CASES FOR STABILITY OF TURBINE - SLUICE CAISSON FIGURE 6.1

The design values for the factors of safety during the different phases are shown in Table 6.1. The values are derived from a study to the feasibility of a tidal power scheme in the Severn Estuary.

CONDITION	FACTORS OF SAFETY (DESIGN VALUES)			
	FLOATATION	SLIDING	OVERTURNING	BEARING
NORMAL	1.4	1.7	1.4	3.0
ABNORMAL	1.2	1.3	1.2	3.0
EXTREME	1.3	1.4	1.3	3.0
TEMPORARY	1.2	1.3	1.2	3.0

Table 6.1 : Design Values for Factors of Safety

The factors of safety for bearing are explained in section 6.4.

6.3 Horizontal Loadings on Caisson

The main horizontal loadings are inflicted by hydrostatic loads, derived from the water levels from the loading cases. On top of that wave loads are calculated. Despite the fact that chances are very small that the maximum wave load acts at the same time over the whole caisson length, these loads have been taken into account for the stability calculations.

The wave loads are calculated using the Miche-Rundgren and Sainflou equations for nonbreaking wave forces. This is explained in Appendix 4.

The maximum wave height at the sea side of the barrage can be expected at a maximum sea level, e.g. an extreme flood (loading case 4). At low sea levels any serious wave will break on the tidal flats. For the other loading cases a seaward wind generating waves in the basin on top of the maximum water levels will be the worst case. However, the waves generated in the basin have a small period and therefore no significant impact on the global stability of the caisson.

The wave force calculations are in Appendix 4. Table 5.2 displays the main aspects of the wave calculations.

Wave Direction	Hi (m)	T (s)	d (m)	h0 (m)	p1 (kN/m^2)	F (kN/m)	M (kNm/m)
Landward	2.0	10	23.2	0.19	11.6	598	6306
Seaward	1.5	3.5	22.5	0.36	-	-	-

Table 6.2 : Wave Parameters

- Hi = Height of the Incoming Wave
- T = Wave Period
- d = Water Depth near Caisson
- h0 = Heigth of Clapotis Orbit Centre Above Stillwater Level
- p1 = Pressure at Sill (Hydrost. Pressure Excluded)
- F = Force due to Waves
- M = Moment around Base due to Waves

The period of the basin waves (direction seaward) is so small that the forces and moments on this side are negligible.

Another type of horizontal loading is resulting from the rockfill slopes at both sides of the caissons. It is assumed that this will result in active pressures on the high water side of the caisson and passive pressures on the low water side. This assumption is rather optimistic, since actual movement of the structure is required to develop passive pressure.

The friction force is the horizontal force under the base that avoids the caisson from sliding. This friction force depends on the weight of the caisson and the foundation material. The sill underneath the caisson is a (grouted) filter construction with a top layer of D_{50} = 0.10 m (see section 7.5). There are two failure scenarios for sliding:

1) The caisson slides over the top layer of the foundation.

2) Internal sliding of the foundation material.

SUB 1) The maximum friction force that can be developed between top layer and base is calculated by the formula:

* $F_{fr} = B * \mu$

in which : F_{fr} = friction force (kN)
B = the resultant force of the bearing (kN)
μ = friction factor

If we apply a ribbed caisson floor the friction factor (μ) will be approximately 0.5, according to Reference 1. If the caisson bottom is flat the friction factor decreases to 0.4, which may be too low to avoid the caisson from sliding.

SUB 2) The maximum friction force in the foundation layer is determined by:

* $F_{fr} = B * \tan \phi$

in which : ϕ = angle of internal friction (°)

Assuming an angle of internal friction for rubblle of 35°, then $\tan \phi$ = 0.7

From this it follows that sliding over the top layer is more likely. Therefore the maximum friction force is based on this failure scenario.

6.4 Vertical Loadings on Caisson

The uplift force is assumed to be linear, except if uplift occurs. The uplift force is assumed to remain constant as long as no positive bearing pressures are developed under the floor.

The dead load of the caisson, the weight of steel and ballast, is calculated in Appendix 5. Further vertical loads include the entrained water in the remaining draft tube and in the sluice channels.

The resultant of all vertical forces is delivered by the bearing. The foundation exists of (anti-scour) filter material, penetrated with grout. The stress on the foundation is calculated using a linear-elastic theory. This theory is valid because :

- the concrete base is relatively stiff.

- the sill will be relatively equal (D_{50} = 0.10m, see section 7.5).

An example of a stress distribution is shown in Figure 6.3. The distribution of stress is linear in both directions. The highest stress always occurs in a corner of the base.

The allowable pressure on the glacial deposits under the bottom protection material is 840 kN/m^2. The underlying mudstones are assumed to be at least as strong.

An example of loads acting on the caisson is shown in Figure 6.2.

6.5 Results

In Appendix 5 the loads are summarized for all loading cases. Table 6.3 shows the obtained safety factors.

The safety factors are obtained by using the following formulas :

- Floatation : $$n = \frac{\text{Resultant of Downward Forces}}{\text{Resultant of Upward Forces}}$$

- Overturning : $$n = \frac{\text{Resultant of Restoring Moments}}{\text{Resultant of Overturning Moments}}$$

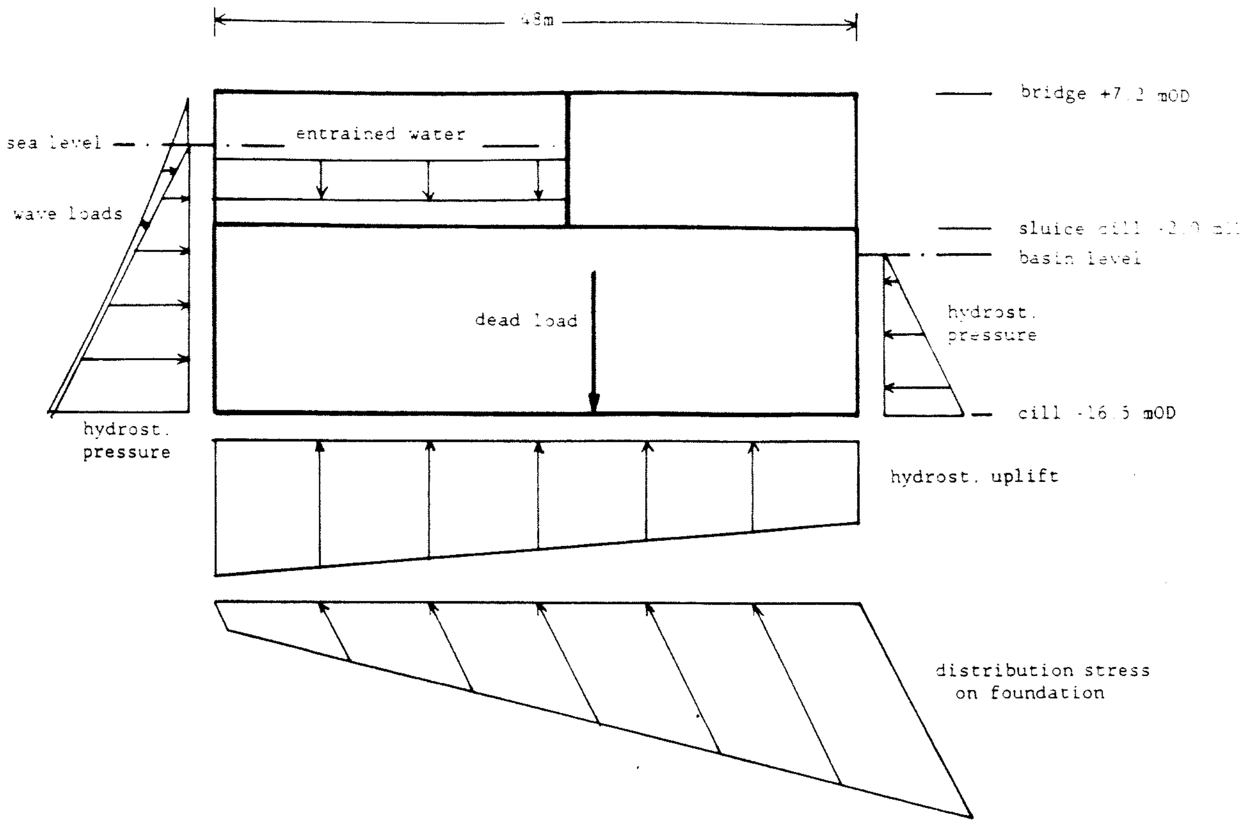

Fig 6.2 Loads and Bearing Pressures during Extreme Flood

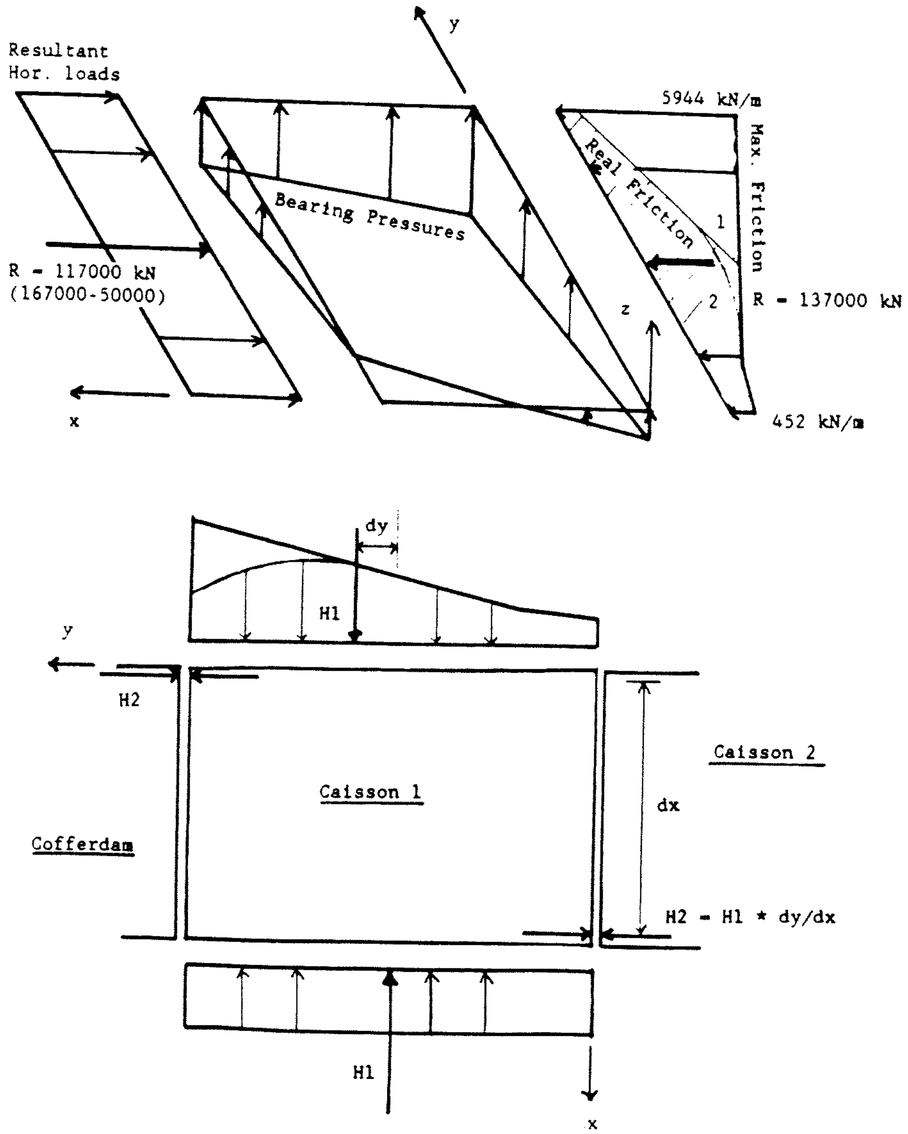

Fig 6.3 3-D Stability; Friction Distribution and Resulting Forces

$$\text{- Sliding :} \quad n = \frac{\text{Resultant of Resisting Forces}}{\text{Resultant of Driving Forces}}$$

$$\text{- Bearing :} \quad n = \frac{\text{Maximum Allowable Pressure}}{\text{Maximum Actual Pressure}}$$

LOADING CASE	OBTAINED SAFETY FACTORS			
	FLOATATION	SLIDING	OVERTURNING	BEARING
1A NORMAL	1.61	2.10	1.44	3.21
1B NORMAL	1.71	2.36	1.53	3.21
2A ABNORMAL	1.62	1.87	1.42	3.10
2B ABNORMAL	1.71	2.10	1.50	3.11
2C ABNORMAL	1.66	2.08	1.47	3.15
3 EXTREME	1.32	1.73	1.30	4.64

Table 6.3 : Obtained Factors of Safety

Comparison of Table 6.3 with Table 6.1 shows that all design values of stability factors have been met. For loading case 3 (extreme), the safety factor for overturning is equal to the design value. Therefore it can be concluded that the global dimensions of the caissson are approximately right.

6.6 3-D Stability

In the 2-dimensional stability calculations the friction was calculated as a function of the total bearing pressure under the caisson base. It was found that the total friction that could be developed was sufficient to avoid the caisson from sliding in all loading cases.

In this particular case of a non-symmetric caisson the actual problems are more complicated. Figure 6.3 shows the the bearing pressures under the base and the maximum accumulated friction along the base. The loading case is 1a (maximum head at start of generation). The bearing pressures are calculated in Appendix 5. The total of the friction that can be developed is sufficient to avoid the caisson from sliding. However, the distribution of the friction along the long side of the caisson is not uniform, and the resultant force is not in the centre of the base. There is no equilibrium of moments about the z-axis.

To avoid the caisson from turning, the resultant friction force should be in the middle of the base. Mathematically, the friction will develop as line 1, but more likely it will be as line 2. If the total driving force, i.e. the force resulting from the head difference across the barrage, exceeds the friction developed according to line 1, extra friction under the heavy side of the caisson will be developed. The resultant moves out of the centre of the base. The only forces that resist the caisson from turning result from the adjacent caisson and cofferdam. This will introduce forces in the y-direction into the caisson.

For this particular loading case the driving force is 117,000 kN. The resisting friction force according to line 1 is 137,000 kN. The safety factor against sliding is then :

$$n = \frac{\text{friction + resisting hydrost. load}}{\text{driving hydrost. load}} = \frac{137000 + 50000}{167000} = 1.12$$

This is lower than the required safety factor, which is 1.7. If the friction develops as line 2 the safety factor may even drop below 1.0, which will result in the effects that are described above.

To avoid these problems the lay-out of the caissons should be reconsidered. If the caisson were shaped more symmetrically (e.g. alternative 3A in section 4.6) the centre of gravity would be more in the centre of the base. Consequently, the 3-D stability problems would not occur. Alternatively, concrete ballast could be used instead of sand near the turbines, so that this side of the caisson would become heavier. Otherwise, the extra forces in y-direction should be accepted and the design should be adjusted to these forces.

REFERENCE

1. The Closure of Tidal Basins
Design and Operations of Closure Works
J.C. Huis in 't Veld
Delft University Press, 1987.

7. TRANSPORT AND PLACING

7.1 Introduction

In this chapter the transport and placing of the caissons in the mouth of the Wyre estuary will be discussed. This is a very important issue, since approximately 80% of the cost of the total project is represented by the caissons. The outcome of any major accident would be fatal for the entire project.

The following issues are described in this chapter :

- The construction sequence of the barrage.
- The stabilty, draft and flow resistance of the caissons during the transport.
- The placing actions and sinking of the caissons.
- The velocities in the closure gap.
- The bed protection and the connection between caisson and sill, and between the caissons and cofferdams.

In this preliminary phase of this project, the placing was represented by a computer model. In further stages, the use of real model tests will be necessary.

The discussion includes both the steel and the concrete caisson. Data of the concrete caisson, such as weights and centres of gravity, have been obtained from studies carried out by T.H.T.

7.2 Construction Sequence

The barrage installation sequence is displayed in Figure 7.1. The placing of the caissons will take place when all other works have been completed. The caissons will be constructed in a dock in Liverpool, 50 miles south of Fleetwood . From there, the caissons are towed to a dredged area immediately north of the barrage.

7.3 Transport

If we assume a transport speed of 2 m/s, then the duration of the sailing from Liverpool to Fleetwood is about 11 hours. This is well within the weather forecast period.

WYRE ESTUARY – FEASIBILITY STUDY FOR TIDAL POWER

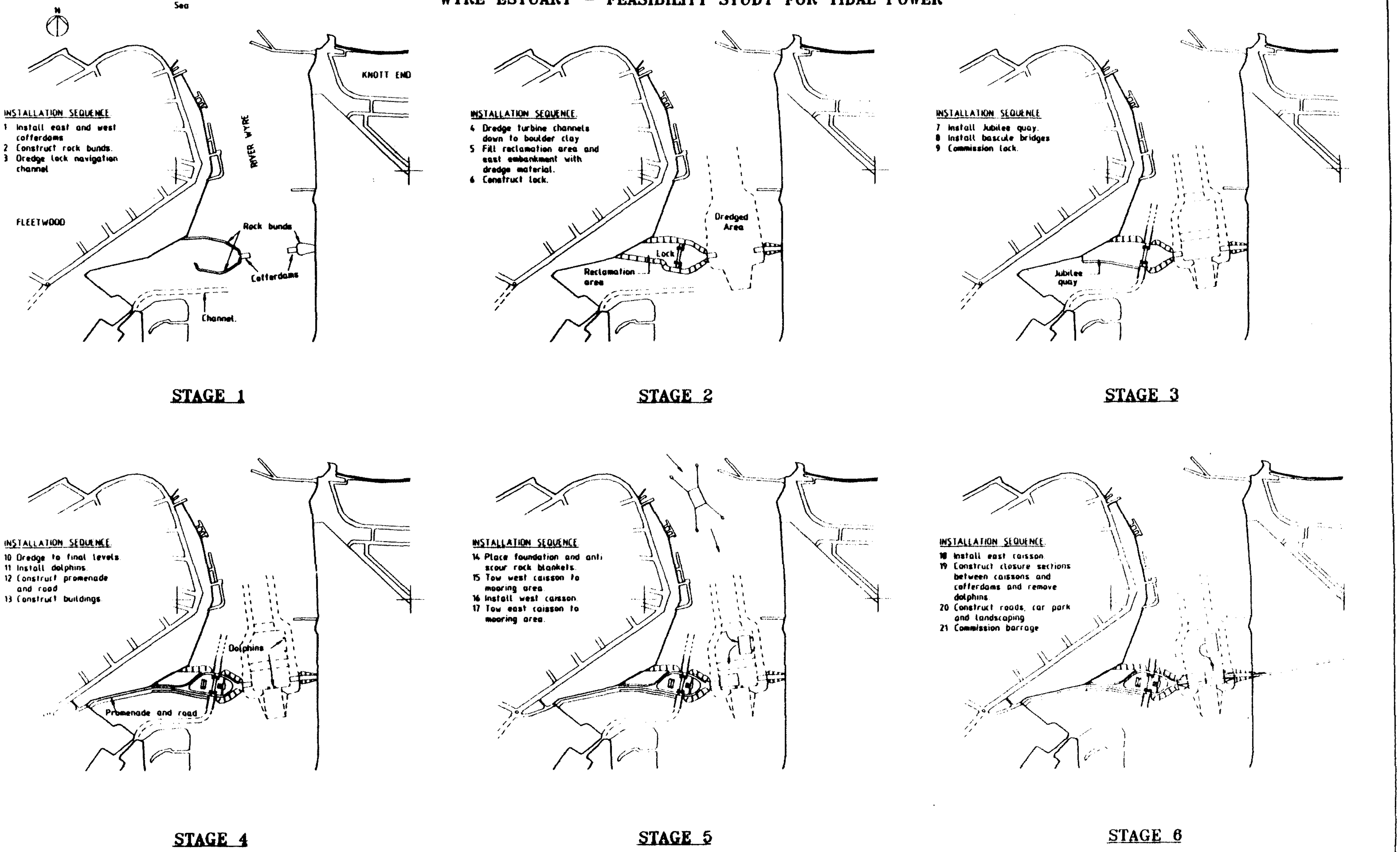

Fig 7.1

TH TECHNOLOGY LTD

IN ASSOCIATION WITH

BINNIE & PARTNERS

BARRAGE INSTALLATION SEQUENCE

DRAWING No. 211

The main aspects of the navigation of the caissons are :

1) Draft
2) Stability
3) Manoeuvrability
4) Flow Resistance

SUB 1) The draft of the caisson and the available depth of the waterway determine the window in which the sailing takes place.

The draft of the steel and concrete caissons is respectively 6m and 10m. The steel caisson draft is calculated in Appendix 5. The draft of the concrete caisson is obtained from calculations carried out by T.H.T. The highest bedlevel on the way between Fleetwood and Liverpool is -18 mOD, so the available depth is adequate at all times. The dredged channel in front the Wyre is maintained at a level of -9.4 mOD over a length of 3150 m. Assuming a keel clearance of 2m, the minimum sea level and available time is given in Table 7.1.

		Steel	Concrete
Draft (m)		6.0	10.0
Min. Sea Level (mOD)		-1.4	+2.6
Tide	Range (m)	Time Available (mins)	
Neap	4.4	582	-
Mean	6.7	487	211
Spring	8.2	474	231

Table 7.1 : Time Available in Low Water Channel

Assuming the speed in the channel is 1.5 m/s (this is approximately the speed used for the caissons of the Brouwershavensche Gat, Reference 1), the duration of the sailing in the channel is only 35 mins, so no real problems should occur here.

SUB 2) The weights and centres of gravity of the various parts of the steel caisson are displayed in Appendix 5. In the unballasted situation the caisson is relatively heavy at the side where the turbines are located. The centre of gravity of the caisson is not at the same location as the centre of uplift forces, i.e. in the centre of the caisson bottom. In order to get the caisson level during transport, it is ballasted in two cells at the opposite side (see Figure 7.2).

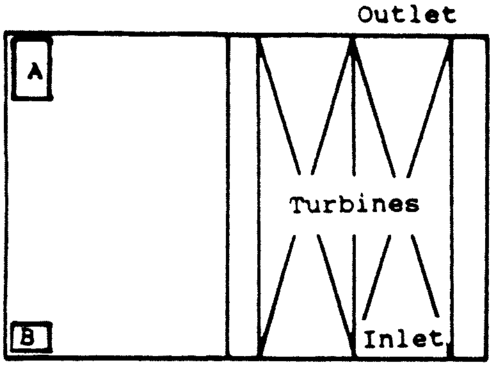

Cell A : 6.5 * 10.0 * 12.5 m^3 : 69% full
Cell B : 6.5 * 4.25 * 12.5 m^3 : 98% full

Fig 7.2 Plan of Caisson during Transport

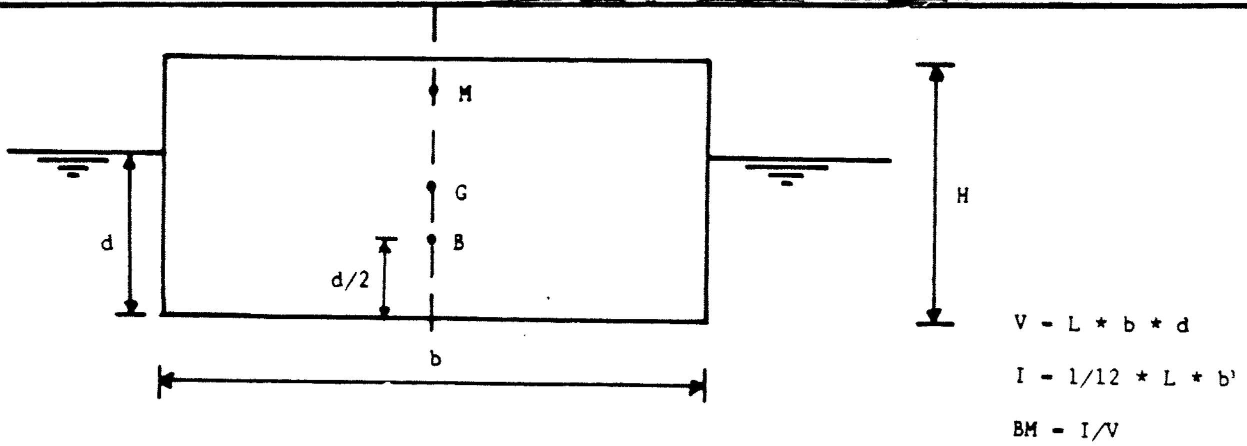

Fig 7.3 Pressure and Centre Points

Stability is assured if the metacentric height is positive, i.e. M is above G (see figure 7.2).

Another important issue concerning the stabilty of the caisson during transport is the dynamic stability. The natural frequency of the caisson is :

$$\omega_e = \frac{\pi \sqrt{MG}}{K_{\phi\phi}}$$

in which :

MG	=	Metacentric Height (m)
$K_{\phi\phi}$	=	Transverse Inertia Radius (m)
	≈	0.5 * Caisson Width

If the caisson meets a wave with a frequency equal to its natural frequency, the response movement of the caisson can be very large, even many times larger than the wave amplitude. Therefore it is necessary that the natural period of the caisson ($T_e = 2\pi/\omega_e$) is substantially larger than the largest suspected wave period (T_w).

Table 7.2 gives the main parameters of the floating caissons.

CAISSON PARAMETERS	STEEL	CONCRETE
Floating Draft, m	5.9	10.1
Submerged Volume, m^3	21031	36118
Moment of Inertia Ixx, m^4	686592	686592
Height of Centre of Buoyancy above Base, m	2.9	5.0
Heigth of Centre of Gravity above Base, m	5.6	9.6
Height of Metacentre above Buoyancy Centre, m	35.6	19.0
Metacentric Height, m	30.0	14.4
Natural Frequency, 1/s	0.72	0.50
Natural Period, s	8.8	12.6

Table 7.2 : Stability and Draft Parameters

It can be concluded that the metacentric height of both caissons are positive. However, the metacentric height of the steel caisson is so large that its natural period is relatively low. At this stage, no data of the wave spectrum in the Irish Sea have been obtained yet. Therefore it is not possible to say if this period is large enough. But since the total sailing will only take about 11 hours, it is assumed that transport safe at calm weather.

SUB 3) From a nautical point of view it is advantageous for the relationship between the width and the length of the caisson to be 1 : 3 or 1 : 4. In this case, the ratio is 1 : 1.5. This is because the width is determined by the lentgh of the turbine. A 1 : 3 ratio would result in one caisson with a length of 150m, which would cause problems with the placing.

SUB 4) The flow resistance is given by :

$$F = 1/2 * C_d * p * g * v^2 * A$$

in which :

F = Drag Force (N)
C_d = Drag Coefficient (-)
p = Density of Water (kg/m^3)
g = Acceleration of Gravity (m/s^2)
v = Velocity relatively to Water (m/s)
A = Area of the Water Plane Perpendicular to the Flow Direction (m^2)

A drag coefficient is obtained from model tests on the Oosterschelde caisson (width = 55m, length = 75m, Reference 1). For a depth of 15m (L.W. spring tide) the following values have been derived :

- Steel caisson : C_d = 1.1
- Concrete caisson : C_d = 1.2

The drag force to be delivered by the tugs for a speed of 2 m/s is then :

- Steel caisson : F = 640 kN
- Concrete caisson : F = 1164 kN

7.4 Placing of Caisson

7.4.1 General

The final closure begins when the whole barrage except the caisson part is completed. The remaining gap between the two cofferdams is 150 m wide. In this stage the velocities are not significantly higher than in the pre-construction situation. A possible sequence of closure would be as follows.

The first caisson is sailed into the mooring area, north of the barrage. Once arrived it is towed to the temporary dolphins. Depending on the chosen tide, it stays moored until just before slack water. Then the caisson is sailed to the required position and turned into the gap. Finally the caisson is sunk down to sill level by pumping water into the ballast areas, while kept in position by mooring dolphins and/or whinches. Alternatively, valves in the floor could be used to sink the caisson. The ballast area is divided into several sections so that the stability of the caisson during the sinking can be controlled.

The gaps between caisson floor and bottom are penetrated with grout, to avoid piping and highly unequal bottom support on the caisson floor. Skirts on all sides of the caisson avoid the grout from flowing away. Finally the ballast chambers are filled with sand.

This leaves a 75 m wide gap between the estuary and the sea. In order to decrease the velocities in this gap, the sluice gates of the first caisson are opened.

Once the first caisson is in place, the second caisson is sailed into the dredged area and moored to the dolphins. It would be advantageous to place the second caisson immediately after the first one on the next neap tide. The use of this scenario would assure that the gap velocities remain low. However, any serious delay of the placing actions could result in a failure of the sill. Therefore it is decided to place the second caisson on a neap tide after the sequence of following spring tides. At this time, the caisson is sailed into the gap. Tugboats at both sides of the caisson keep the caisson into position. By mooring to winches or dolphins the positioning should be assured. The caisson is sunk, grouted and filled with ballast.

Placing and mooring operations demand low current velocities and can therefore only be carried out safely during Slack Water periods.

While the caisson is sailed into position and sunk onto the sill, the remaining gap decreases. This affects the basin levels and gap velocities. The total duration of these actions should be reduced to a minimum so that the head difference between sea and basin remain low and thus the velocities under the caisson acceptable.

Once the caisson is sunk, the following actions need to be undertaken :

* Opening of the sluice gates

* Partially filling of the ballast area. The amount of ballast is determined by the requirements that :

  - the temporary safety factors of stability have to be met

  - the load on the caisson floor may not be too high because the sill has not yet been equalised by grouting yet

* Grouting of the space between sill and caisson floor in order to

  - avoid piping and washing out of bed protection material

  - obtain a more uniform bottom support

* Closing of the gaps between the two caissons and between caisson and cofferdam (see Figure 7.11).

* Filling of the remaining ballast areas

The velocities during and immediately after the placing actions have been calculated using a computer model, which is described in the next section.

7.4.2 Model Description

In order to estimate the velocities in the gap and the head differences over the barrage a spreadsheet model has been developed. The barrage is represented by the remaining gap between the first caisson and the cofferdam with the sea and the estuary on either side.

* For simplicity it is assumed that the sea level follows a sinusoidal tidal cycle.

* The discharge is determined by

  - the cross sectional area of the gap (see Figure 7.7)
  - the head difference between sea and basin
  - the friction losses in the gap (see Figure 7.4)
  - inlet and outlet losses.

* The basin level depends on the discharge through the gap and the surface area of the estuary (see Figure 7.6).

Losses at the outlet were taken as $V^2/2g$: since the estuary is regarded as a basin with zero velocity, all velocity head is lost at the outlet. Inlet losses were taken as Ks * $V^2/2g$ with Ks varying between 0.3 and 0.5, depending on the area of the gap (see Figure 7.5, from Reference 3).

Other losses (inertia) were neglected after they were proved to be small (see Appendix 6). They resulting equation for discharge through the gap is:

* $$Q = A * \left(\frac{2gL}{C^2R} + 1 + Ks \right)^{-1/2} * \sqrt{(2g*dH)}$$

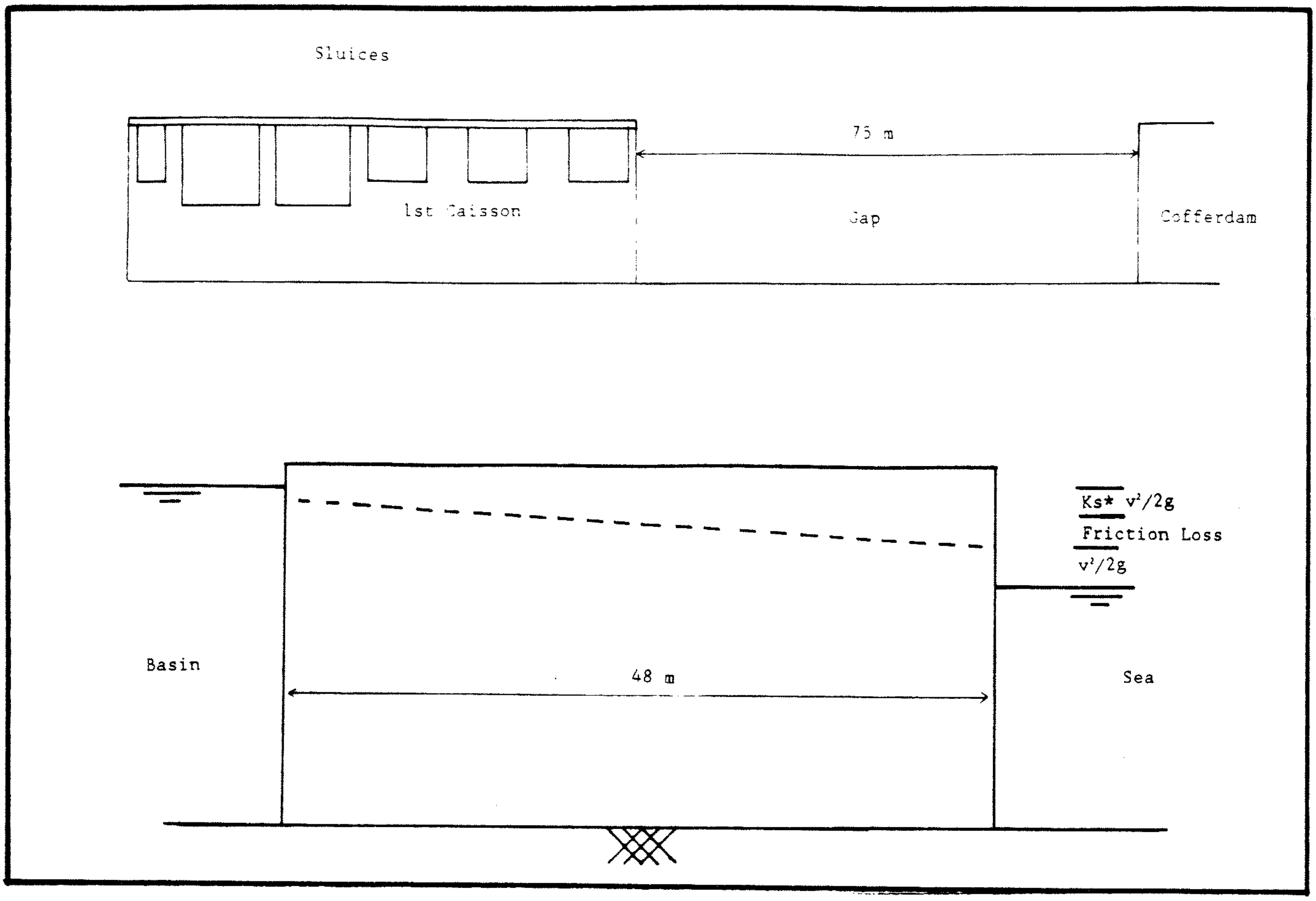

Fig 7.4 Head Losses in Gap

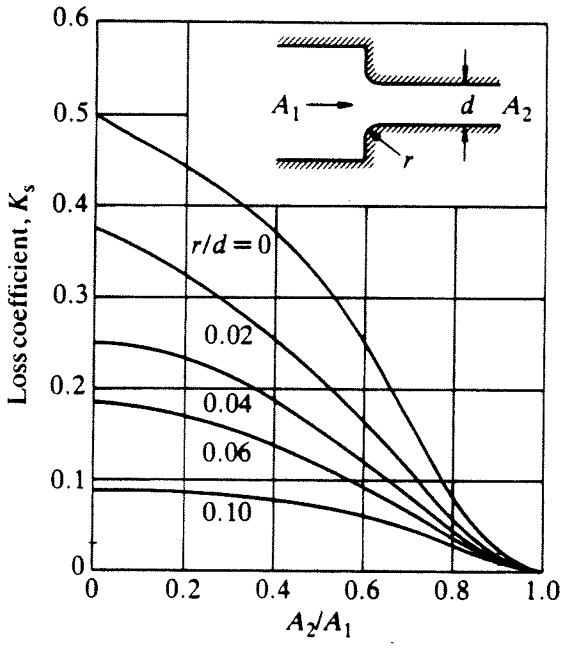

Fig 7.5 Inlet Loss Coefficients

Surface Area

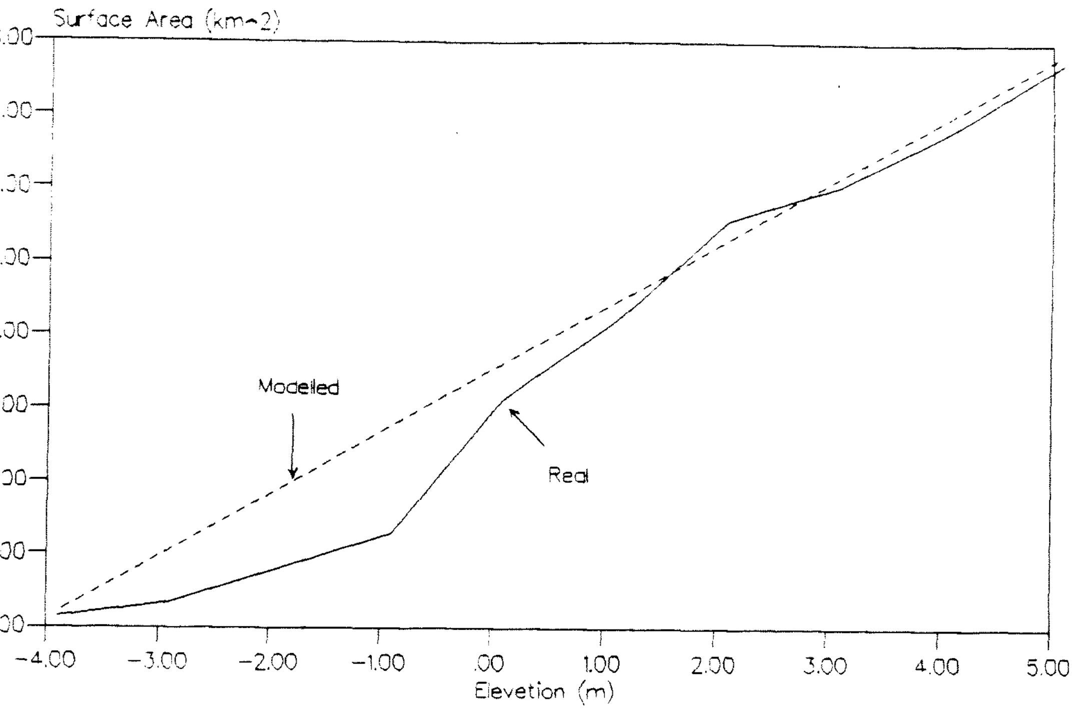

Fig 7.6

Cross Area of Gap (m~2)

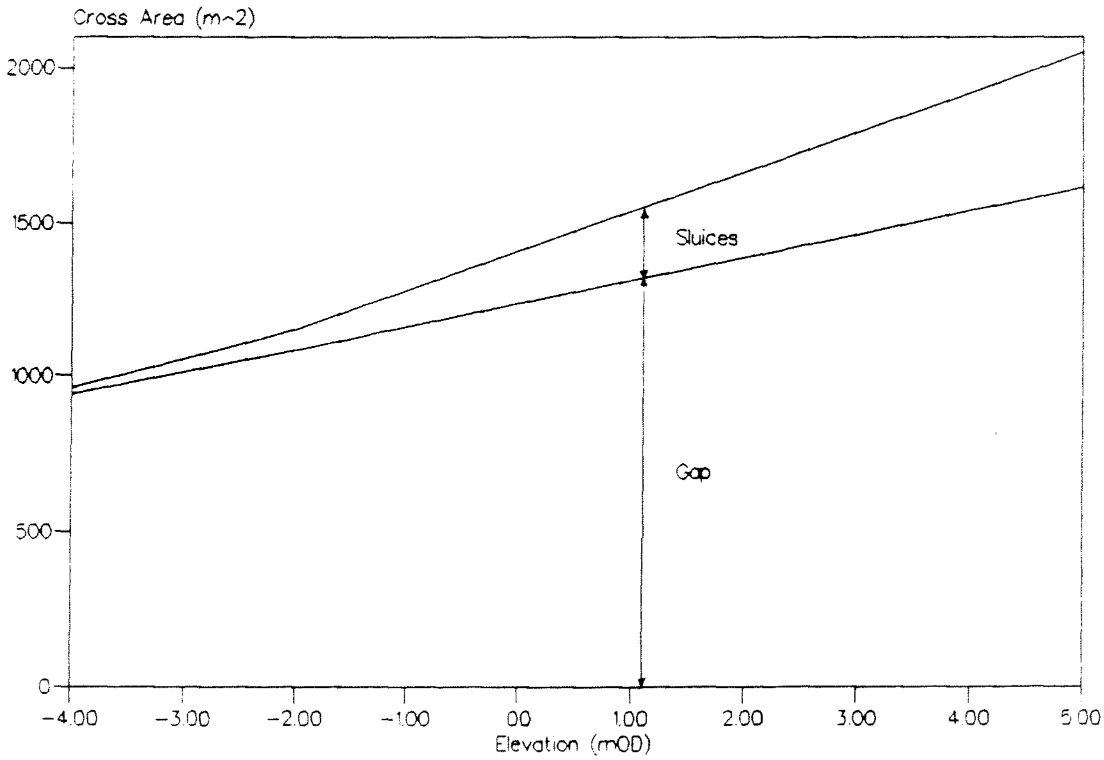

Fig 7.7

with :	Q	=	Discharge through Gap (m^3/s)
	A	=	Flow Area of Gap (m^2)
	g	=	Acceleration of Gravity (m/s^2)
	L	=	Length of Gap (m)
	C	=	Chezy Coefficient ($m^{1/2}/s$)
	R	=	Hydraulic Radius (m)
	Ks	=	Inlet Loss Coefficient (-)
	dH	=	Head Difference across Barrage (m)

7.4.3 Friction in Gap and Sluices

It is assumed that the friction in the gap is dominated by the bed protection material rather than to the concrete or steel side walls. This is justified by examining the equivalent sand roughness of the materials according to Nikuradse (k). For the bed protection this is approximately the same as the diameter of the stones, say 0.3m. The k-value for concrete and steel is respectively 10^{-3} and 10^{-4} m.

The applicable Chezy formula depends on wether the situation is hydraulicly smooth or rough.

If we make the following assumptions for the gap :

* Velocity :	V	= 2m/s
* Basin Level :	Hb	= +1.0 mOD, so d = 17.5m (depth above sill)
* Chezy factor :	C	= 50 $m^{1/2}/s$
* Viscosity :	v	= $1.0*10^{-6}$

Since the stones are only present on the bottom (and not on the sides) the value of the hydraulic radius (R) is taken equal to the depth.

* Hydraulic Radius : R = d = 17.5m

* Slope of Friction : $i_f = V^2/C^2R = 9.1*10^{-5}$

* Thickness of Laminar Sublayer :

$$\delta = 11.6 * \frac{v}{\sqrt{(gRi_f)}} = 3.2*10^{-4}$$

The condition for hydraulic roughness is :

* $k/4 > \delta$

This is the case. An applicable formula for this situation is Strickler's :

* $C = 25 * (R/k)^{1/6}$ $(m^{1/2}/s)$

For the sluices the k-value for both the steel and the concrete caisson is taken as 10^{-3} m. If we take one of the 9m wide sluices with a sill level of -2.0 mOD and make the following assumptions :

* $V = 2$ m/s

* Hbasin = +1.0 mOD : d = 3m

* $C = 80\ m^{1/2}/s$

* $R = 9*3/(2*3+9) = 1.8m$

* $i_f = V^2/C^2R = 3.5*10^{-4}$

* $\delta = 11.6 \frac{v}{\sqrt{(gRiw)}} = 1.5*10^{-4} < k/4 = 2.5*10^{-4}$

Thus Strickler's formula may be applied for the sluices as well.

7.4.4 One Caisson in Place

Figure 7.8 shows the velocities in the gap during a tidal cycle. The tidal range is 8.2 m, which is the mean spring tidal range. The graph shows the effect of opening of the sluices. Since the sill level of most of the sluices is at -2.0 mOD, the velocities at low water levels are not affected. At higher levels the reduction of the velocities is significant. Figure 7.9 shows the results during a neap tide.

Because the surface area at low water is relatively low, the L.W. slack period is considerably longer than the H.W. slack period. Table 7.3 summarises the maximum velocities and the slack water periods. In this context the slack water period is somewhat arbitrarily defined as the time in which the velocity is lower than 0.5 m/s.

	Slack Water Period (mins)		Maximum Velocity (m/s)	
Tide	H.W.	L.W.	Sluices incl.	Sluices excl.
Neap	140	229	0.8	1.0
Spring	50	187	1.6	2.0

Table 7.3 : Slack Water Periods and Max. Velocities

The maximum velocity can be calculated for every possible tidal range. This results in a relationship between the tidal range and the maximum velocity (see Figure 7.10).

7.4.5 Placing of second Caisson

In Figure 7.12 the action sequence for the placing of the second caisson is displayed. The estimated times are derived from the closure of the Brouwershavense Gat in the Netherlands (Reference 1). The caissons involved were sluice caissons and were 68m long, 18m wide and 16.2m high. The last gap was large enough to be able to turn the caisson into position, rotating it about one corner. Because the Wyre caissons are so much wider this is not possible for the last Wyre caisson.

Therefore the following sequence is suggested:

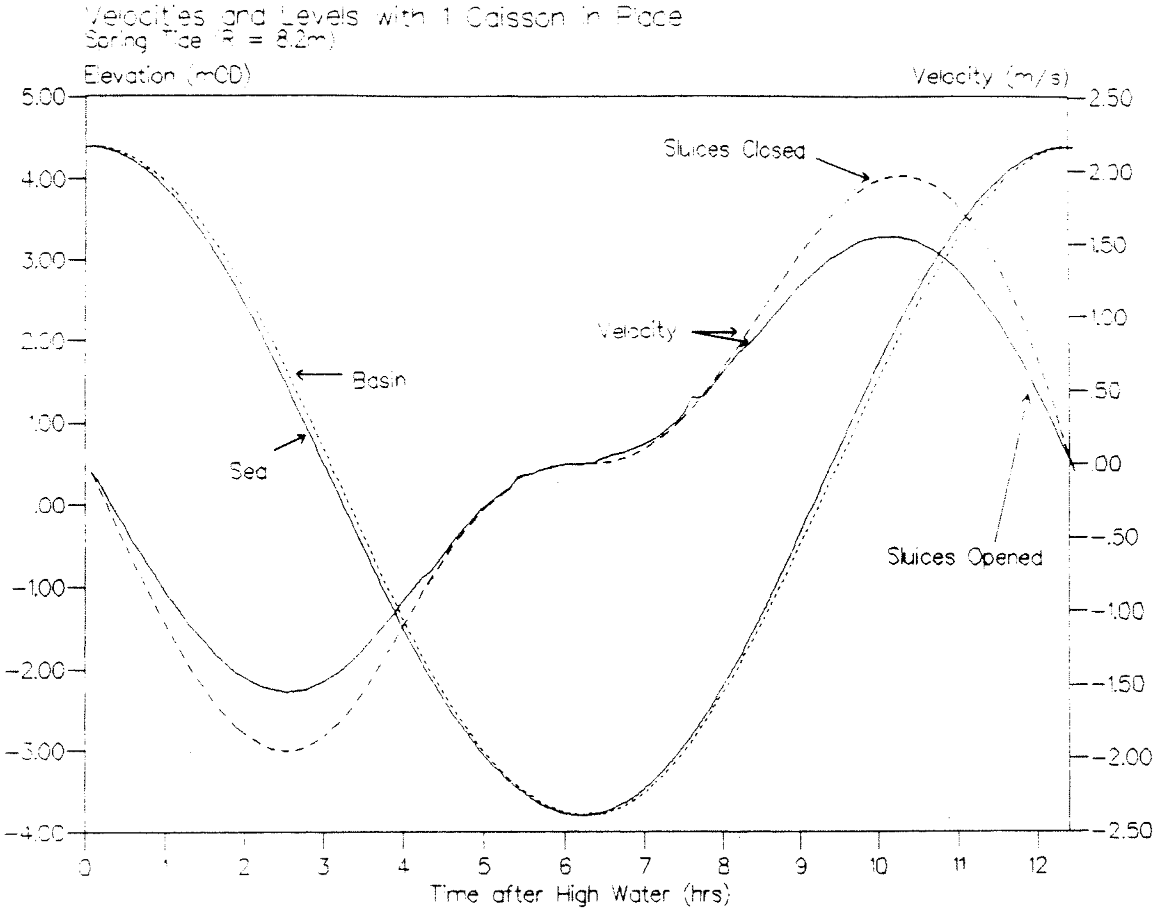

Velocities and Levels with 1 Caisson in Place
Spring Tide (R = 8.2m)
Elevation (mCD)
Velocity (m/s)
Sluices Closed
Velocity
Basin
Sea
Sluices Opened
Time after High Water (hrs)

Fig 7.8

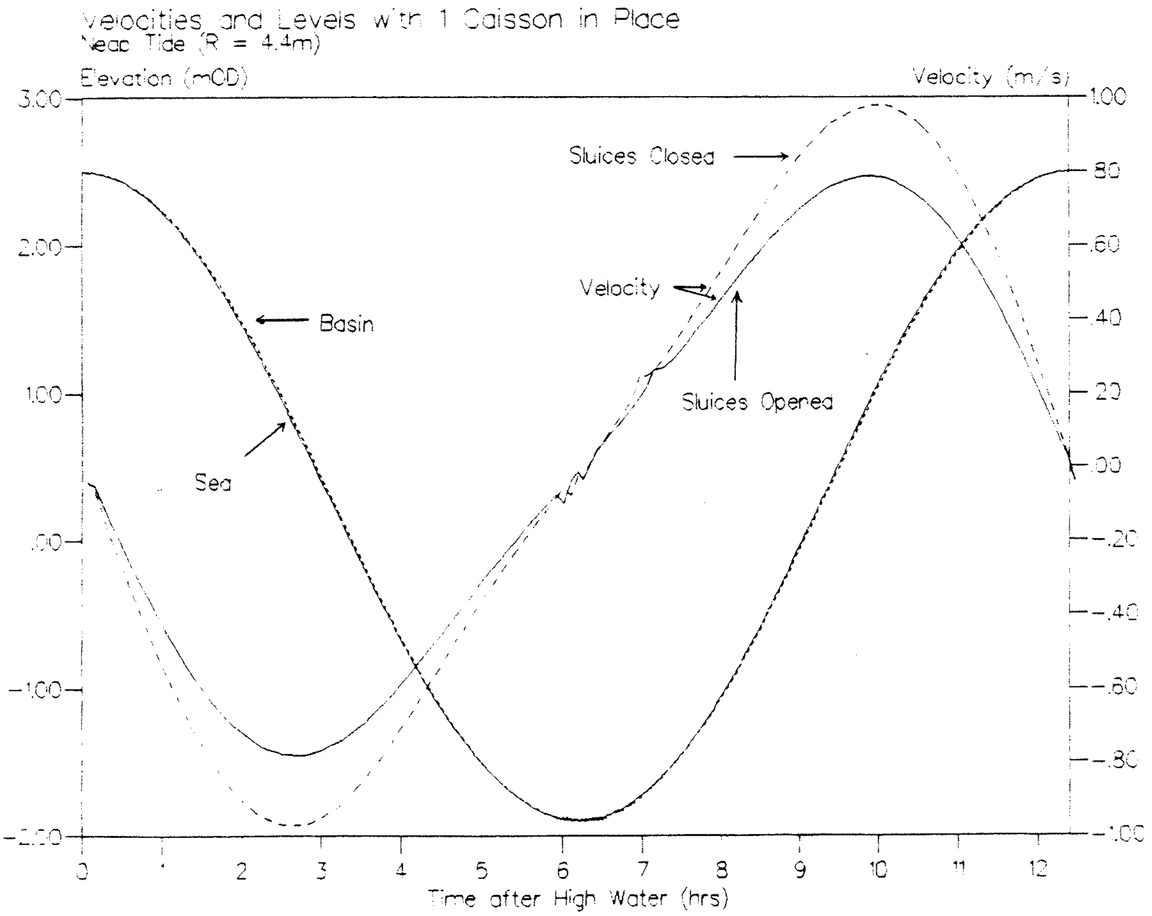

Velocities and Levels with 1 Caisson in Place
Neap Tide (R = 4.4m)
Elevation (mCD)
Velocity (m/s)
Sluices Closed
Velocity
Basin
Sluices Opened
Sea
Time after High Water (hrs)

Fig 7.9

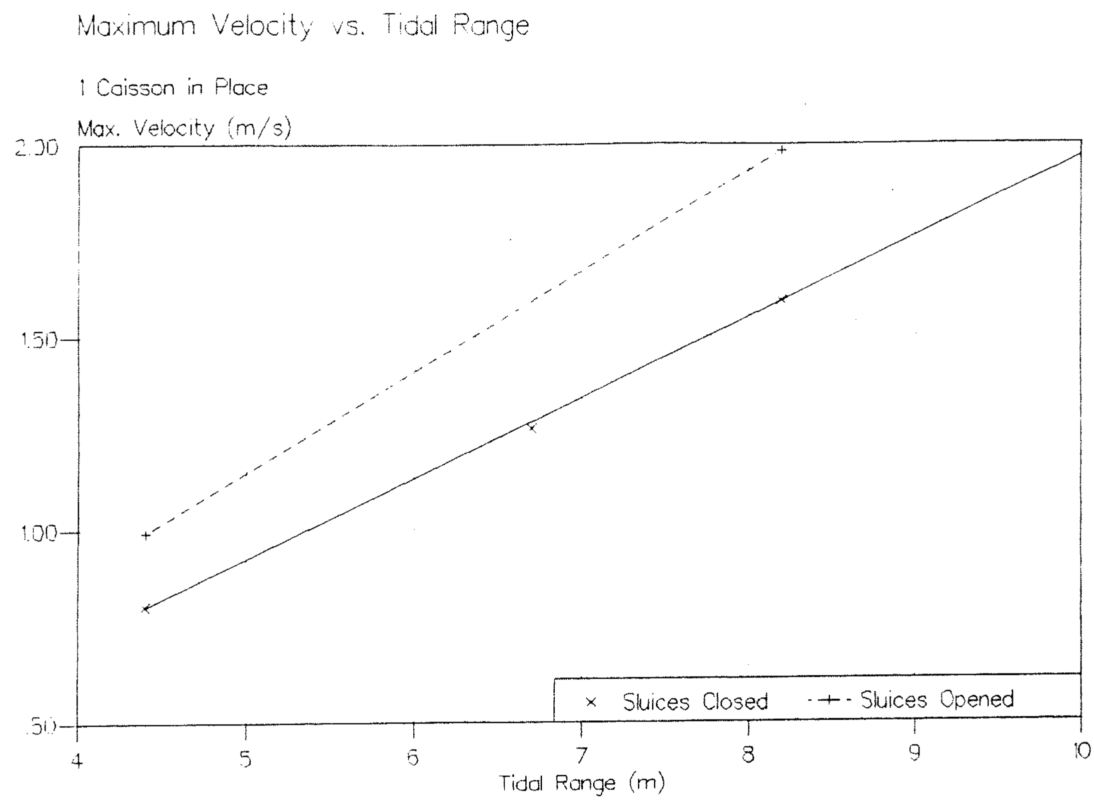

Fig 7.10

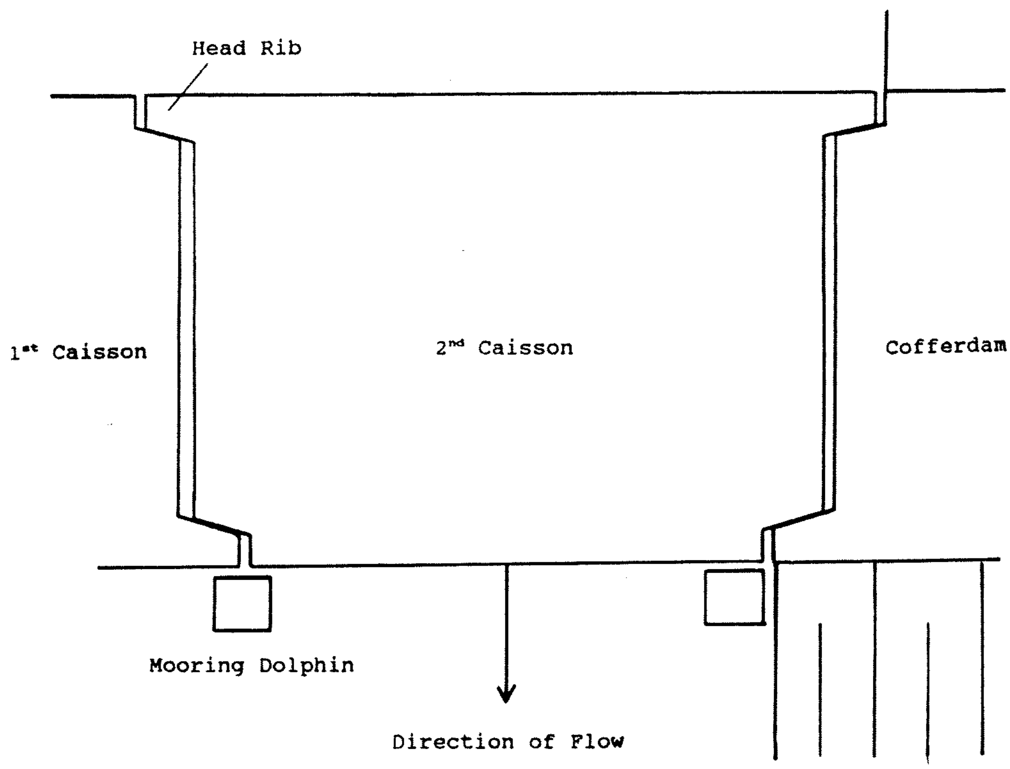

Fig 7.11 Plan of Caisson showing Head Ribs

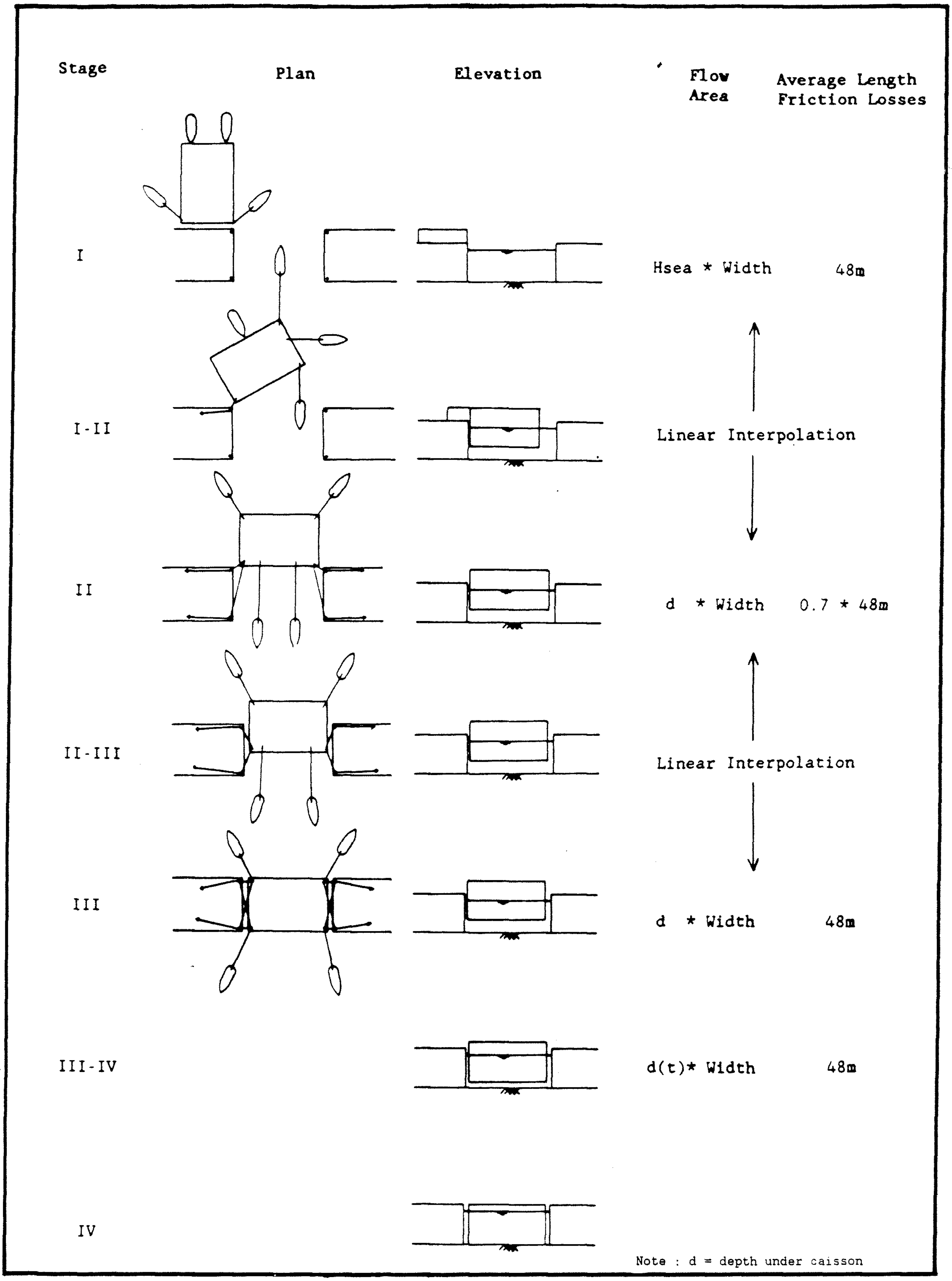

Fig 7.12 Placing Actions

- The caisson is sailed towards the first caisson, and tied into position with one corner to a corner of the first caisson (stage I).

- Tugboats turn the caisson to a position in front of the gap (stage II), both caisson corners are tied to the adjacent caisson and cofferdam.

- The caisson is manoeuvred onto the correct place (stage III).

- The caisson is sunk onto the sill, while tugboats control its position. If more safety is required during the sinking, the use of mooring dolphins, installed at the basin side, could be a solution.

The actions and the assumptions for the hydraulic variables during the stages are displayed in Figure 7.12. In stage I the cross sectional area equals the water depth times the width of the gap. In stage II it is assumed that the friction losses will occur under the caisson : the flow area is the width times the depth under the caisson. The average length of the flow under the caisson is assumed to be 0.7 * 48m, because the water will also flow to the sides of the caisson. In stage III the flow area is the depth under the caisson times the width, and the length of the friction losses is 48m. In the intermediate stages the parameters are unknown, so they are linear interpolated.

The duration of these actions depends on the water level and the depth under the caisson.

Figure 7.11 shows the second caisson floating above the sill. At the corners of the caissons and the cofferdam head ribs are attached. The functions of these head ribs are :

- To close the gaps between the caissons.

- To assure the position of the second caisson during the placing actions. The tugboats pull the caisson against the ribs. If the resulting force on the first caisson or cofferdam would be too large, it is suggested to apply mooring dolphins along the basin side of the barrage.

After the caisson is sunk onto the sill the intermediate gaps are filled with rubble and grout.

The preference for floating in against the tide and at Slack Water leaves two alternatives for starting the operations :

1) Starting at High Water
2) Starting just before Low Water

SUB 1) This alternative is favourable if the water depth above the sill is to small to drag the caisson into the gap. This may be the case for the concrete caisson. An advantage is that the sluice area at High Water is larger than at Low Water. Another possible advantage is that in case of delays the floating-in action still occurs against the current.

SUB 2) The sinking time is reduced because the depth above the sill is smaller. This is important because a longer sinking time results in an increase of the velocities under the caisson. Another advantage is that the Low Water Slack is longer than the High Water Slack (see Figure 7.8 and 7.9). This means a longer possible operation time.

Naturally the tidal range at the moment of action is an important factor. The feasibility of these scenarios depends on :

1) the current velocities
2) the drag forces on the caisson

SUB 1) The actions of mooring the caisson require a velocity of about 0.5 m/s (max. 0.75 m/s) above the sill. These maximum current elcities are recommended in Reference 1. Furthermore the velocity is an important factor concerning stone sizing of the bed protection material.

SUB 2) The drag force may not exceed the maximum possible force delivered by the tugboats.

The velocities and water levels are modelled by making certain assumptions about the hydraulic parameters (see Figure 7.12). Four placing scenarios have been modelled :

1) Concrete Caisson :

a) Neap Tide, Low Water Slack (Fig. 7.13a)
Keel Clearance = 4.6m

b) Neap Tide, High Water Slack (Fig. 7.13b)
Keel Clearance = 9.0m

2) Steel Caisson :

a) Neap Tide, Low Water Slack (Fig. 7.14a)
Keel Clearance = 8.6m

b) Spring Tide, Low Water Slack (Fig. 7.14b)
Keel Clearance = 6.7m

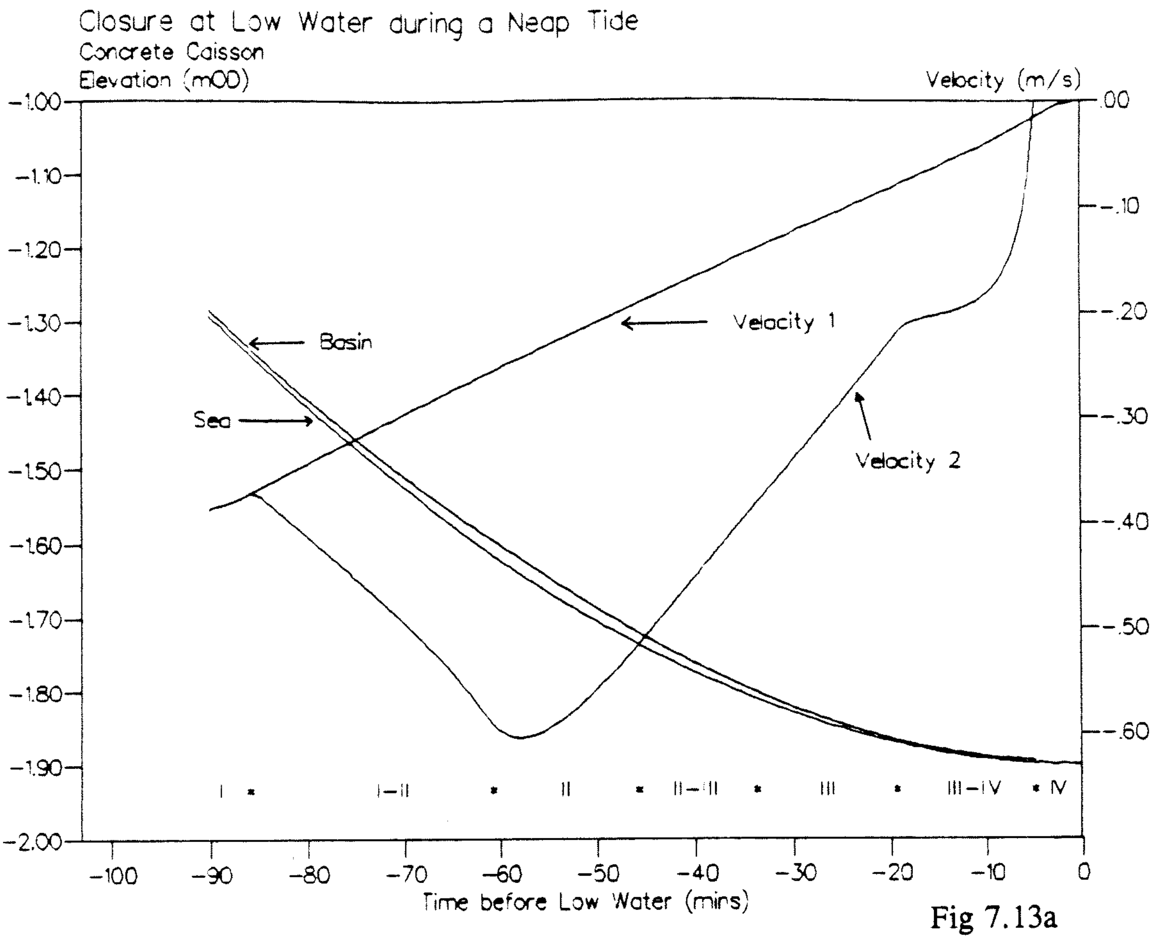

Fig 7.13a

Velocity 1 = Current Velocity before Placing
Velocity 2 = Current Velocity under Influence of Placing Actions

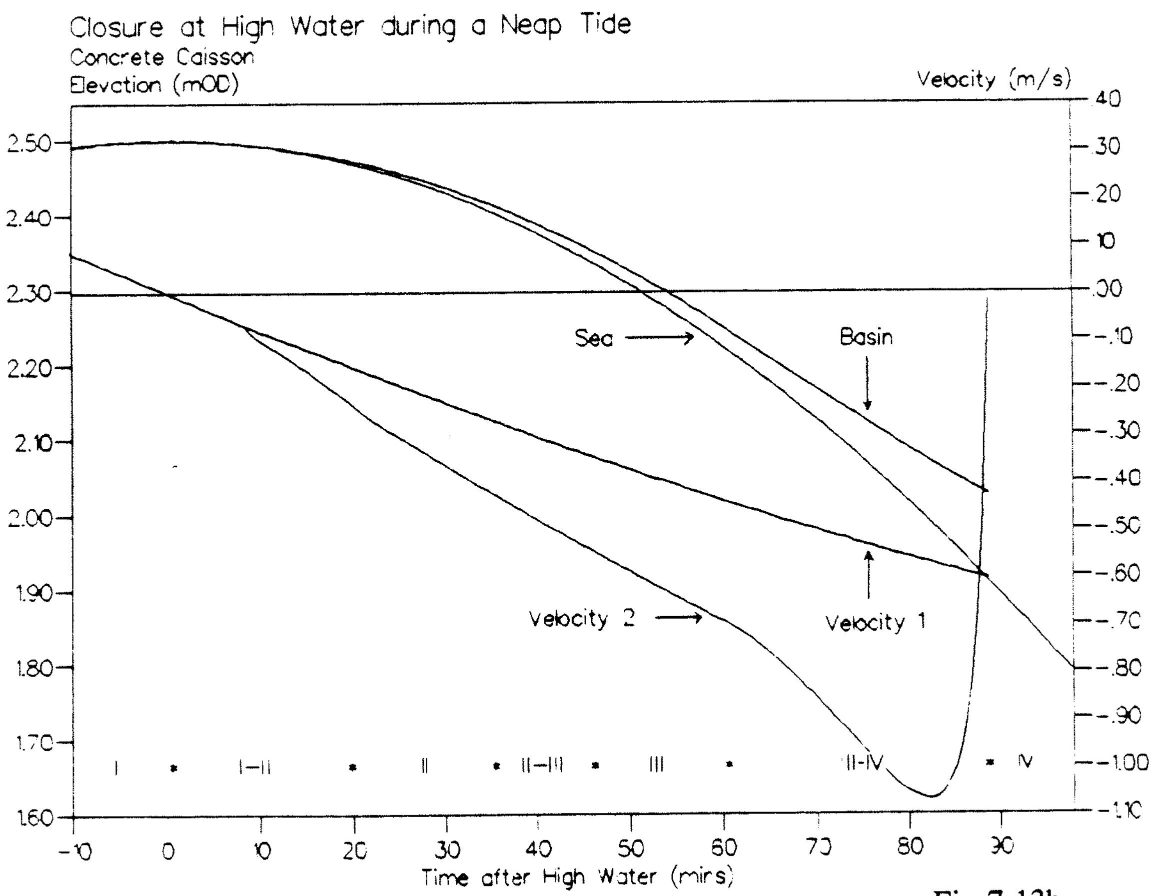

Fig 7.13b

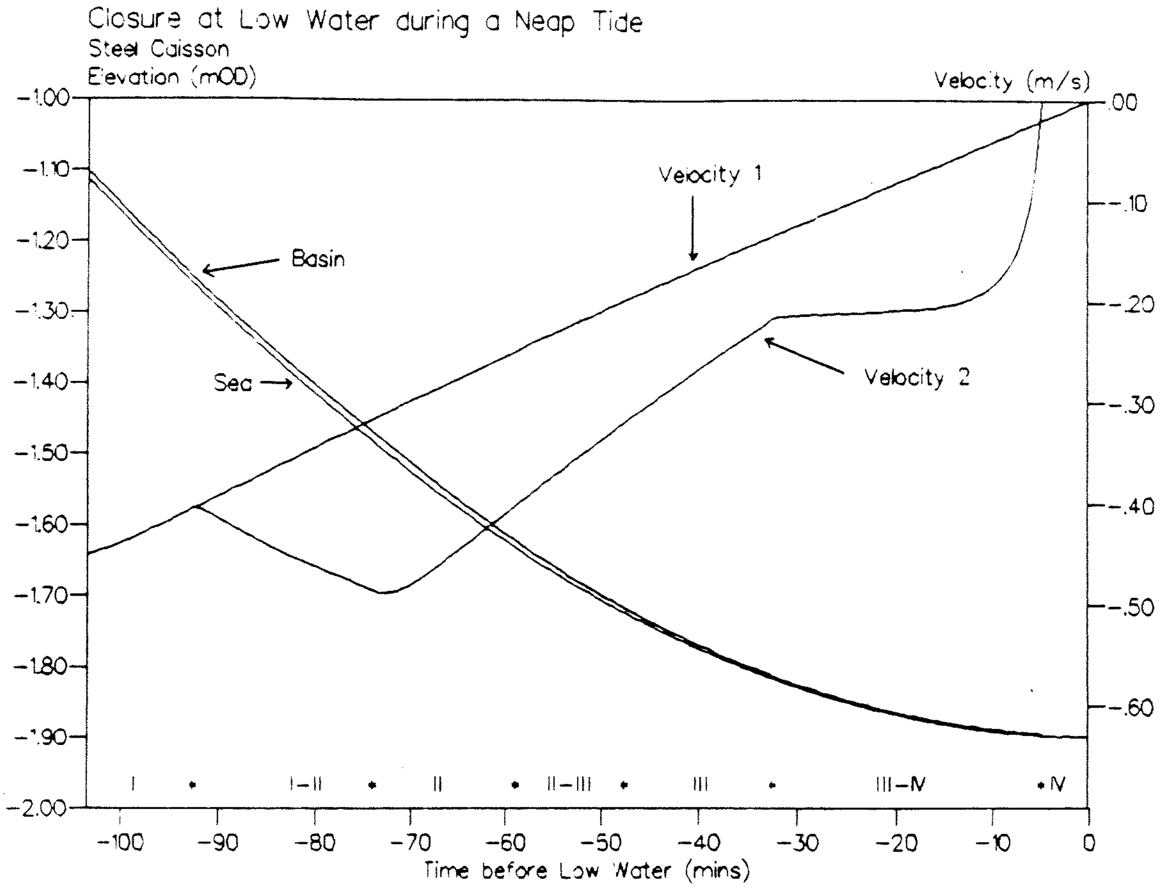

Fig 7.14a

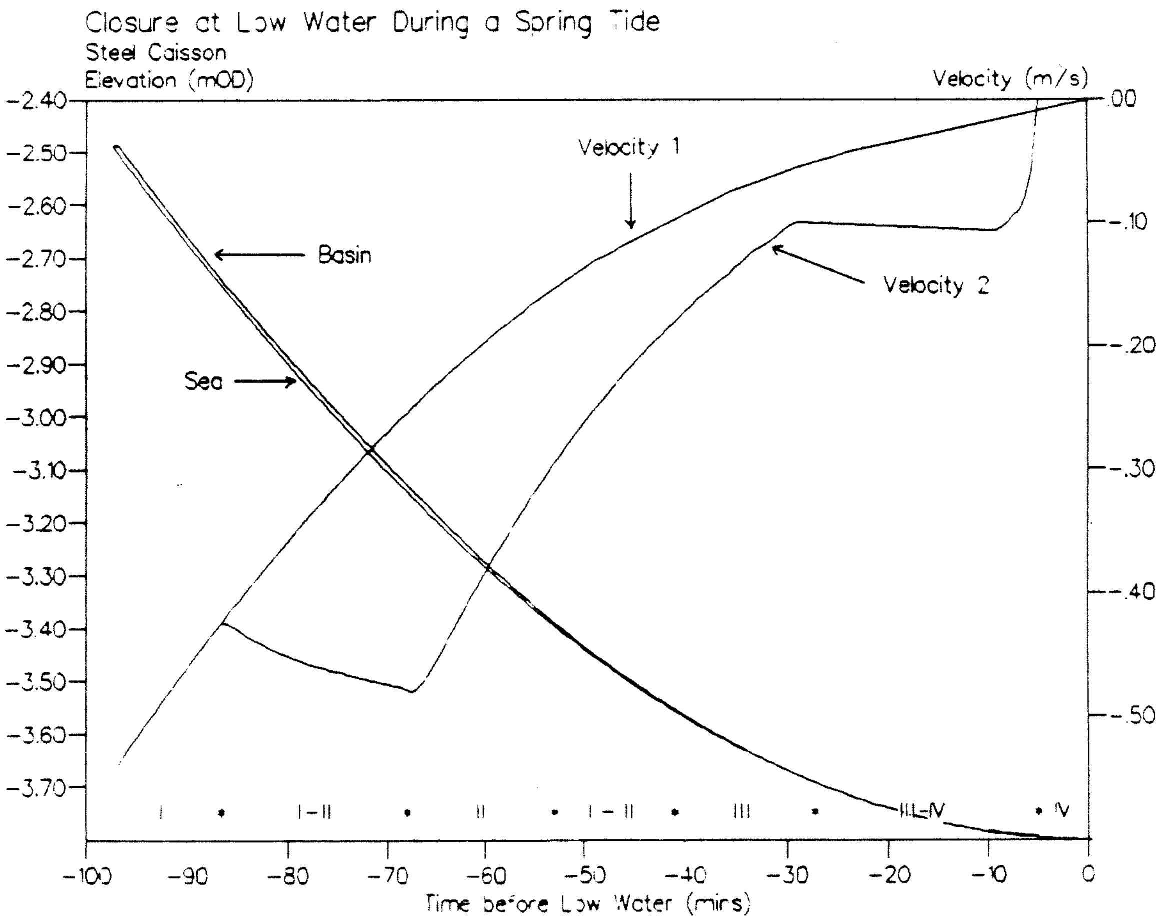

Fig 7.14b

The duration of the stages for these scenarios is given in Table 7.4. The durations are obtained by comparing with the placing of the Brouwershavense Gat caisson. Adjustments were made for the differences in draft and keel clearance.

		DURATION OF STAGES (MINS)			
	SCENARIO	1a	1b	2a	2b
STAGE	I-II	25	20	19	19
	II	15	15	15	15
	II-III	12	11	11	9
	III	15	15	15	15
	III-IV	14	28	28	22

Table 7.4 : Assumed Duration of Stages

We assume that the drag force results from the head difference across the caisson:

$$F = 1/2 * p * g * [(H_s - d)^2 - (H_b - d)^2] * L$$

in which

F = Drag Force (N)
H_s = Depth at Seaward Side (m)
H_b = Depth at Basin Side (m)
p = Density of Water (kg/m^3)
d = Keel Clearance (m)
L = Length of Caisson = 75 m

The maximum velocities and drag forces are displayed in Table 7.5.

Placing Scenario	Maximum Velocity (m/s)	Maximum Head Difference (m)	Maximum Drag Force (kN)
1A Concrete	0.60	0.021	159
1B Concrete	1.07	0.116	873
2A Steel	0.49	0.014	64
2B Steel	0.54	0.018	82

Table 7.5 : Calculated Current Velocities and Drag Forces

The following can be concluded.

In general :

- Using the L.W. slack period leads to substantially lower velocities than the H.W slack period.

- Placing at High Water results in velocities higher than the maximum permitted 0.75 m/s.

For the concrete caisson :

- Despite the fact that the velocity exceeds 0.5 m/s, the placing on a low water certainly does not look impossible. One way of decreasing the velocities is to start slightly later with the placing, to end it just after L.W. slack.

For the steel caisson :

- On a neap tide, the velocities stay under 0.5 m/s and even on a spring tide the velocities remain acceptable.

7.4.6 Both Caissons in Place

Figure 7.15 and 7.16 show the water levels and discharges through the sluices after the closure of the estuary. Immediately after the placing of the second caisson, its safety considering stability is not very high, because the permanent ballast is not present yet. Because this is a temporary case, the design values are lower than in the permanent stage. When placing on a low neap tide, the most crucial moment is at the following high water. The safety factors for stability at that moment are listed in Table 7.6.

FACTORS OF SAFETY	FLOATATION	SLIDING	OVERTURNING
DESIGN VALUES	1.20	1.30	1.20
OBTAINED VALUES			
STEEL CAISSON	1.20	1.97	1.10
CONCRETE CAISSON	1.34	2.36	1.23

Table 7.6 : Safety Factors after Placing

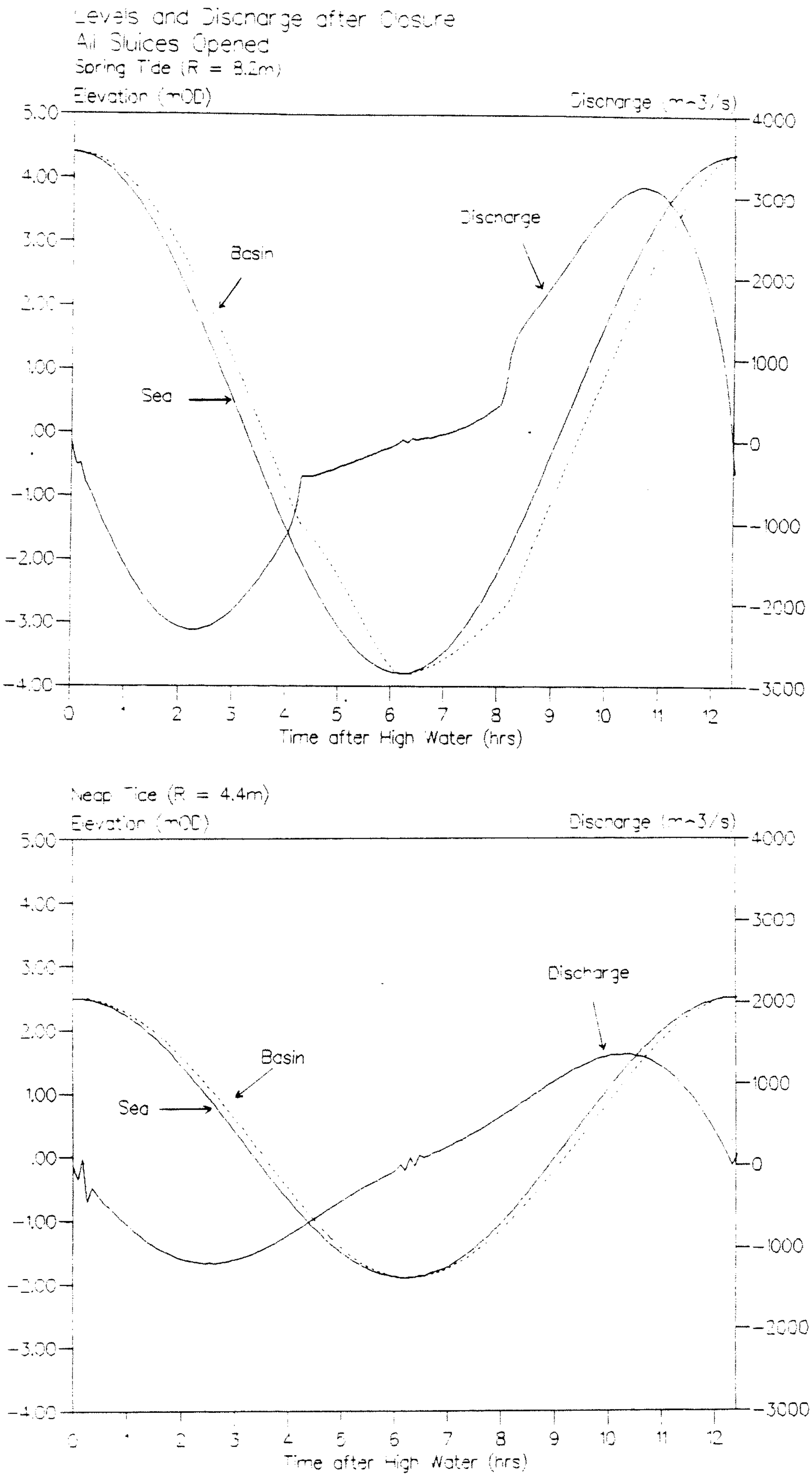

Levels and Discharge after Closure
All Sluices Opened
Spring Tide (R = 8.2m)
Elevation (mOD)
Discharge (m^3/s)
5.00
4.00
3.00
2.00
1.00
.00
-1.00
-2.00
-3.00
-4.00
4000
3000
2000
1000
0
-1000
-2000
-3000
Discharge
Basin
Sea
0 1 2 3 4 5 6 7 8 9 10 11 12
Time after High Water (hrs)
Neap Tide (R = 4.4m)
Elevation (mOD)
Discharge (m^3/s)
5.00
4.00
3.00
2.00
1.00
.00
-1.00
-2.00
-3.00
-4.00
4000
3000
2000
1000
0
-1000
-2000
-3000
Discharge
Basin
Sea
0 1 2 3 4 5 6 7 8 9 10 11 12
Time after High Water (hrs)

Fig 7.15

The following can be concluded.

In general :

- Using the L.W. slack period leads to substantially lower velocities than the H.W slack period.

- Placing at High Water results in velocities higher than the maximum permitted 0.75 m/s.

For the concrete caisson :

- Despite the fact that the velocity exceeds 0.5 m/s, the placing on a low water certainly does not look impossible. One way of decreasing the velocities is to start slightly later with the placing, to end it just after L.W. slack.

For the steel caisson :

- On a neap tide, the velocities stay under 0.5 m/s and even on a spring tide the velocities remain acceptable.

7.4.6 Both Caissons in Place

Figure 7.15 and 7.16 show the water levels and discharges through the sluices after the closure of the estuary. Immediately after the placing of the second caisson, its safety considering stability is not very high, because the permanent ballast is not present yet. Because this is a temporary case, the design values are lower than in the permanent stage. When placing on a low neap tide, the most crucial moment is at the following high water. The safety factors for stability at that moment are listed in Table 7.6.

FACTORS OF SAFETY	FLOATATION	SLIDING	OVERTURNING
DESIGN VALUES	1.20	1.30	1.20
OBTAINED VALUES			
STEEL CAISSON	1.20	1.97	1.10
CONCRETE CAISSON	1.34	2.36	1.23

Table 7.6 : Safety Factors after Placing

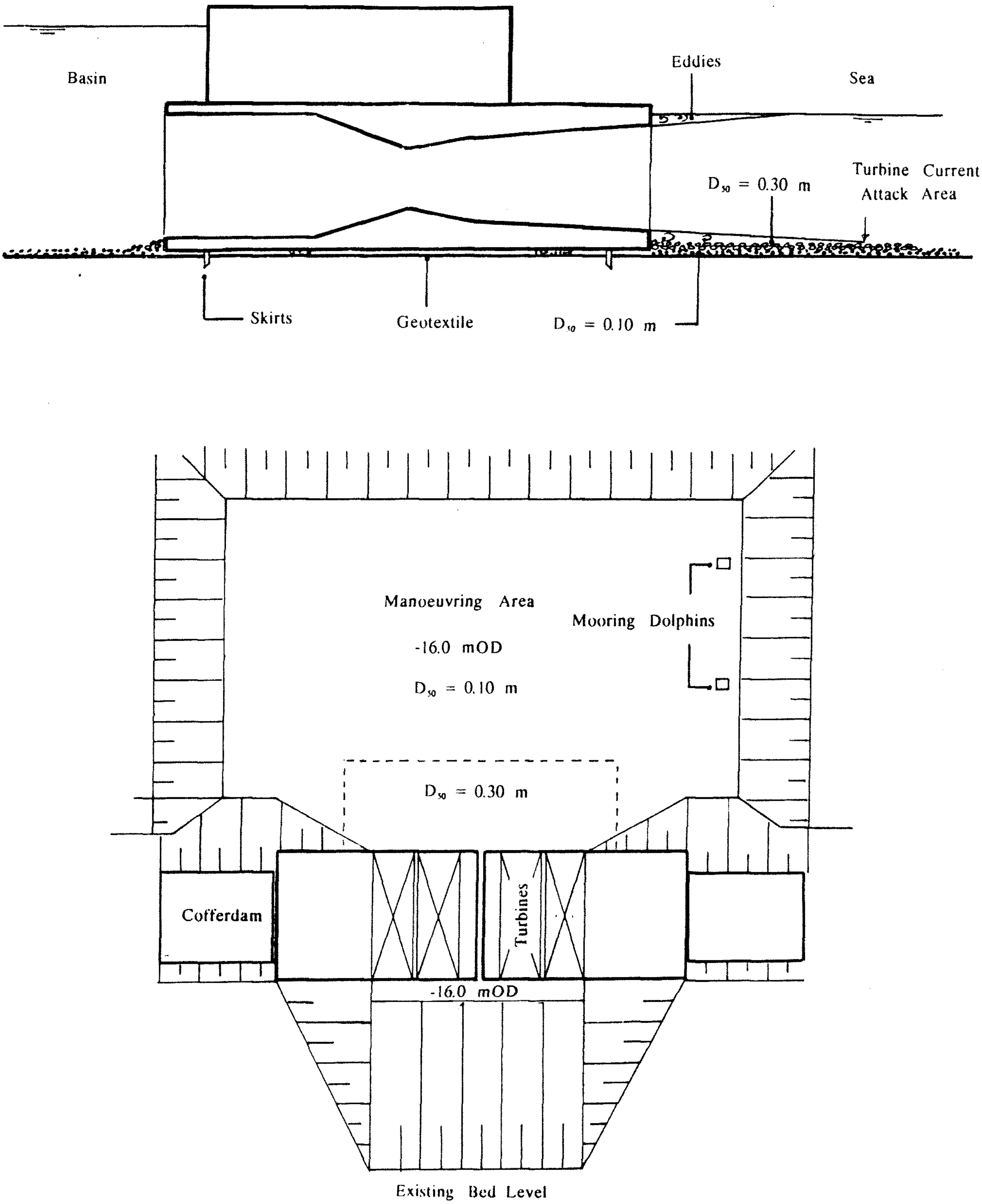

Fig 7.16 Scour Protection around Caisson

There are several formulas for stone seizing. The Isbash formula for the critical velocity for a stone on top of a sill is given by :

$$* \qquad U_{cr} = 1.2 * \sqrt{g\delta D_{50}} \qquad (1)$$

in which :

g = Acceleration of Gravity (m/s^2)

δ = Relative Density of Stones = 1.65 (-)

D_{50} = Equivalent Diameter of the Average Weight of Stones (m)

This formula is valid for a non-developed boundary layer (e.g. at outlets) or if the waterdepth - stone diameter ratio (h/D) is smaller than 5. This means that it is applicable for the permanent situation at the outlet of the turbine (load case I), but not for the temporary situation in the closure gap (load case II). A formula for this situation has been developed by the Delft Hydraulics Laboratorium :

$$\frac{U_{cr}}{\sqrt{g\delta D_{50}}} = 1.4 * \log \frac{5.5*h}{D_{50}} \qquad (2)$$

in which : h = Water Depth (m)

This formula suggests that when the depth - stone diameter is large, the velocity near the bed is less due to friction, so that the mean velocity must be greater for greater depths to produce the same critical shear stress on the sill. This conclusion, however, is not sufficiently supported by experimental data. Table 7.7 gives the results for the stone seizing.

Load Case	Form.	U_{mean} (m/s)	r (-)	g_t (-)	U_{cr} (m/s)	D_{50} (m)
I	1	1.5	0.50	1.7	2.6	0.30
II	1	1.8	0.25	1.7	1.9	0.15
II	2	1.8	0.25	1.2	1.9	0.02

Table 7.7 : Critical Velocities and Stone Diameters

If we compare the D50 for both cases, it appears that it is very important which formula is applied : the Isbash formula is far more conservative. It is recommended to study this matter more extensively in a further stage of the study. In this stage, it is assumed that the D50 of the toplayer will be 0.10 m. The thickness of this layer will be 2.0 * D50 = 0.20 m.

In order to avoid the clay from washing out, the use of a geotextile or matrass is suggested. A filter consruction of gravel would require approximately 5 layers of different diameters; this would be very difficult ti construct. In order to get a relatively smooth sill, the use of a bucket dredger is suggested, so that the depth variations can be kept under 20 cm.

The grouting of the sill requires an enclosed area. In order to achieve this, the use of skirts is suggested. These skirts could be :

1) attached to the bottom of the caisson
2) attached to hydraulic jacks at either side of the caisson

SUB 1) The skirts would be pushed through the sill by the weight of the caisson. With a toplayer of 0.10 m, this should not cause many problems. The length of these skirts would be about 0.7 m, depending on the thickness of the sill construction. This has a slight influence on the transport and placing operations, because effectively the draft of both caissons would increase by 0.7 m. For the steel caisson, this would not cause many problems. The draft of the concrete caisson would increase to 10.7 m, which will cause the following problems:

The time available for crossing the low water channel will be less. In order to cross the tidal flats, the sea level should be at least +3.3 mOD. This will only occur at high water during a spring tide. The window for crossing the channel will decrease to 170 minutes. Normally, this will be enough. If more security is desired, the channel could be dredged to a deeper level. Alternatively, the buoyancy could be increased by the use of floating bags.

During the placing operation, the current velocity would probably exceed 0.75 m/s.

SUB 2) Along both long sides of the caisson hydraulic jacks are connected. Skirts are attached to these hydraulic jacks. During the transport and sinking of the caisson the skirts are held beneath the caisson floor. After the caisson is sunk, the hydraulic jacks would push the skirts downwards, through the sill. The use of this system means that the casisson draft will not increase. Therefore no additional problems during the placing would occur. This is one of the systems suggested for the Severn Tidal Power scheme (see Reference 5).

For the steel caisson both systems would be suitable. For the concrete caisson the hydraulic jack system is probably favourable.

7.6 Conclusions and Recommendations

- The stability during transport is safe for both types of caissons, although the window for sailing of the concrete is substantially larger, due to its higher natural period.

- During the placing, the flow velocity will remain acceptable (approx. 0.5 m/s) in case of a steel caisson. With a concrete caisson, the velocity will probably be higher (approx. 0.65 m/s). It should be studied what the maximum allowable velocity during placing actions can be.

- Despite the fact that the tidal range at the mouth of the Wyre is large, the velocities in the closure gap remain acceptable. This is mainly due to the relatively small surface area of the estuary at low water levels. Consequently the bed protection material is of relatively small seize. Therefore the sill will be smooth, which is necessary for levelling the caissons. However, more clarity is required about stone seizing formulas at large water depths.

- Because the applied model is relatively simple (no hydrau-dynamic influences are taken into account) it is advisable to check the results by the use of a more accurate model. For the transport and placing actions of the caissons, real model tests are absolutely necessary.

REFERENCES

1. Rapport Doorlaat Caisson Oosterschelde
   Nederlandsch Scheepsbouwkundig Proefstation Wageningen

2. Closure of the Brouwershavensche Gat
   J.M. van Westen
   The Closure of Tidal Basins
   Delft University Press, 1987

3. Internal Flow Systems
   D.S. Miller
   2nd Edition

4. Interaction Water Motion and Closing Elements
   K.W. Pilarczyk
   The Closure of Tidal Basins
   Delft Univerity Press, 1987

5. Tidal Power from the Severn Estuary, Volume II
   The Severn Barrage Committee, 1979

APPENDIX 1 : WAVE HEIGHT CALCULATIONS

Offshore Wave Conditions

Extreme Wave Height[1] = 14 m, i.e. Significant Wave Height = 7 m.
Wave Period[1] = 10 s
Depth at MHWS (d) = 5.7 m

$H/gT^2 = 7/(9.81*10^2) = 0.00713$
Beach Slope (m) = ∞
(Fig. A1.1[2]) : constant depth $d/H = 1.28$
Max. Wave Height on Tidal Flats : $H_0 = 5.7/1.28 = 4.5$ m

Friction on Tidal Flats:

Length of Tidal Flats (dx) = 3150 m
Water Depth (d) = 5.7 m
$T^2/h = 10^2/5.7 = 17.5$ s2/m = 5.3 s2/ft
f = 0.01 say
$f * H * dx / d^2 = 0.01 * 4.5 * 3150 / 5.7^2 = 4.4$
Portschneider and Leid (Fig. A1.2) : Reduction Factor (K_f) = 0.55
i.e. $H_{inshore} = 0.55 * 4.4 = 2.5$ m

Other reductions :
- Refraction
- Diffraction
- Reflection

Assume $H_{inshore} = 2$ m

Internal Waves

Southerly Fetch = 3.8 km
Average Water Depth on MHWS = 6.2 m
Max. Wind Speed (U) = 34 m/s
Wind Stress Factor (Ua) = $0.71 * U^{1.23} = 54.3$ m/s

(Fig. A1.3[2]) :
- $H_s = 1.5$ m
- $T = 3.5$ s

1 Source : Environmental Parameters in UK Continental Shelf
Noble Denton 1984

2 Source : Shore Protection Manual
Department of the Army, 1984

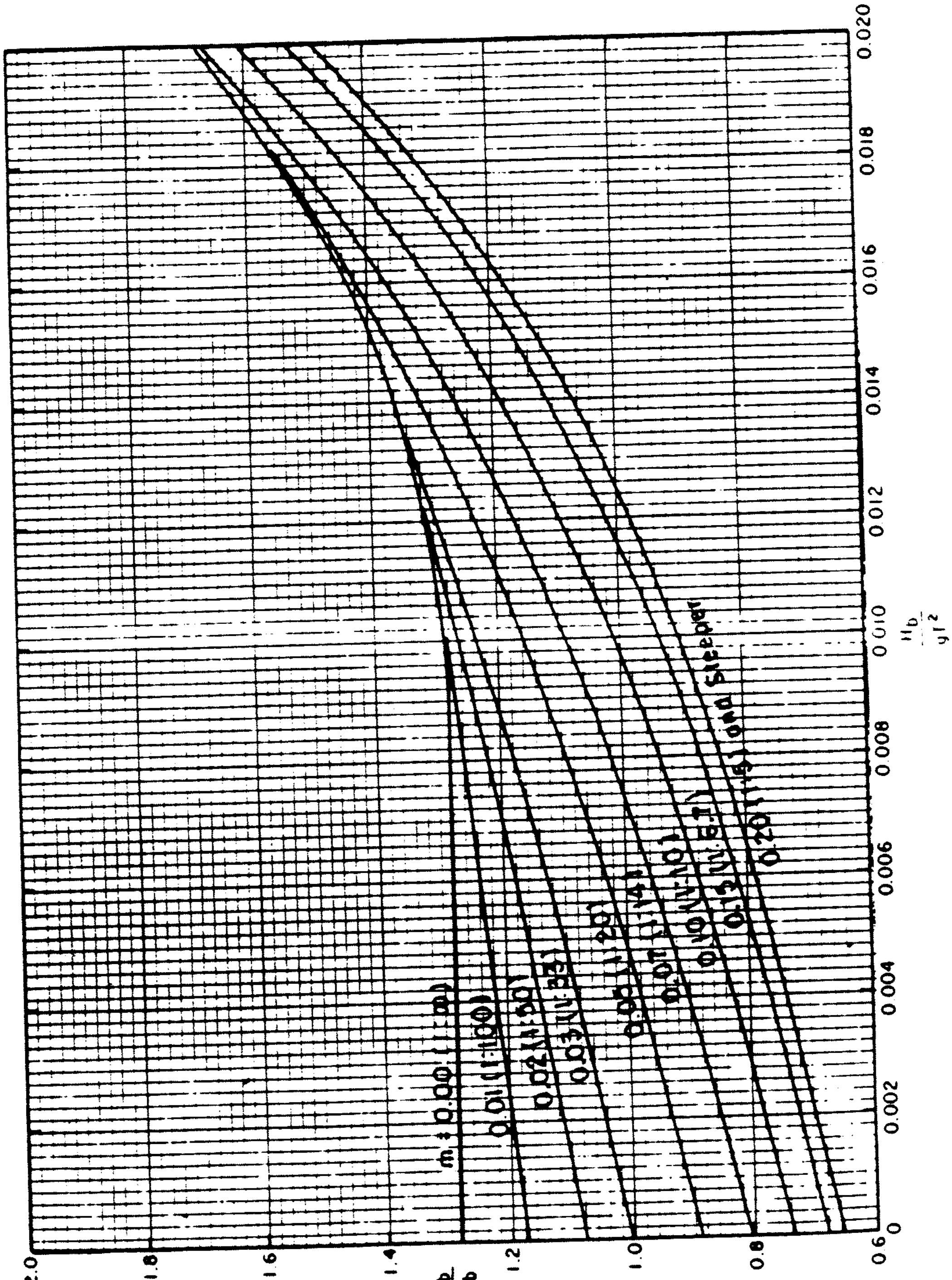

Dimensionless depth at breaking versus breaker steepness.

Fig A1.1

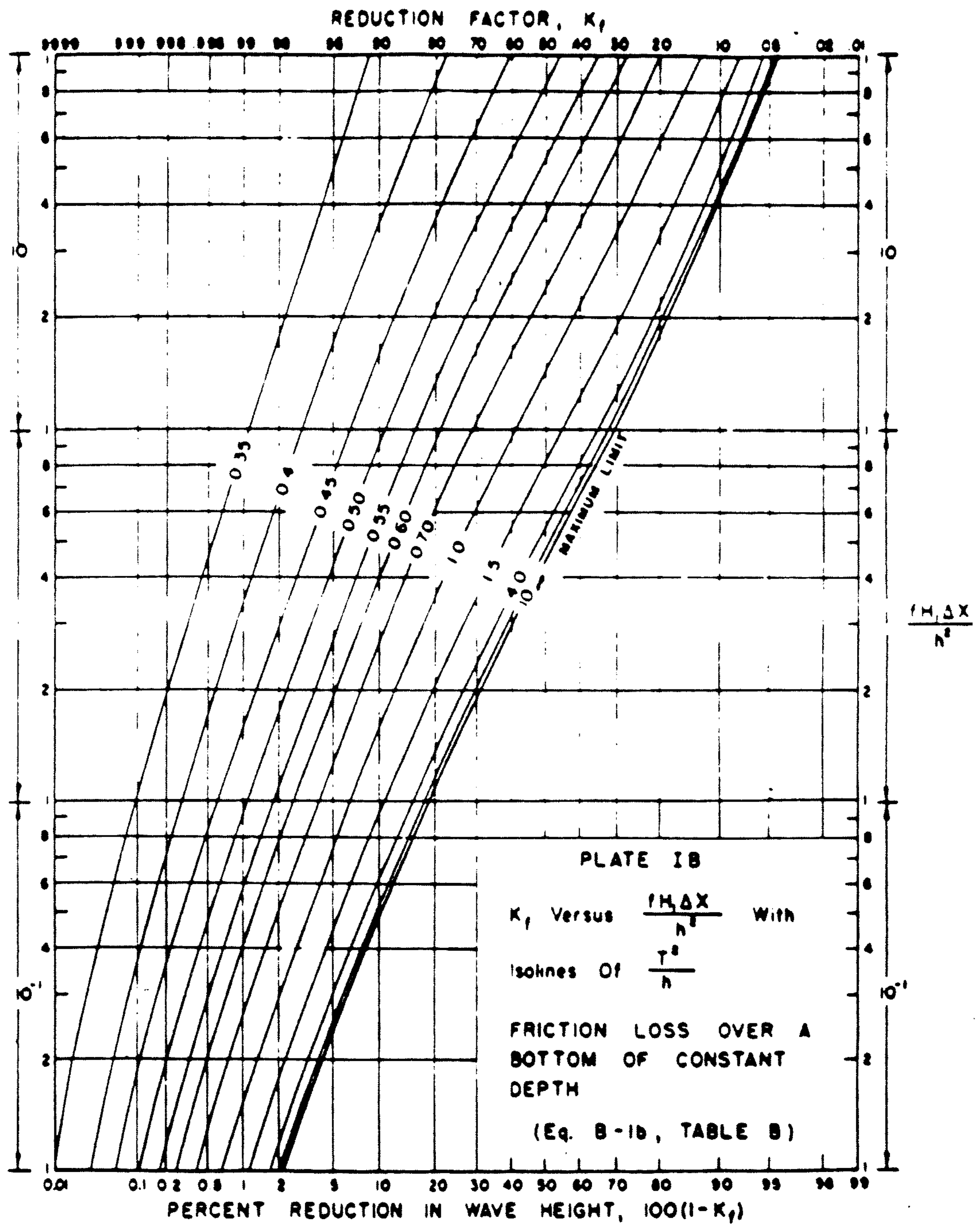

Fig A1.2 Friction Loss over a Bottom of Constant Depth

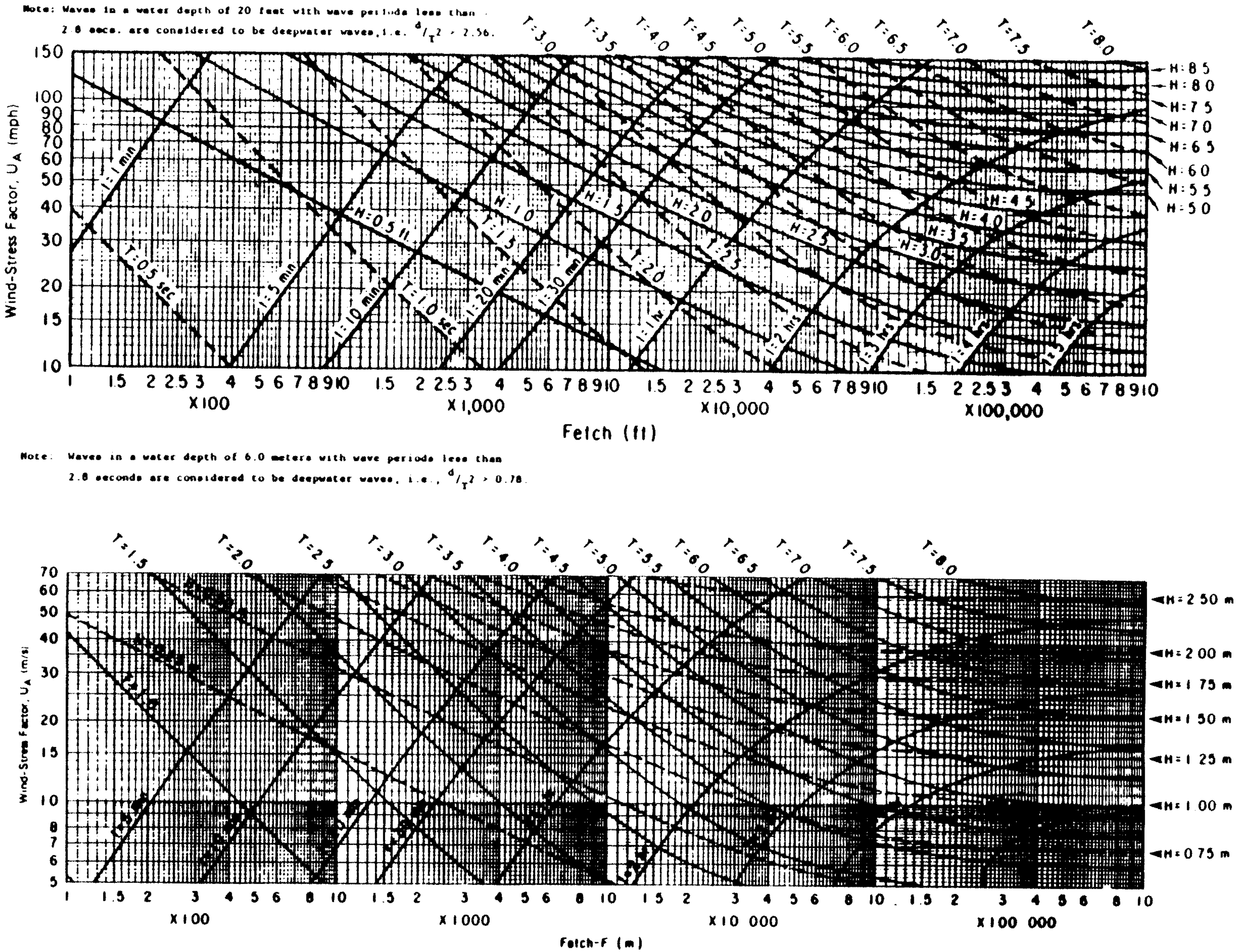

Fig A1.3

Forecasting curves for shallow-water waves; constant depths = 20 feet (upper graph) and 6.0 meters (lower graph).

APPENDIX 2 : FRAME CALCULATIONS

Strap produces output for every member in the model. In order to simplify the output, the members were seized by using the following procedure.

The 3-D frame is divided into 10 2-D frames in the X1-X2 plane and two frames in the X2-X3 plane. Each frame is divided into 5 parts :

* Horizontal members at the bottom : H1
* Horizontal members in the middle : H2
* Horizontal members at the top : H3
* Diagonal members : D
* Vertical members : V

The numbering of the frames is shown in Figure A2.1. The number of a member is found by adding its own number (1-72) to it X1-X2 frame number (000-1100). A representative member of each part is selected. On the following pages, the axial and shear forces, bending and torsional moments are displayed. The selected Universal Beam and its areas shown. Axial stress (f_c or f_t), shear stress (f_q) and bending stress (f_{bc}) are calculated with the following formulas (see Figure A2.2):

$$f_c = \text{axial force}/At$$
$$f_q = V2/A$$
$$f_{bc} = M3*h/(2*I3)$$

The equivalent stress is calculated using the following formulas :

$$f_e = \sqrt{((f_t + f_{bt})^2 + 3 * f_q^2)}$$

or

$$f_e = \sqrt{((f_c + f_{bc})^2 + 3 * f_q^2)}$$

This stress should be less than 230 kN/mm² (BS 449:part 2 : 1969).
The following remarks must be made :

- Most bottom members (H1) have torsional moments. This is ignored because in reality the floor will be massive concrete.

- V3 shear and M3 moments are small enough to be ignored.

- Some members were too heavily loaded to be seized as one single UB. This is the case for the members near the inlet and outlet area of the tube. These members were seized as 2 or 3 UB's. In reality, these members would be trusses.

- Some top members were too heavily loaded. In this case the plate thickness was taken into account, so increasing area and moment of inertia of the member.

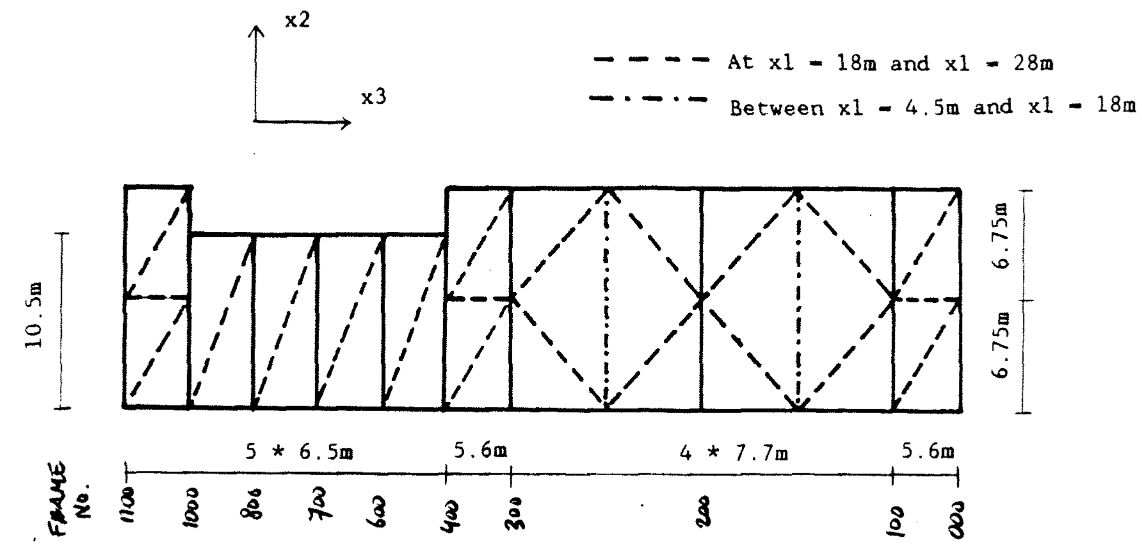

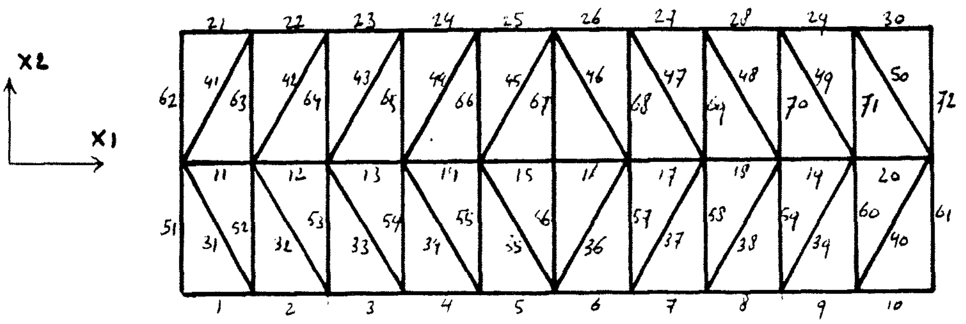

Fig A2.1 Frame Numbering

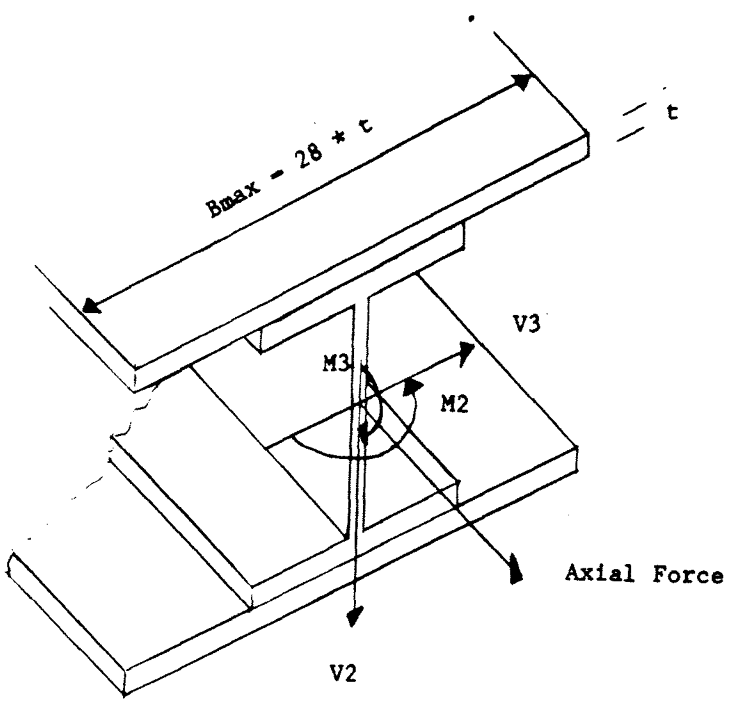

Fig A2.2 Moment and Force Definition

Frame : 000

Member	Load Case	Axial (kN)	V2 (kN)	V3 (kN)	MT (kNm)	M2 (kNm)	M3 (kNm)	UB	Weight (kg/m)	Plate Th. (mm)	Aw (mm^2)	A (mm^2)	I3 (mm^4)	fq (N/mm^2)	fc (N/mm^2)	fbc (N/mm^2)	fe (N/mm^2)	Length (m)	Weight (kN)
005 H1	2	-3781	-75	-6	280	-14	185	686*284*152	170	-	8854	21630	1.70	8.50	174.80	37.70	213.10	48.00	81.60
011 H2	2	-2413	102	20	-	-10	289	610*229*140	140	-	7115	17820	1.12	14.30	135.40	79.80	216.60	48.00	67.20
025 H3	2	-2708	-67	-2	-	-6	448	686*284*170	170	-	8854	21630	1.70	7.60	125.20	91.40	217.00	48.00	81.60
035 D	1	1524	33	-15	-	85	172	533*210*92	92	-	4822	11760	.55	6.80	129.60	83.00	212.90	148.50	136.62
060 V	2	-1025	-55	-5	-	58	-229	533*210*92	92	-	4822	11760	.55	11.40	87.20	110.50	198.70	133.10	122.45
																			489.47

Frame : 100, 300

Member	Load Case	Axial (kN)	V2 (kN)	V3 (kN)	MT (kNm)	M2 (kNm)	M3 (kNm)	UB	Weight (kg/m)	Plate Th. (mm)	Aw (mm^2)	A (mm^2)	I3 (mm^4)	fq (N/mm^2)	fc (N/mm^2)	fbc (N/mm^2)	fe (N/mm^2)	Length (m)	Weight (kN)
106 H1	2	-13946	61	100	4732	-251	-377	914*305*388	388	30	17017	99790	18.50	3.60	139.80	9.96	149.80	48.00	186.20
111 H2	2	4987	134	-5	-	23	365	914*305*224	224	-	13025	28490	3.75	10.30	175.00	44.30	220.00	48.00	107.50
126 H3	2	9383	1174	-42	-	108	4499	914*419*388	388	30	17017	99790	18.56	69.00	94.00	111.60	237.80	48.00	186.20
140 D	2	2890	-27	-6	-	-8	-144	610*229*125	125	-	6463	15940	.98	4.20	181.70	44.80	226.60	139.60	174.50
170 V	2	-5205	157	13	-	166	-535	914*305*253	253	-	14172	32250	4.36	11.10	161.40	56.40	218.40	126.50	320.00
																			974.40

Member	Load Case	Axial (kN)	V2 (kN)	V3 (kN)	MT (kNm)	M2 (kNm)	M3 (kNm)
307 H1	2	-16098	36	-54	3513	-135	-320
311 H2	2	5034	144	1	-	-12	390
325 H3	2	-10823	-716	2	-	6	2693
340 D	2	2858	-36	11	-	-45	-187
370 V	2	-5159	155	-23	-	-208	-529

SAME AS 100

Frame : 200

Member	Load Case	Axial (kN)	V2 (kN)	V3 (kN)	MT (kNm)	M2 (kNm)	M3 (kNm)	UB	Weight (kg/m)	Plate Th. (mm)	Aw (mm^2)	A (mm^2)	I3 (mm^4)	fq (N/mm^2)	fc (N/mm^2)	fbc (N/mm^2)	fe (N/mm^2)	Length (m)	Weight (kN)
206 H1	2	18536	123	9	8555	-23	544	914*419*388	388	-	17017	99790	18.56	7.20	185.80	23.40	209.60	48.00	186.24
211 H2	2	6136	105	4	-	-13	244	914*305*253	253	-	14172	32250	4.36	7.40	190.20	25.70	216.30	48.00	121.44
226 H3	2	12294	1574	4	-	-10	4048	914*419*388	388	30	17017	99790	18.56	92.50	123.20	89.40	266.20	48.00	186.24
240 D	2	-3718	-5	5	-	-12	99	762*267*147	147	-	8787	18780	1.69	-	198.00	22.10	199.20	139.60	205.21
269 V	2	-6648	285	2	-	19	-1063	914*419*343	343	-	15355	43690	6.24	18.50	152.20	77.60	232.00	126.50	433.90
																			------+
																			1133.03

Frame : 400, 1000

Member	Load Case	Axial (kN)	V2 (kN)	V3 (kN)	MT (kNm)	M2 (kNm)	M3 (kNm)
406 H1	2	-6293	56	-19	630	-46	-210
420 H2	2	-4583	115	-16	-	-42	-488
426 H3	2	3466	548	3	-	-9	1402
435 D	1	2535	24	7	-	-30	163
481 V	2	2680	-240	26	-	3	-465

SAME AS 1000

Member	Load Case	Axial (kN)	V2 (kN)	V3 (kN)	MT (kNm)	M2 (kNm)	M3 (kNm)	UB	Weight (kg/m)	Plate Th. (mm)	Aw (mm^2)	A (mm^2)	I3 (mm^4)	fq (N/mm^2)	fc (N/mm^2)	fbc (N/mm^2)	fe (N/mm^2)	Length (m)	Weight (kN)
1006 H1	2	-6579	39	-16	-233	-40	-151	914*305*253	253	-	14172	32250	4.36	2.80	204.00	15.90	220.00	48.00	121.44
1020 H2	2	-4772	136	14	-	40	-554	914*305*253	253	-	14172	32250	4.36	9.60	148.00	58.40	207.00	48.00	121.44
1026 H3	2	-3855	-437	-13	-	-33	1111	914*305*289	289	-	16056	36850	5.04	27.20	104.60	102.20	212.10	48.00	138.72
1046 D	1	-2111	-15	14	-	80	115	533*210*101	101	-	8225	12910	.62	1.80	163.50	50.40	213.90	141.60	143.02
1081 V	2	2792	-234	26	-	3	-470	686*284*170	170	-	8854	21630	1.70	26.40	129.10	95.90	229.60	126.50	215.05
																			------+
																			739.67

Frame : 600, 700, 800

Member	Load Case	Axial (kN)	V2 (kN)	V3 (kN)	MT (kNm)	M2 (kNm)	M3 (kNm)	UB	Weight (kg/m)	Plate Th. (mm)	Aw (mm^2)	A (mm^2)	I3 (mm^4)	fq (N/mm^2)	fc (N/mm^2)	fbc (N/mm^2)	fe (N/mm^2)	Length (m)	Weight (kN)
605 H1	2	-6620	-116	7	-175	18	286	914*305*289	289	-	16056	36850	5.04	7.22	179.60	26.30	206.30	48.00	138.72
620 H2	2	-4274	-66	-	-	3	-53	686*254*170	170	-	9360	21630	1.70	3.10	197.60	10.80	208.50	48.00	81.60
626 H3	2	-4679	-1599	2	-	5	4066	914*419*338	388	25	17017	66890	18.56	94.00	70.00	146.10	270.50	48.00	186.24
634 D	1	2046	19	-	-	-3	-1052	838*292*226	226	-	12178	28840	3.39	1.60	70.90	132.00	202.90	126.60	286.12
670 V	2	4162	-214	-3	-	7	-592	838*292*226	226	-	12178	28840	3.39	17.60	144.30	74.30	220.70	107.80	243.63
																			------+
																			936.30

Member	Load Case	Axial (kN)	V2 (kN)	V3 (kN)	MT (kNm)	M2 (kNm)	M3 (kNm)
706 H1	2	-6729	53	-19	-21	-46	-196
720 H2	2	-4199	12	-	-	-	-61
726 H3	2	-4804	-1668	3	-	8	239
746 D	1	-2637	162	1	-	8	-870
770 V	1	3707	-189	-4	-	-	-542

SAME AS 600

Member	Load Case	Axial (kN)	V2 (kN)	V3 (kN)	MT (kNm)	M2 (kNm)	M3 (kNm)
805 H1	2	-6764	56	-17	-29	-43	-200
820 H2	2	-4293	18	-1	-	-2	-70
826 H3	2	-4644	-1625	4	-	10	4135
846 D	1	-2515	170	4	-	22	-902
870 V	2	4145	-211	-7	-	-5	-717

SAME AS 700

Frame : 1100

Member	Load Case	Axial (kN)	V2 (kN)	V3 (kN)	MT (kNm)	M2 (kNm)	M3 (kNm)	UB	Weight (kg/m)	Plate Th. (mm)	Av (mm^2)	A (mm^2)	I3 (mm^4)	fq (N/mm^2)	fc (N/mm^2)	fbc (N/mm^2)	fe (N/mm^2)	Length (m)	Weight (kN)
1105 H1	2	-4991	-83	8	-856	19	210	914*419*224	224	-	13025	28490	3.75	6.40	175.20	25.50	201.00	48.00	107.52
1120 H2	2	-2939	48	3	-	5	-171	610*229*140	140	-	7115	17820	1.12	6.70	164.90	47.30	212.50	48.00	67.20
1126 H3	2	-2612	-397	-13	-	-33	1011	838*292*226	226	-	12178	28840	3.39	32.60	90.60	126.80	224.60	48.00	108.48
1146 D	1	-1336	-16	-16	-	-94	89	457*191*74	74	-	3680	9490	.33	4.30	140.80	61.10	202.00	141.60	104.78
1169 V	2	-1428	76	-18	-	-124	-255	533*210*101	101	-	5152	12910	.62	14.80	110.60	111.20	223.30	126.50	127.77
																			-------+
																			515.75

APPENDIX 3 : PANEL CALCULATIONS

Panels

The caisson panels have been divided into groups with similar loadings and sizes (see Figure A3.1). The input for the Bagpus program exists of the coordinates of the corners of the panels, the design sea level and the density of the water. Bagpus calculates the hydrostatic load on the panel. When the loads are not just hydrostatic (e.g. hydrost. load minus ballast), the input is not so straightforward. The way across this problem is to turn the panel upside down and change the density of water and the water level. This is done for the panels b1 to b6. Figure A3.3 shows the side wall of the caisson at the sluice side with the real pressures and the pressures used for Bagpus.

Figure A3.2 shows the schematisation for the sluice piers when one sluice is dewatered and the water level in the adjacent sluice is at a maximum. The problem is that :

a) Bagpus requires that all panels are fully submerged.

b) Bagpus expects that all panels are simply supported at two sides, while the sluice pier is cantilevered at one side.

The aim of the schematisation is to find the adequate water level so that the maximum bending moment in the Bagpus program is equal to the the real maximum moment.

Figure A3.4 shows the schematisation of the conning towers.

The Bagpus output is to be found on the next pages.

Explanation of variables:

- **Flange** : Flange Width, according to BS 449 this is 28 * the plate thickness
- **Depth** : Total depth of the panel
- Web : Web depth
- fbc : maximum bending stress
- pbc : permissible bending stress
- fq : maximum shear stress
- UFb : Utilisation factor in bending
- UFs : Utilisation factor in shear
- FW th : Fillet weld size

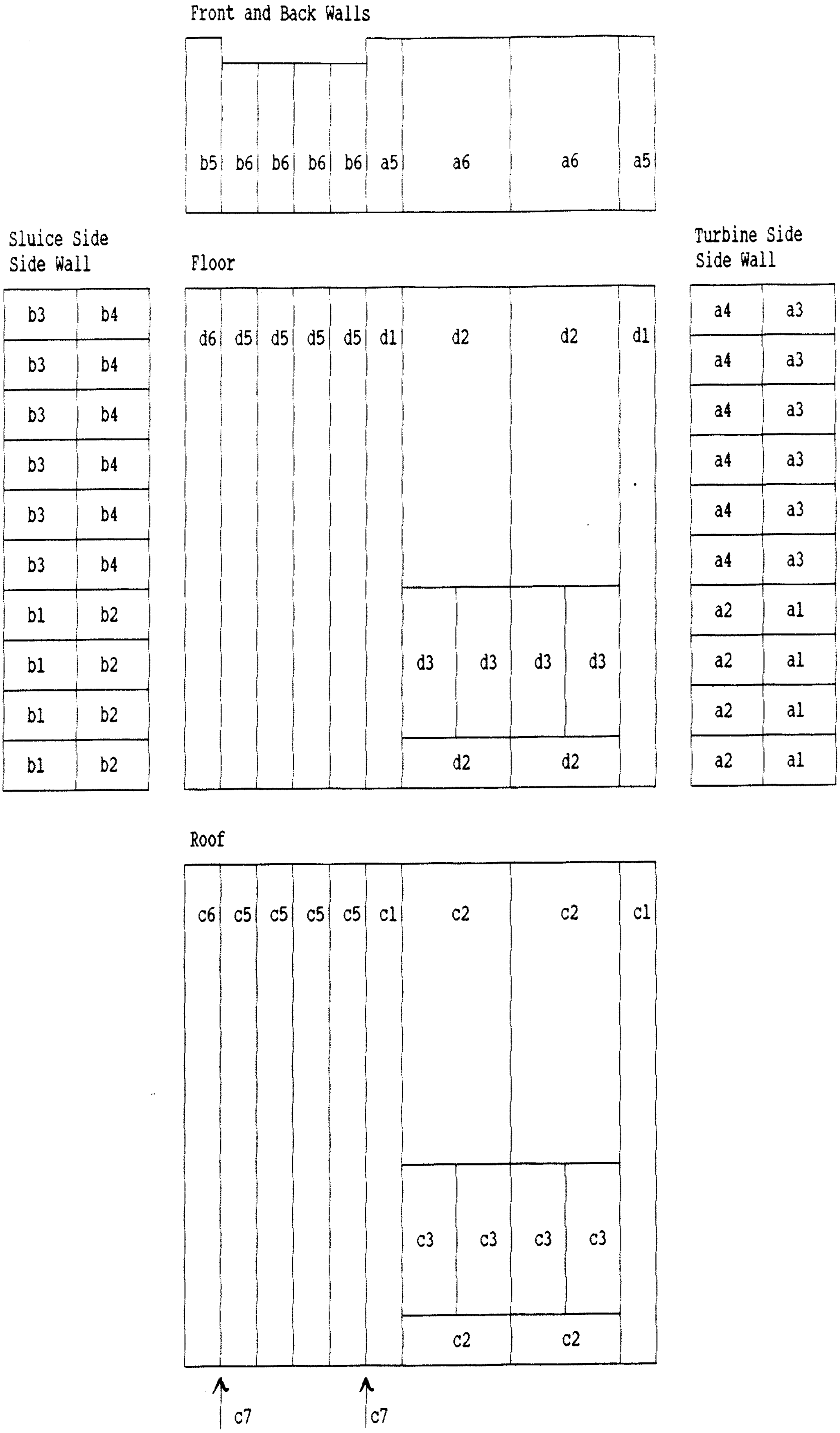

Fig A3.1 Panels in Caisson

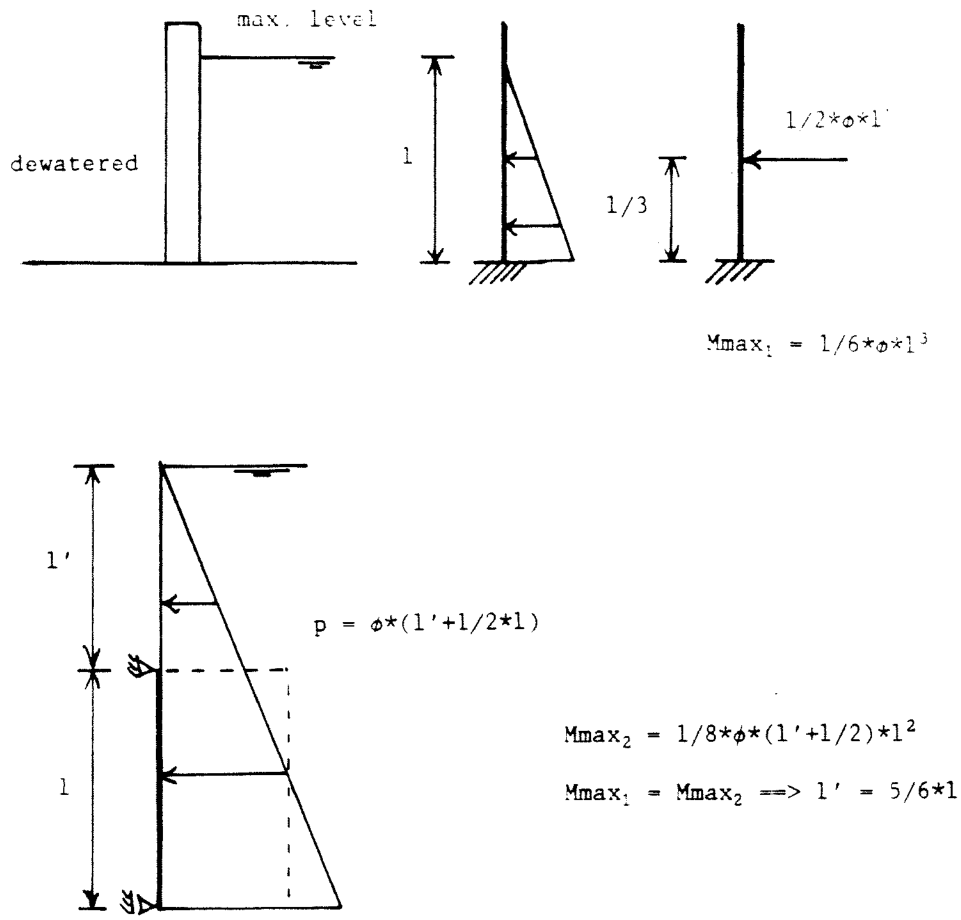

Fig A3.2 Sluice Pier Schematisation

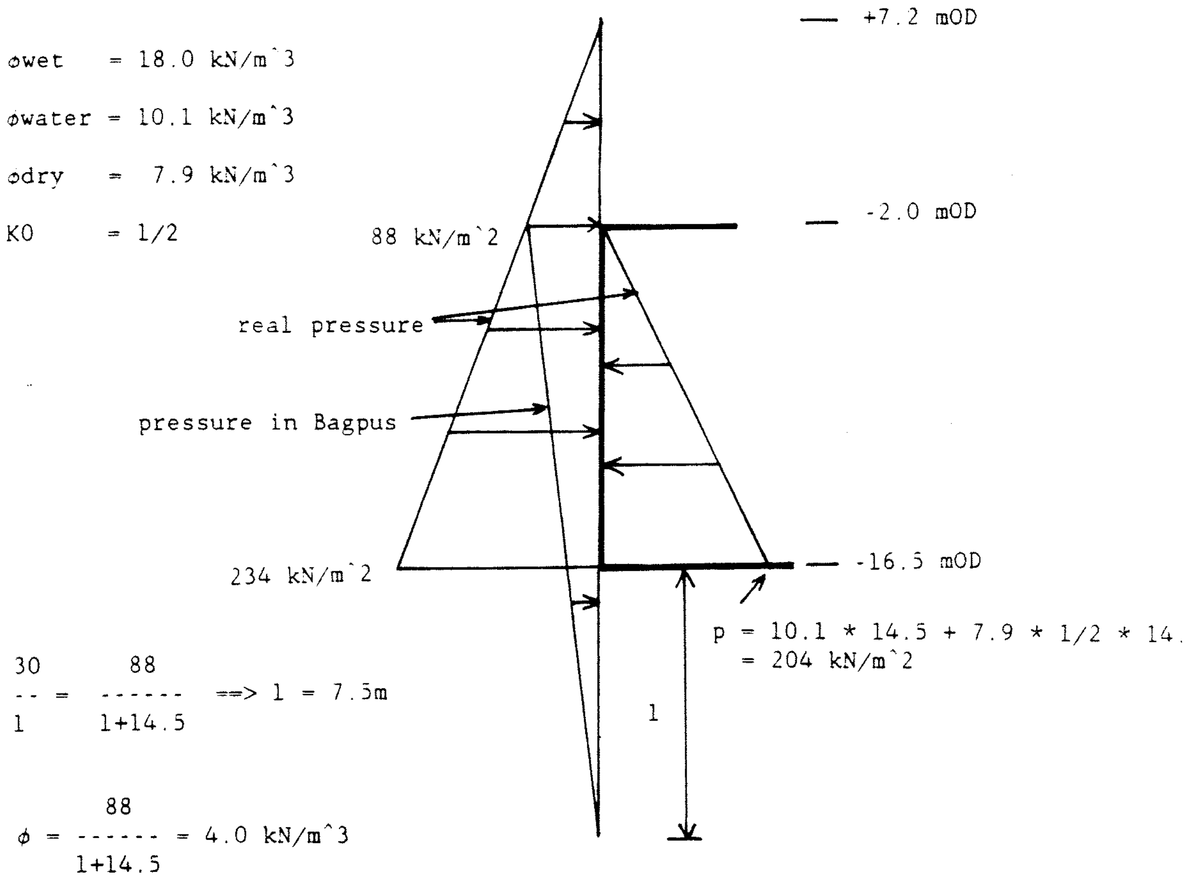

Fig A3.3 Schematisation for Walls with Ballast Loads

Panel number A1

****
OPTIMISED SOLUTION
****

****

Panel width = 7.250 metres
Panel breadth = 4.500 metres
Head of water = 13.850 metres variable head
Construction type = SINGLE SKIN
Main beams = BREADTHWAYS

****

Plate Thickness = 20.000 mm
Panel depth = 450.000 mm
Widthwise spans = 1.208 metres
Breadthwise spans:
b(1) = 4.500 metres

	Flange (mm)	depth (mm)	web (mm)	fbc (N/mm^2)	pbc (N/mm^2)	fq (N/mm^2)	UFb	UFs	FW th (mm)
Primary	560.	410.	6.0	44.0	215.0	75.7	.2	.5	5.0
Secondary	560.	410.	8.0	210.5	215.0	141.9	1.0	.9	5.0

Plt. Wt.(tonnes)	Stiff. Wt.(tonnes)	Total Wt.(tonnes)
8.48	.98	9.46

X c.g. (metres)	Y c.g. (metres)	Z c.g. (metres)
2.25	.00	10.88

Plt. Cost	Stiff.Cost	Plt.Weld Cost	Stiff.Weld Cost	Total Cost
2543.	294.	392.	4210.	7439.

****

PANEL NUMBER 12

Panel width = [illegible].150 metres
Panel breadth = 4.500 metres
Head of water = 23.7[illegible] metres variable head
Construction type = SINGLE SKIN
Main beams = BREADTHWAYS

****

Plate Thickness = [illegible] mm
Panel depth = [illegible] mm
Widthwise spans = .72[illegible] metres
Breadthwise spans:
b(1) = 1.790 metres

b(2) = 2.710 metres

	Flange	depth	web	fbc	pbc	fq	UFb	UFs	FW th
	(mm)	(mm)	(mm)	(N/mm^2)	(N/mm^2)	(N/mm^2)			(mm)
Primary	560.	160.	8.0	196.1	215.0	158.3	.9	1.0	5.0
Secondary	560.	160.	7.0	16.5	215.0	150.2	.1	.9	5.0

Plt. Wt.(tonnes)	Stiff. Wt.(tonnes)	Total Wt.(tonnes)
9.76	.69	10.45

X c.g. (metres)	Y c.g. (metres)	Z c.g. (metres)
2.25	.00	3.63

Plt. Cost	Stiff.Cost	Plt.weld Cost	Stiff.weld Cost	Total Cost
2928.	207.	392.	6487.	10014.

J. R. [illegible] A4

```
            ******************************
                  OPTIMISED SOLUTION
            ******************************

*******************************************

Panel width          =       [illegible].250 metres
Panel breadth        =       5.000 metres
Head of water        =      2[illegible].750 metres   variable head
Construction type    =       SINGLE SKIN
Main beams           =       BREADTHWAYS
*******************************************


Plate thickness      =      20.000 mm
Panel depth          =     220.000 mm
Widthwise spans      =        .725 metres
Breadthwise spans:
 b( 1)                =        1.790 metres

 b( 2)                =        3.210 metres

           Flange depth    web       fbc       pbc       fq        UFb      UFs    FW th
            (mm)   (mm)    (mm) (N/mm^2)(N/mm^2) (N/mm^2)                          (mm)
Primary     560.   180.    9.0    209.1     215.0    150.2      1.0       .9     5.3
Secondary   560.   1[illegible]    7.0     16.6     215.0    150.4       .1       .9     5.0

   Plt. wt.(tonnes   Stiff. wt.(tonnes)  Total wt.(tonnes)
     10.81                .91                 11.73

   X c.g. (metres)     Y c.g. (metres)    Z c.g. (metres)
     2.5[illegible]                .00                  3.63

   Plt. Cost      Stiff.Cost     Plt.Weld Cost  Stiff.Weld Cost  Total Cost
    3244.           274.          392.            7242.           11152.
-----------------------------------------------------------------------------
```

Panel design details from file turb8.DAT

Panel number A5

****
OPTIMISED SOLUTION
****

****

Panel width	=	5.600 metres	
Panel breadth	=	14.500 metres	
Head of water	=	23.700 metres	variable head
Construction type	=	SINGLE SKIN	
Main beams	=	BREADTHWAYS	

****

Plate Thickness	=	30.000 **mm**
Panel depth	=	890.000 **mm**
Widthwise spans	=	1.120 metres
Breadthwise spans:		
b(1)	=	2.590 **metres**
b(2)	=	4.320 **metres**
b(3)	=	7.590 **metres**

	Flange (mm)	depth (mm)	web (mm)	fbc (N/mm^2)	pbc (N/mm^2)	fq (N/mm^2)	UFb	UFs	FW th (mm)
Primary	840.	830.	12.0	192.7	193.1	104.9	1.0	.7	5.1
Secondary	840.	830.	12.0	5.9	215.0	55.7	.0	.3	5.0

Plt. Wt.(tonnes)	Stiff. Wt.(tonnes)	Total Wt.(tonnes)
36.78	8.55	45.33

X c.g. (metres)	Y c.g. (metres)	Z c.g. (metres)
.00	2.80	7.25

Plt. Cost	Stiff.Cost	Plt.Weld Cost	Stiff.Weld Cost	Total Cost
11033.	2566.	4006.	10681.	28286.

Panel number 16

****

OPTIMISED SOLUTION

****

****

Panel width = 15.400 metres
Panel breadth = 14.500 metres
Head of water = 23.700 metres variable head
Construction type = SINGLE SKIN
Main beams = BREADTHWAYS

****

Plate Thickness = 25.000 mm
Panel depth = 955.000 mm
Widthwise spans = .906 metres
Breadthwise spans:
b(1) = 2.410 metres

b(2) = 12.090 metres

	Flange (mm)	depth (mm)	web (mm)	fbc (N/mm^2)	pbc (N/mm^2)	fq (N/mm^2)	UFb	UFs	FW tr (mm)
Primary	700.	905.	13.0	158.8	171.6	98.2	.9	.6	5.(
Secondary	700.	905.	13.0	8.9	215.0	58.9	.0	.4	5.(

Plt. Wt.(tonnes)	Stiff. Wt.(tonnes)	Total Wt.(tonnes)
80.83	28.37	109.20

X c.g. (metres)	Y c.g. (metres)	Z c.g. (metres)
.00	7.70	7.25

Plt. Cost	Stiff.Cost	Plt.Weld Cost	Stiff.Weld Cost	Total Cost
24249.	8511.	5399.	29364.	67524.

Panel number 82

****
OPTIMISED SOLUTION
****

****

Panel width = 7.250 metres
Panel breadth = 4.500 metres
Head of water = 21.100 metres variable head
Construction type = SINGLE SKIN
Main beams = BREADTHWAYS

****

Plate Thickness = 20.000 mm
Panel depth = 150.000 mm
Widthwise spans = 1.208 metres
Breadthwise spans:
b(1) = 2.060 metres

b(2) = 2.440 metres

	Flange	depth	web	fbc	pbc	fq	UFb	UFs	FW th
	(mm)	(mm)	(mm)	(N/mm^2)	(N/mm^2)	(N/mm^2)			(mm)
Primary	560.	110.	8.0	208.0	215.0	147.3	1.0	.9	5.
Secondary	560.	110.	7.0	28.2	215.0	155.2	.1	1.0	5.

Plt. Wt.(tonnes)	Stiff. Wt.(tonnes)	Total Wt.(tonnes)
8.77	.35	9.12

X c.g. (metres)	Y c.g. (metres)	Z c.g. (metres)
2.25	.00	3.63

Plt. Cost	Stiff.Cost	Plt.Weld Cost	Stiff.Weld Cost	Total Cost
2631.	105.	392.	4750.	7877.

Panel number B3

```
        *********************************
              OPTIMISED SOLUTION
        *********************************

************************************************

Panel width          =     7.250 metres
Panel breadth        =     5.000 metres
Head of water        =    13.850 metres  variable head
Construction type    =       SINGLE SKIN
Main beams           =       BREADTHWAYS
************************************************


Plate Thickness      =    15.000 mm
Panel depth          =   155.000 mm
Widthwise spans      =     1.036 metres
Breadthwise spans:
 b( 1)                =       2.090 metres

 b( 2)                =       2.910 metres
```

	Flange (mm)	depth (mm)	web (mm)	fbc (N/mm^2)	pbc (N/mm^2)	fq (N/mm^2)	UFb	UFs	FW th (mm)
Primary	420.	125.	6.0	207.4	215.0	107.5	1.0	.7	5.0
Secondary	420.	125.	6.0	22.1	215.0	92.3	.1	.6	5.0

Plt. Wt.(tonnes)	Stiff. Wt.(tonnes)	Total Wt.(tonnes)
6.82	.36	7.19

X c.g. (metres)	Y c.g. (metres)	Z c.g. (metres)
2.50	.00	10.88

Plt. Cost	Stiff.Cost	Plt.Weld Cost	Stiff.Weld Cost	Total Cost
2047.	109.	363.	5522.	8040.

Panel design details from file turb12.DAT

Panel number 84

****
OPTIMISED SOLUTION
****

****

Panel width	=	7.250 metres
Panel breadth	=	5.000 metres
Head of water	=	21.100 metres variable head
Construction type	=	SINGLE SKIN
Main beams	=	BREADTHWAYS

****

Plate Thickness	=	20.000 mm
Panel depth	=	160.000 mm
Widthwise spans	=	1.036 metres

Breadthwise spans:

b(1)	=	2.500 metres
b(2)	=	2.500 metres

	Flange (mm)	depth (mm)	web (mm)	fbc (N/mm^2)	pbc (N/mm^2)	fq (N/mm^2)	UFb	UFs	FW th (mm)
Primary	560.	120.	6.0	200.9	215.0	155.4	.9	1.0	5.(
Secondary	560.	120.	6.0	20.8	215.0	155.4	.1	1.0	5.(

Plt. Wt.(tonnes)	Stiff. Wt.(tonnes)	Total Wt.(tonnes)
9.94	.35	10.29

X c.g. (metres)	Y c.g. (metres)	Z c.g. (metres)
2.50	.00	3.63

Plt. Cost	Stiff.Cost	Plt.Weld Cost	Stiff.Weld Cost	Total Cost
2982.	105.	392.	5522.	8999.

Panel design details from file turb12.DAT

Panel number 86

****
OPTIMISED SOLUTION
****

****

Panel width	=	6.500 metres
Panel breadth	=	11.500 metres
Head of water	=	28.100 metres variable head
Construction type	=	SINGLE SKIN
Main beams	=	WIDTHWAYS

****

Plate Thickness	=	20.000 mm
Panel depth	=	440.000 mm
Widthwise spans	=	1.300 metres
Breadthwise spans:		
b(1)	=	1.630 metres
b(2)	=	1.720 metres
b(3)	=	1.820 metres
b(4)	=	1.960 metres
b(5)	=	2.170 metres
b(6)	=	2.200 metres

	Flange (mm)	depth (mm)	web (mm)	fbc (N/mm^2)	pbc (N/mm^2)	fq (N/mm^2)	UFb	UFs	FW th (mm)
Primary	560.	400.	8.0	211.0	215.0	158.5	1.0	1.0	5.1
Secondary	560.	400.	6.0	11.4	215.0	54.3	.1	.3	5.0

Plt. Wt.(tonnes)	Stiff. Wt.(tonnes)	Total Wt.(tonnes)
19.73	2.44	22.18

X c.g. (metres)	Y c.g. (metres)	Z c.g. (metres)
.00	3.25	5.75

Plt. Cost	Stiff.Cost	Plt.Weld Cost	Stiff.Weld Cost	Total Cost
5920.	733.	1242.	11104.	18999.

Optimum design for thickness = 40.000 mm:

Plate Thickness = 40.000 mm
Panel depth = 500.000 mm
Widthwise spans = 4.000 metres
Breadthwise spans = 2.800 metres

	Flange	depth	web	fbc	pbc	fq	UFb	UFs	FW t
	(mm)	(mm)	(mm)	(N/mm^2)	(N/mm^2)	(N/mm^2)			(mm)
Primary	1120.	420.	8.0	74.4	215.0	151.9	.3	.9	5.
Secondary	1120.	420.	8.0	26.6	215.0	151.9	.1	.9	5.

Plt. Wt.(tonnes)	Stiff. Wt.(tonnes)	Total Wt.(tonnes)
145.29	5.72	151.00

X c.g. (metres)	Y c.g. (metres)	Z c.g. (metres)
24.00	2.80	14.50

Plt. Cost	Stiff.Cost	Plt.Weld Cost	Stiff.Weld Cost	Total Cost
43586.	1715.	9024.	19746.	74071.

PANEL NUMBER C1

Optimum design for thickness =   30.000 mm:

Plate Thickness   =   30.000 mm
Panel depth   =   310.000 mm
Widthwise spans   =   2.250 metres
Breadthwise spans   =   2.567 metres

	Flange (mm)	depth (mm)	web (mm)	fbc (N/mm^2)	pbc (N/mm^2)	fq (N/mm^2)	UFb	UFs	FW th (mm)
Primary	840.	250.	14.0	207.4	215.0	150.4	1.0	.9	8.1
Secondary	840.	250.	7.0	22.9	215.0	150.4	.1	.9	5.[illegible]

Plt. Wt.(tonnes)	Stiff. Wt.(tonnes)	Total Wt.(tonnes)
41.17	2.22	43.40

X c.g. (metres)	Y c.g. (metres)	Z c.g. (metres)
36.75	3.85	14.50

Plt. Cost	Stiff.Cost	Plt.Weld Cost	Stiff.Weld Cost	Total Cost
12352.	667.	2592.	11181.	26791.

PANEL NUMBER C8

Optimum design for thickness = 40.000 mm:

Plate Thickness	=	40.000 mm
Panel depth	=	700.000 mm
Widthwise spans	=	4.500 metres
Breadthwise spans	=	2.567 metres

	Flange (mm)	depth (mm)	web (mm)	fbc (N/mm^2)	pbc (N/mm^2)	fq (N/mm^2)	UFb	UFs	FW th (mm)
Primary	1120.	620.	14.0	211.8	215.0	151.6	1.0	.9	8.[illegible]
Secondary	1120.	620.	9.0	20.8	215.0	94.3	.1	.6	5.[illegible]

Plt. Wt.(tonnes)	Stiff. Wt.(tonnes)	Total Wt.(tonnes)
43.52	3.48	47.00

X c.g. (metres)	Y c.g. (metres)	Z c.g. (metres)
32.25	7.70	14.50

Plt. Cost	**Stiff.Cost**	**Plt.Weld Cost**	**Stiff.Weld Cost**	**Total Cost**
13056.	1044.	3184.	6591.	23875.

PANEL NUMBER C4

Optimum design for thickness =   60.000 mm:

Plate Thickness   =   60.000 mm
Panel depth   =   500.000 mm
Widthwise spans   =   4.800 metres
Breadthwise spans   =   3.250 metres

	Flange (mm)	depth (mm)	web (mm)	fbc (N/mm^2)	pbc (N/mm^2)	fq (N/mm^2)	UFb	UFs	FW th (mm)
Primary	1680.	380.	17.0	83.8	215.0	157.9	.4	1.0	10.1
Secondary	1680.	380.	17.0	30.9	215.0	157.9	.1	1.0	10.1

Plt. Wt.(tonnes)	Stiff. Wt.(tonnes)	Total Wt.(tonnes)
273.60	10.93	284.53

X c.g. (metres)	Y c.g. (metres)	Z c.g. (metres)
24.00	3.25	10.50

Plt. Cost	Stiff.Cost	Plt.Weld Cost	Stiff.Weld Cost	Total Cost
82081.	3278.	13629.	27026.	126015.

PANEL NUMBER C5

Optimum design for thickness = 45.000 mm:

Plate Thickness = 45.000 mm
Panel depth = 425.000 mm
Widthwise spans = 3.250 metres
Breadthwise spans = 4.500 metres

	Flange (mm)	depth (mm)	web (mm)	fbc (N/mm^2)	pbc (N/mm^2)	fq (N/mm^2)	UFb	UFs	FW th (mm)
Primary	1260.	335.	15.0	126.5	215.0	151.6	.6	.9	8.
Secondary	1260.	335.	16.0	32.8	215.0	151.0	.2	.9	9.

Plt. Wt.(tonnes)	Stiff. Wt.(tonnes)	Total Wt.(tonnes)
71.42	3.55	74.97

X c.g. (metres)	Y c.g. (metres)	Z c.g. (metres)
9.00	3.25	14.50

Plt. Cost	Stiff.Cost	Plt.Weld Cost	Stiff.Weld Cost	Total Cost
21426.	1066.	6401.	10408.	39301.

PANEL NUMBER C6

$6.5 \times 18\ m^2$

HEAD = 9.2 M

Optimum design for thickness = 50.000 mm:

Plate Thickness = 50.000 mm
Panel depth = 400.000 mm
Widthwise spans = 5.000 metres
Breadthwise spans = 3.250 metres

	Flange (mm)	depth (mm)	web (mm)	fbc (N/mm^2)	pbc (N/mm^2)	fq (N/mm^2)	UFb	UFs	FW th (mm)
Primary	1400.	300.	16.0	110.6	215.0	154.3	.5	1.0	9.2
Secondary	1400.	300.	16.0	42.5	215.0	154.3	.2	1.0	9.2

Plt. Wt.(tonnes)	Stiff. Wt.(tonnes)	Total Wt.(tonnes)
134.84	5.11	139.95

X c.g. (metres)	Y c.g. (metres)	Z c.g. (metres)
15.00	3.25	14.50

Plt. Cost	Stiff.Cost	Plt.Weld Cost	Stiff.Weld Cost	Total Cost
40452.	1532.	6384.	16323.	64691.

PANEL NUMBER c6

6.5 x 30 M²

HEAD = 9.2M

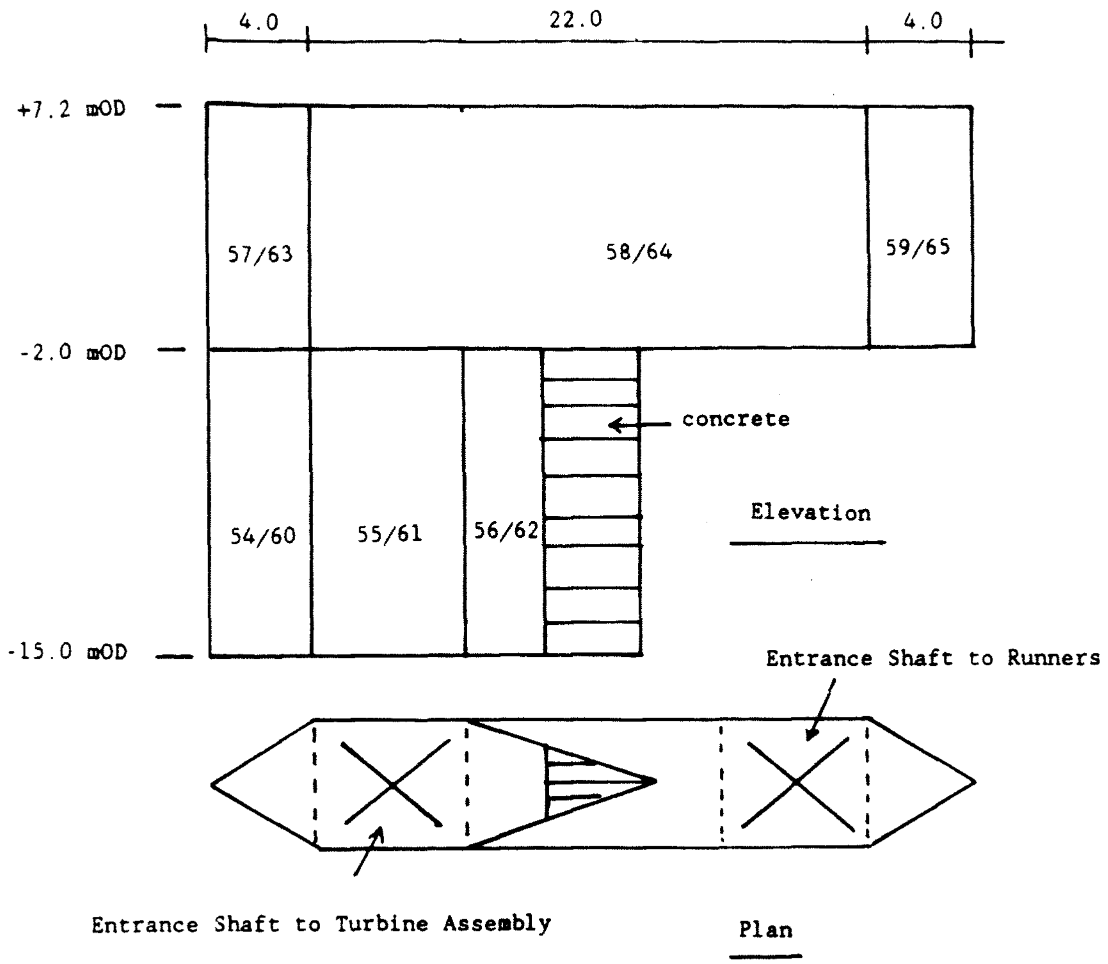

Fig A3.4 Panels in Conning Tower

NO	WIDTH (m)	BREADTH (m)	MAX HEAD (m)	SKIN TH. (mm)	PANEL DEPTH (mm)	PLATE WEIGHT (T)	STIFF WEIGHT (T)	CONC. WEIGHT (T)	TOTAL WEIGHT (T)	C. OF G. X (m)	C. OF G. Y (m)	C. OF G. Z (m)
54	4.1	14.5	23.7	35.	835.	32.	5.	0.	37.	42.8	6.1	7.3
55	10.1	14.5	23.7	30.	1070.	65.	21.	0.	85.	36.5	4.5	7.3
56	5.3	14.5	23.7	25.	985.	29.	11.	0.	41.	29.4	6.2	7.3
57	4.1	8.5	9.2	20.	270.	9.	1.	0.	10.	42.8	6.1	18.8
58	20.6	8.5	9.2	20.	330.	43.	3.	0.	46.	31.3	4.5	18.8
59	7.7	8.5	9.2	20.	250.	17.	1.	0.	18.	17.5	6.2	18.8
60	4.1	14.5	23.7	35.	835.	32.	5.	0.	37.	42.8	9.4	7.3
61	10.1	14.5	23.7	30.	1070.	65.	21.	0.	85.	36.5	11.1	7.3
62	5.3	14.5	23.7	25.	985.	29.	11.	0.	41.	29.4	9.5	7.3
63	4.1	8.5	9.2	20.	270.	9.	1.	0.	10.	42.8	9.4	18.8
64	20.6	8.5	9.2	20.	330.	43.	3.	0.	46.	31.3	11.1	18.8
65	7.7	8.5	9.2	20.	250.	17.	1.	0.	18.	17.5	9.5	18.8

Venturi

The draft tube has been split into 4 segments with a constant diameter. At both seaward and basin side, the draft tube is represented by the plates at the inside of the twin skin panels in the adjacent walls, roof and floor. Table A4.1 lists the venturi characteristics.

Length	Size
15.2m	12.0*14.4 m^2
2.0m	8.4m Diameter
3.5m	6.0m Diameter
8.7m	5.4m Diameter
10.6m	6.6m Diameter
8.0m	11.0m Diameter

Table A4.1

The four middle sections have been designed with a Bagpus subroutine. The output is on the following pages.

Venturi Tube design details from file turb3.DAT

Venturi tube number 1
Max. centreline depth of turbine shaft below water level 21.200 m
Turbine runner blade diameter 6.000 m
Tube type is non-standard
Length of section A 2.000 m
Length of section B 3.500 m
Length of section C 8.700 m
Length of section D 10.600 m
Tube is not cantilevered at first end
Tube is not cantilevered at last end

Material grade 50.

Section 1

The least cost for section 1 of the tube occurs when:
Plate thickness 25.000 mm
Length between ring stiffeners 2.000 m
Number of ring stiffeners 2
Number of longitudinal stiffeners 44
Spacing (circumferentially, from bottom):

750.	750.	750.	760.	760.	770.	780.	790.	800.	820.	830.
850.	880.	900.	930.	960.	990.	1030.	1060.	1080.	1090.	1100.

UB section 305x102 x 28.000

Ring stiffener design (mm): Fillet weld thicknesses (mm)

Web thick	Web depth	Flange thick	Flange width	U.B.-tube	ring-flange	ring-tube
25.	1430.	25.	310.	6.	8.	10.

Steel Weights (Tonnes):

Tube Plate	U.B. stringers	Ring stiffeners	Total Weight
14.76	2.46	29.41	46.64

Costs:

Plate supply	U.B. supply	Ring supply	Plate welding	U.B. welding	Ring welding	Total cost
4429.45	739.20	8824.30	1534.00	4595.04	10334.07	30456.06

Section 2

The least cost for section 2 of the tube occurs when:
Plate thickness 30.000 mm
Length between ring stiffeners 1.750 m
Number of ring stiffeners 3
Number of longitudinal stiffeners 22
Spacing (circumferentially, from bottom):
1070. 1070. 1090. 1120. 1160. 1200. 1230. 1270. 1310. 1340. 1360.
UB section 305x102 x 28.000

Ring stiffener design (mm): Fillet weld thicknesses (mm)

Web thick	Web depth	Flange thick	Flange width	U.B.- tube	ring- flange	ring- tube
20.	1110.	20.	70.	6.	6.	15.

Steel Weights (Tonnes):

Tube Plate	U.B. stringers	Ring stiffeners	Total Weight
21.39	2.16	16.58	40.13

Costs:

Plate supply	U.B. supply	Ring supply	Plate welding	U.B. welding	Ring welding	Total cost
6418.29	646.80	4974.32	1664.00	4028.14	10834.72	28566.25

Section 3

The least cost for section 3 of the tube occurs when:
Plate thickness 25.000 mm
Length between ring stiffeners 2.175 m
Number of ring stiffeners 5
Number of longitudinal stiffeners 28
Spacing (circumferentially, from bottom):
770. 770. 780. 790. 800. 810. 830. 850. 870. 890. 910.
930. 950. 960.
UB section 305x102 x 33.000

Ring stiffener design (mm): Fillet weld thicknesses (mm)

Web thick	Web depth	Flange thick	Flange width	U.B.- tube	ring- flange	ring- tube
20.	1240.	20.	10.	6.	6.	14.

Steel Weights (Tonnes):

Tube Plate	U.B. stringers	Ring stiffeners	Total Weight
39.50	8.04	26.70	74.24

Costs:

Plate supply	U.B. supply	Ring supply	Plate welding	U.B. welding	Ring welding	Total cost
11849.90	2411.64	8010.00	3835.00	12753.73	16217.64	55077.91

Section 4

The least cost for section 4 of the tube occurs when:
Plate thickness 25.000 mm
Length between ring stiffeners 2.650 m
Number of ring stiffeners 5
Number of longitudinal stiffeners 38
Spacing (circumferentially, from bottom):

730.	730.	730.	740.	740.	750.	760.	770.	790.	800.	820.
830.	850.	870.	890.	910.	930.	940.	950.			

UB section 406x140 x 39.000

Ring stiffener design (mm): Fillet weld thicknesses (mm)

Web thick	Web depth	Flange thick	Flange width	U.B.- tube	ring- flange	ring- tube
25.	1540.	25.	140.	6.	6.	14.

Steel weights (Tonnes):

Tube Plate	U.B. stringers	Ring stiffeners	Total Weight
62.60	15.71	58.50	136.81

Costs:

Plate supply	U.B. supply	Ring supply	Plate welding	U.B. welding	Ring welding	Total cost
18780.88	4712.76	17550.14	6136.00	21156.44	20948.13	89284.35

APPENDIX 4 : WAVE FORCE CALCULATIONS

The Miche-Rungren equations are based on the following theory[1], see Figure A4.1.

An incoming wave, wave height Hi, reflects at the structure, so that the actual wave height is the sum of both incoming and reflected waves:

- Hw = Hi + Hr = (1+X) * Hi

X is the the wave reflection coefficient. The value for X is in between 0.9 and 1.

The height of the Clapotis or standing wave crest above the bottom is given by

- yc = d + h0 + (1+X)/2 * Hi

while the height of the clapotis trough above the bottom is given by

- yt = d + h0 - (1+X)/2 * Hi

in which h0 is the height of the Clapotis Orbit Centre above the Stillwater Level.

The pressure at the bottom is approximated as

- p1 = (1+X)/2 * w * Hi / cosh(2*π*d/L)

Moments and forces are derived from the Figures A4.2 and A4.3.

<u>Landward Wind</u>

H_i = 2.0 m
T = 10 s
Max. Sea Level = +6.7 mOD, so d = 6.7 + 16.5 = 23.2 m
==> H_i/gT^2 = 2.0/(9.81*10^2) = 0.002
==> H_i/d = 2.0/23.2 = 0.087 (deep water)
Assume X = 0.9
(Fig A4.2) Sainflou : F/wd^2 = 0.055 ==> F = 10.1 * 23.2^2 * 0.055 = 299 kN/m
Total Wave Force on Caisson : 299 * 75.2 = 22484 kN
(Fig A4.3) Sainflou : M/wd^2 = 0.035 ==> M = 10.1 * 23.2^3 * 0.035 = 4416 kNm/m
Total Wave Moment on Caisson : 4416 * 75.2 = 331975 kNm

1 Source : Shore Protection Manual, Department of the Army, 1984

Seaward Wind

H_i = 1.5 m

T = 3.5 s

Max. Basin Level = +5.0 mOD, so d = 5.0 + 16.5 = 21.5 m

==> H_i/gT^2 = 1.5/(9.81*3.5^2) = 0.012

==> H_i/d = 1.5/21.5 = 0.070 (deep water)

Assume X = 0.9

(Fig A4.2) Sainflou : F/wd^2 is negligible, so

Total Wave Force on Caisson = 0 kN

(Fig A4.3) Sainflou : M/wd^2 is negligible, so

Total Wave Moment on Caisson = 0 kNm

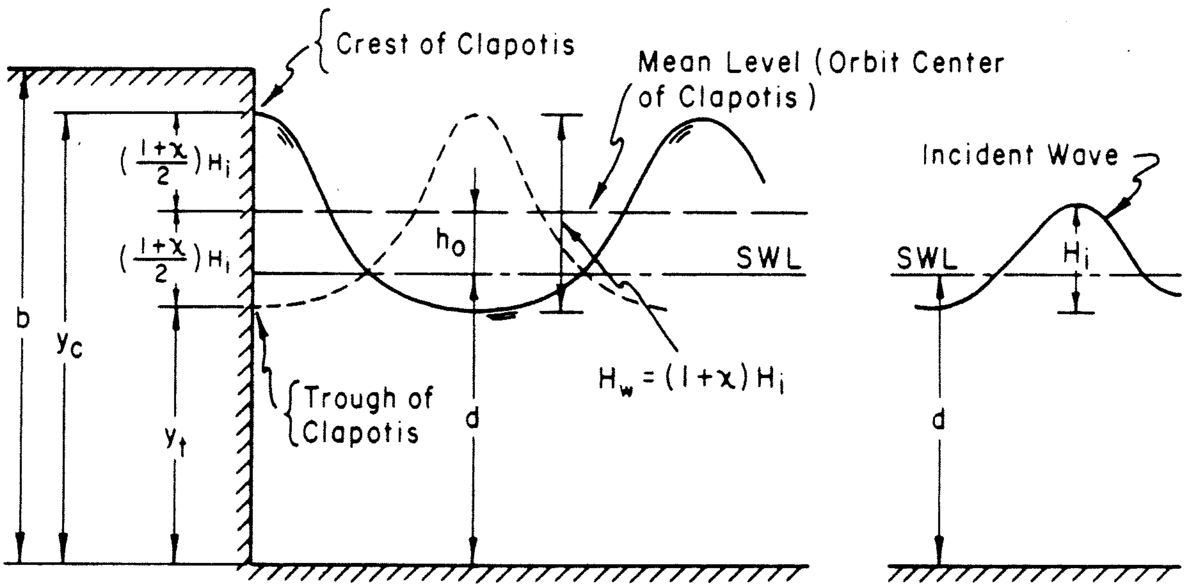

d = Depth from Stillwater Level

H_i = Height of Original Free Wave (In Water of Depth, d)

χ = Wave Reflection Coefficient

h_o = Height of Clapotis Orbit Center (Mean Water Level at Wall) Above the Stillwater Level (See Figures 7-90 and 7-93)

y_c = Depth from Clapotis Crest = $d + h_o + \left(\frac{1+\chi}{2}\right) H_i$

y_t = Depth from Clapotis Trough = $d + h_o - \left(\frac{1+\chi}{2}\right) H_i$

b = Height of Wall

Fig A4.1 Definition of Terms: nonbreaking wave forces.

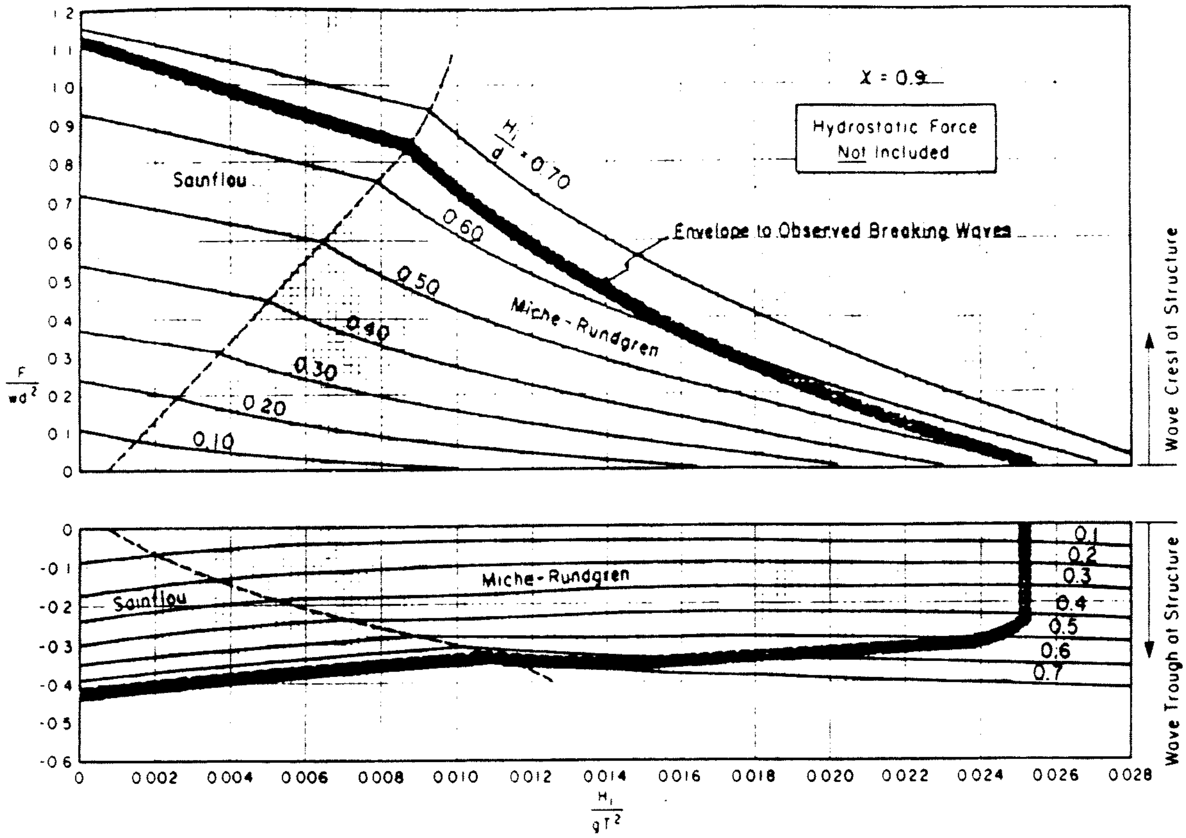

Fig A4.2 Nonbreaking wave forces; $\chi = 0.9$.

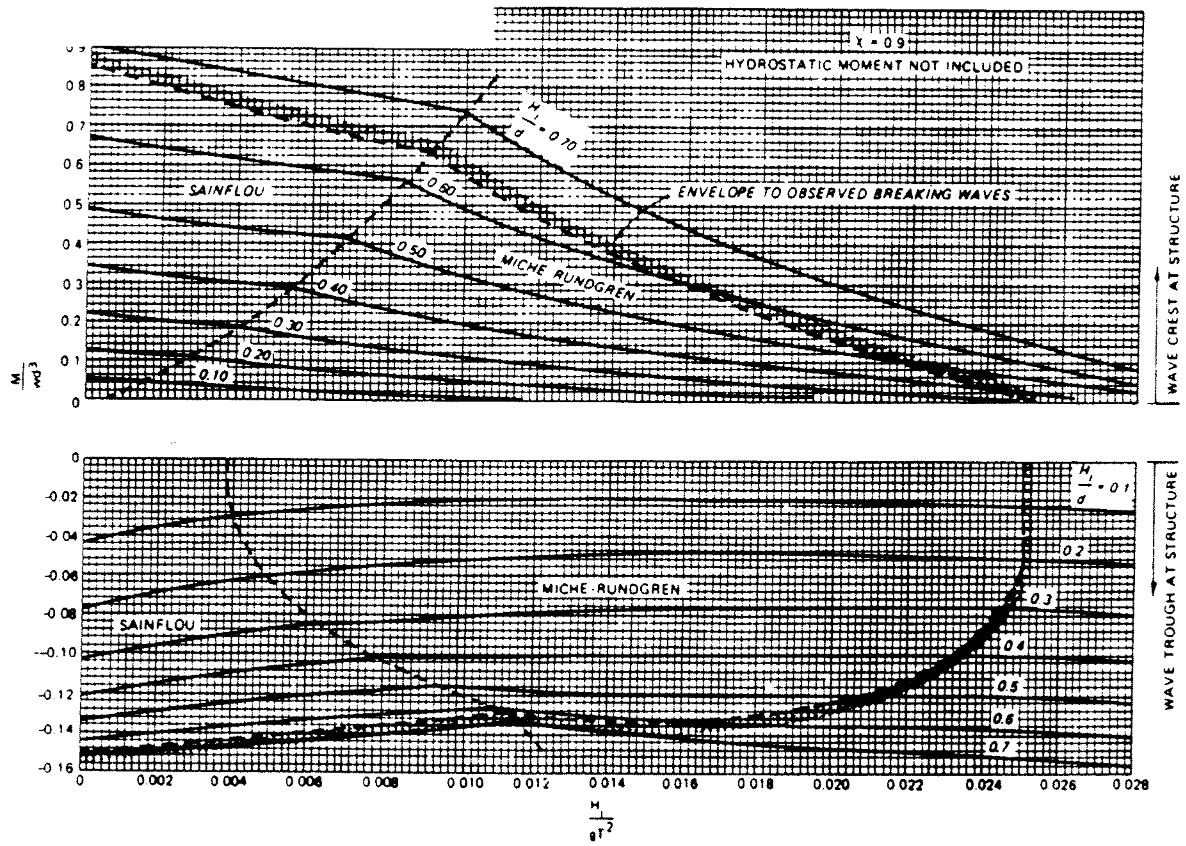

Fig A4.3 Nonbreaking wave moment; $\chi = 0.9$.

APPENDIX 5 : STABILITY AND DRAFT CALCULATIONS

In the first part of this appendix, the floating draft calculation, all parts of the caisson, such as panels, U.B. 's, are displayed with their volumes, weights and centroids of volume.

The panel calculations are displayed in Appendix 3. The numbers in front of the descriptions relate to the numbers in this appendix. The frame numbers are explained in Appendix 2. The data of rotating parts, around stay rings and gates have been derived from T.H.T.

The totals of the weights and moments determine the centre of gravity of the caisson. In order to assure that the centre of gravity is in the middle of the base, so that the caisson is level during transport, the caisson is ballasted in two cells. The total weight determines the floating draft of the caisson.

The ballast calculations have been carried out in order to determine the amount of ballast that can be placed inside the caisson. The caisson below -2.0 mOD is a box with a volume of 74.5 * 48 m^2. All members, panels, draft tubes, machinery rooms etc. inside this box have been subtracted from this volume, and the voids inside the sluice piers have been added to it. This results in the total volume left for the ballast.

On the next pages all loads are summarized for all loading cases.

The other vertical loadings are dependant from the basin and sea levels:

- The hydrostatic uplift under the caisson
- The loads of the entrained water in the sluices
- The loads of the entrained water in the draft tube (one tube is dewatered)
- The bearing pressures result from equilibrium equations :
    * the equilibrium of the vertical forces gives the total bearing force
    * the equilibrium of moments about the x and y axis results in the distribution of the bearing pressure under the base

The horizontal loads comprise :

- The hydrostatic loads at both sides of the caisson
- The wave loads (only significant at the seaward side)
- The passive and active loads resulting from the stones embedding the caisson
- The friction is a function of the bearing pressure, the friction factor is 0.5

The forces and moments are summarized for all loading cases. From these the resulting bearing pressures and factors of safety for stability are calculated.

Figure A5.1 explains the axis. (These are different from the axis used for the Strap model)

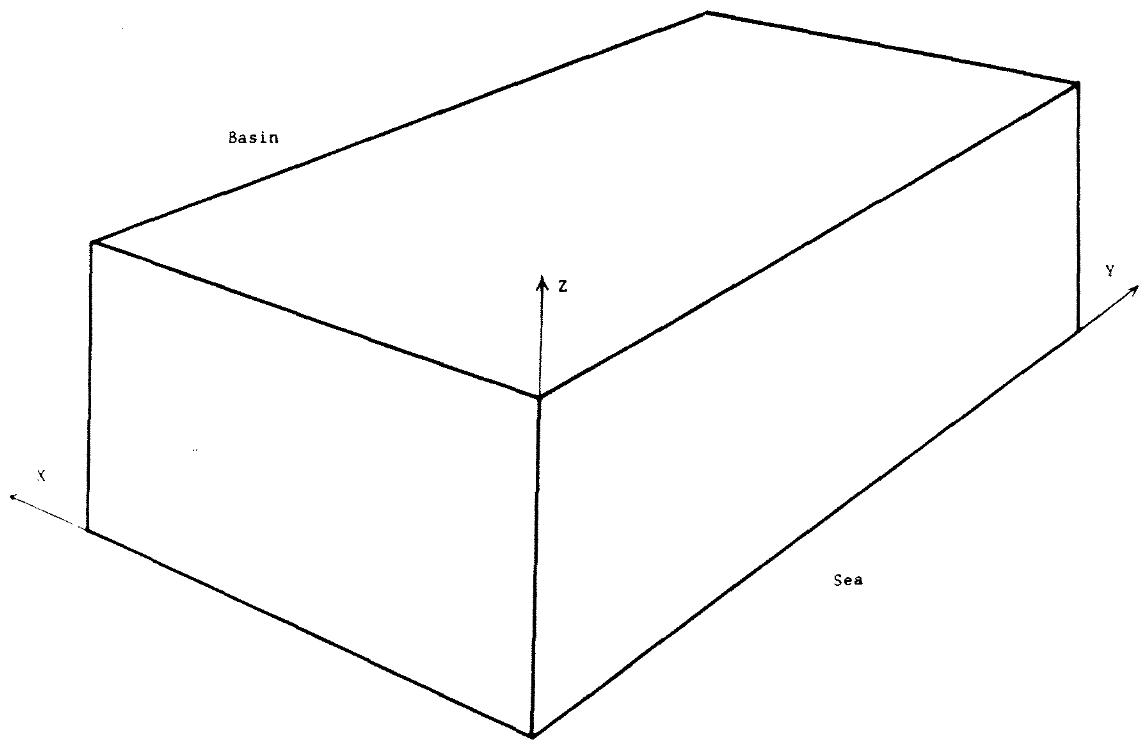

Fig A5.1 Definition of Axis for Stability Calculations

REFERENCE		VOLUME (m^3)	SPEC. WEIGHT (kN/m^3)	WEIGHT (kN)	CENTROID OF VOLUME (m) X	Y	Z	MOMENTS (kNm) Mx	My	Mz	CONTRIBUTION TO FLOATING DRAFT (m)
1 FRAMES	000	6.36	77.00	490.00	24.00	.00	7.25	.00	11760.00	3552.50	.01
	100	12.65	77.00	974.00	24.00	5.60	7.25	5454.40	23376.00	7061.50	.03
	200	14.71	77.00	1133.00	24.00	21.00	7.25	23793.00	27192.00	8214.25	.03
	400	9.61	77.00	740.00	24.00	42.00	7.25	31080.00	17760.00	5365.00	.02
	600	12.16	77.00	936.00	24.00	48.50	5.75	45396.00	22464.00	5382.00	.03
	700	12.16	77.00	936.00	24.00	55.00	5.75	51480.00	22464.00	5382.00	.03
	800	12.16	77.00	936.00	24.00	61.50	5.75	57564.00	22464.00	5382.00	.03
	1100	6.70	77.00	516.00	24.00	74.50	7.25	38442.00	12384.00	3741.00	.01
	DIAGONALS	2.14	77.00	165.00	25.00	37.25	7.00	6146.25	4125.00	1155.00	.00
SUBTOTAL		88.65		6826.00	24.02	38.00	6.63	259355.65	163989.00	45235.25	.19
2 CONNING TOWERS		123.12	77.00	9480.00	34.10	21.00	10.90	199080.00	323268.00	103332.00	.26
3 SLUICE PIERS											
1 : 2*25.2*9.2		32.77	77.00	2523.00	22.00	48.50	19.10	122365.50	55506.00	48189.30	.07
2 : 1*30.0*9.2		19.50	77.00	1501.80	21.50	.00	19.10	.00	32288.70	28684.38	.04
3 : 1*44.0*9.2		28.61	77.00	2202.60	27.00	68.00	19.10	149776.80	59470.20	42069.66	.06
4 : 1*48.0*9.2		31.21	77.00	2402.80	24.00	74.50	19.10	179008.60	57667.20	45893.48	.07
SUBTOTAL		112.08		8630.20	23.75	52.28	19.10	451150.90	204932.10	164836.82	.24
4 VENTURIES		77.40	77.00	5960.00	20.72	21.00	7.50	125160.00	123491.20	44700.00	.17
5 PLATES											
a. walls near turbine											
1 : 4*4.5*7.25 up		5.18	77.00	398.80	39.00	.00	13.88	.00	15553.20	5533.35	.01
2 : 4*4.5*7.25 down		5.43	77.00	418.00	39.00	.00	4.63	.00	16302.00	1933.25	.01
3 : 4*5.0*7.25 up		8.49	77.00	653.40	15.00	.00	13.88	.00	9801.00	9065.93	.02
4 : 4*5.0*7.25 down		9.14	77.00	703.80	15.00	.00	4.63	.00	10557.00	3255.08	.02
5 : 8*5.6*14.5		47.10	77.00	3626.40	24.00	21.00	7.25	76154.40	87033.60	26291.40	.10
6 : 2*15.4*13.5 stop logs		28.36	77.00	2184.00	24.00	21.00	7.25	45864.00	52416.00	15834.00	.06
b. walls near ballast											
1 : 4*4.5*7.25 up		3.24	77.00	249.20	39.00	74.50	10.88	18565.40	9718.80	2710.05	.01
2 : 4*4.5*7.25 down		4.74	77.00	364.80	39.00	74.50	3.63	27177.60	14227.20	1322.40	.01
3 : 6*5.0*7.25 up		5.60	77.00	431.40	15.00	74.50	10.88	32139.30	6471.00	4691.48	.01
4 : 6*5.0*7.25 down		8.02	77.00	617.40	15.00	74.50	3.63	45996.30	9261.00	2238.08	.02
5 : 8*6.5*11.5		23.04	77.00	1774.40	24.00	55.00	5.75	97592.00	42585.60	10202.80	.05
6 : 2*5.6*11.5		7.03	77.00	541.00	24.00	71.25	7.25	38546.25	12984.00	3922.25	.01
c. roof											
1 : 2*5.6*48.0		39.22	77.00	3020.00	24.00	21.00	14.50	63420.00	72480.00	43790.00	.08
2 : 2*15.4*30.0		53.99	77.00	4157.00	15.00	21.00	14.50	87297.00	62355.00	60276.50	.12
3 : 4*7.7*13.5		22.55	77.00	1736.00	39.00	21.00	14.50	36456.00	67704.00	25172.00	.05
4 : 2*15.4*4.5		12.21	77.00	940.00	45.75	21.00	14.50	19740.00	43005.00	13630.00	.03
5 : 4*6.5*48.0		147.81	77.00	11381.20	24.00	55.00	11.50	625966.00	273148.80	130883.80	.32
6 : 1*6.5*48.0		27.91	77.00	2149.20	24.00	71.25	14.50	153130.50	51580.80	31163.40	.06
7 : 2*48.0*3.0		20.95	77.00	1613.00	24.00	55.00	13.00	88715.00	38712.00	20969.00	.04

d. floor										
1 : 2*5.6*48.0	48.15	77.00	3707.50	24.00	21.00	.50	77857.50	88980.00	1853.75	.10
2 : 2*15.4*30.0	113.88	77.00	8768.40	15.00	21.00	.50	184136.40	131526.00	4384.20	.24
3 : 4*7.7*13.5	31.31	77.00	2410.60	39.00	21.00	.50	50622.60	94013.40	1205.30	.07
4 : 2*15.4*4.5	17.08	77.00	1315.30	45.75	21.00	.50	27621.30	60174.98	657.65	.04
5 : 5*6.5*48.0	70.07	77.00	5395.20	24.00	58.25	.50	314270.40	129484.80	2697.60	.15
SUBTOTAL	760.47		58556.00	23.91	36.06	7.24	2111267.95	1400075.18	423683.25	1.62
6 ROTATING PARTS	157.99	77.00	12165.00	27.13	21.00	7.25	255465.00	330036.45	88196.25	.34
7 AROUND STAY RING										
sea-side	112.96	77.00	8698.00	21.00	20.00	7.25	173960.00	182658.00	63060.50	.24
basin-side	54.09	77.00	4165.00	21.00	29.00	7.25	120785.00	87465.00	30196.25	.12
SUBTOTAL	167.05		12863.00	21.00	22.91	7.25	294745.00	270123.00	93256.75	.36
8 GATES										
3 small gates	20.06	77.00	1545.00	19.30	21.00	18.65	32445.00	29818.50	28814.25	.04
2 large gates	24.88	77.00	1916.00	18.90	55.00	17.15	105380.00	36212.40	32859.40	.05
SUBTOTAL	44.95		3461.00	19.08	39.82	17.82	137825.00	66030.90	61673.65	.10
9 CONCRETE IN FLOOR										
48.0*74.5*1.0	3576.00	22.00	78672.00	24.00	37.25	.50	2930532.00	1888128.00	39336.00	2.18
10 BALLAST										
cell A	525.00	18.00	9450.00	2.50	71.25	7.25	673312.50	23625.00	68512.50	.26
cell B	390.28	18.00	7025.00	45.75	71.25	7.25	500531.25	321393.75	50931.25	.19
SUBTOTAL	915.28		16475.00	20.94	71.25	7.25	1173843.75	345018.75	119443.75	.46
TOTALS			213088.20	24.00	37.25	5.55	7938425.25	5115092.58	1183693.72	5.90

Submerged Volume (m^3) = 21097.84
Moment of Inertia Ixx (m^4) = 686592.00
Height of Centre of Buoyancy above base (m) = 2.95
Height of Metacentre above Centre of Buoyancy (m) = 35.49
Metacentric Height (m) = 29.94

BALLAST CALCULATIONS

REFERENCE	VOLUME	CENTROID OF VOLUME (m)			MOMENTS (m^4)		
		X	Y	Z	Mx	My	Mz
TOTAL OF CAISSON BELOW -2 mOD	52548.00	24.00	37.75	7.25	1983687.00	1261152.00	380973.00
1 FRAMES	-88.65	24.02	38.00	6.63	-3368.26	-2129.73	-587.47
4 VENTURIES	-77.40	20.72	21.00	7.50	-1625.45	-1603.78	-580.52
5 PLATES	-760.47	23.91	36.06	7.24	-27419.06	-18182.79	-5502.38
7 AROUND STAY RING	-167.05	21.00	22.91	7.25	-3827.86	-3508.09	-1211.13
9 CONCRETE IN FLOOR	-3576.00	24.00	37.25	.50	-133206.00	-85824.00	-1788.00
10 BALLAST	-915.28	20.94	71.25	7.25	-65213.54	-19167.71	-6635.76
2 MACHINERY ROOMS	-756.00	24.00	21.00	7.25	-15876.00	-18144.00	-5481.00
DRAFT TUBES							
1	-1562.40	31.40	21.00	7.25	-32810.40	-49059.36	-11327.40
2	-652.40	18.40	21.00	7.25	-13700.40	-12004.16	-4729.90
3	-3248.80	7.50	21.00	7.25	-68224.80	-24366.00	-23553.80
4	-6415.20	39.75	21.00	7.25	-134719.20	-255004.20	-46510.20
5	-420.40	24.00	21.00	7.25	-8828.40	-10089.60	-3047.90
VOIDS IN SLUICE PIERS							
2*25.2*9.2*2.0	927.36	22.00	28.50	19.10	26429.76	20401.92	17712.58
1*30.0*9.2*1.5	414.00	21.50	.00	19.10	.00	8901.00	7907.40
1*44.0*9.2*2.0	809.60	27.00	68.00	19.10	55052.80	21859.20	15463.36
1*48.0*9.2*1.5	662.40	24.00	74.50	19.10	49348.80	15897.60	12651.84
TOTAL LEFT FOR BALLAST	36721.31	22.58	43.73	8.82	1605698.99	829128.30	323752.72

VERTICAL LOADINGS

REFERENCE	VOLUME (m^3)	SPEC. WEIGHT (kN/m^3)	WEIGHT (kN)	CENTROID OF VOLUME (m) X	Y	Z	MOMENTS Mx	My
FLOATING WEIGHT			213088.20	24.00	37.25	5.55	7938425.25	5115092.58
BALLAST	36721.31	18.00	660983.59	22.58	43.73	8.82	28902581.77	14924309.35
OFF:								
2 stop logs	-14.18	77.00	-1092.00	24.00	28.70	7.25	-31340.40	-26208.00
TOTAL DEAD WEIGHT			872979.79	22.93	42.17	8.02	36809666.62	20013193.92
ENTRAINED WATER								
DRAFT TUBE								
1	781.20	10.10	7890.12	31.40	28.70	7.25	226446.44	247749.77
2	326.20	10.10	3294.62	18.40	28.70	7.25	94555.59	60621.01
3	1624.40	10.10	16406.44	7.50	28.70	7.25	470864.83	123048.30
4	3207.60	10.10	32396.76	39.75	28.70	7.25	929787.01	1287771.21
5	210.20	10.10	2123.02	24.00	28.70	7.25	60930.67	50952.48
6	-1001.00	10.10	-10110.10	34.50	28.70	7.25	-290159.87	-348798.45
SUBTOTAL			52000.86	27.33	28.70	7.25	1492424.68	1421344.32
SLUICE CHANNELS								
basin side :								
3 above turbines	5046.30	10.10	50967.63	34.65	21.00	17.00	1070320.23	1766028.38
2 deep sluices	5874.00	10.10	59327.40	34.65	55.00	14.00	3263007.00	2055694.41
1 fish pass	747.60	10.10	7550.76	34.65	71.25	17.00	537991.65	261633.83
sea side								
3 above turbines	5112.64	10.10	51637.65	10.65	21.00	17.95	1084390.73	549941.01
2 deep sluices	5571.65	10.10	56273.71	10.65	55.00	14.95	3095053.80	599314.96
1 fish pass	757.43	10.10	7650.02	10.65	71.25	17.95	545064.12	81472.74
SUBTOTAL			233407.17	22.77	41.11	15.98	9595827.53	5314085.34

HYDROSTATIC UPLIFT	PRESSURE	FORCE (kN)	CENTROID OF FORCE (m) X	Y	MOMENTS (kNm) Mx	My
RECTANGLE	234.32	-845801.47	24.00	37.60	-31802135.35	-20299235.33
TRIANGLE	-17.17	-30988.42	32.00	37.60	-1165164.44	-991629.31
TOTALS		-876789.89	24.28	37.60	-32967299.79	-21290864.64

LOAD CASE : 1A MAXIMUM HEAD AT START OF GENERATION

	WATERLEVEL (m)	CLAPOTIS SET UP (m)	WAVE FORCE (kN)	WAVE MOMENT (kNm)	WATER DENS. (kN/m^3)
BASIN	5.00	.00	.00	.00	10.10
SEA	-2.00	.00	.00	.00	10.10

	PRESSURE (kN/m^2)	FORCE (kN)	CENTROID OF FORCE (m) y	z	MOMENTS (kNm) My	Mz
BASIN	217.15	-175544.06	37.60	7.17	-1258065.76	-6600456.66
SEA	146.45	79844.54	37.60	4.83	385915.28	3002154.70
	TOTALS	-95699.52	37.60	9.11	-872150.49	-3598301.95

RESULTANT FORCES LOAD CASE : 1A MAXIMUM HEAD AT START OF GENERATION

DESCRIPTION	FORCE (kN)				MOMENTS (kNm)			
	VERTICAL		HORIZONTAL		Mx		My	
	UPWARD	DOWNWARD	DRIVING	RESISTING	OVERTURNING	RESTORING	OVERTURNING	RESTORING
VERTICAL LOADINGS								
DEAD LOAD		872979.79				36809666.62		20013193.92
ENTRAINED WATER								
- turbine		52000.86				1492424.68		1421344.32
- sluice channels		132044.37				5652240.78		4234571.50
HYDROST. UPLIFT	-656225.28				-24674070.53		-16770201.60	
HORIZONTAL LOADINGS								
HYDROST. LOADS			-175544.06	79844.54			-1258065.76	385915.28
EARTH PRESSURE			-2686.00	53245.20			-8456.90	170371.87
FRICTION				200399.87				
	-656225.28	1057025.02	-178230.06	333489.61	-24674070.53	43954332.08	-18028267.36	26055025.02
	TOTAL	400799.74		155259.55		19280261.55		8026757.65
FACTORS OF SAFETY	Flotation	1.61	Sliding	1.87	Overturning	1.78	Overturning	1.45
DESIGN VALUES	STABLE	1.40	STABLE	1.70	STABLE	1.40	STABLE	1.40

BEARING PRESSURES

y / x	.00	24.00	48.00
.00	70.84	15.70	-39.45
37.60	166.18	111.04	55.89
75.20	261.52	206.38	151.23

LOAD CASE : 1B MAXIMUM HEAD DURING GENERATION

	WATERLEVEL (m)	CLAPOTIS SET UP (m)	WAVE FORCE (kN)	WAVE MOMENT (kNm)	WATER DENS. (kN/m^3)
BASIN	3.50	.00	.00	.00	10.10
SEA	-4.00	.00	.00	.00	10.10

	PRESSURE (kN/m^2)	FORCE (kN)	CENTROID OF FORCE (m) y	z	MOMENTS (kNm) My	Mz
BASIN	202.00	-151904.00	37.60	6.67	-1012693.33	-5711590.40
SEA	126.25	59337.50	37.60	4.17	247239.58	2231090.00
	TOTALS	-92566.50	37.60	8.27	-765453.75	-3480500.40

RESULTANT FORCES LOAD CASE : 1B MAXIMUM HEAD DURING GENERATION

DESCRIPTION	FORCE (kN)				MOMENTS (kNm)			
	VERTICAL		HORIZONTAL		Mx		My	
	UPWARD	DOWNWARD	DRIVING	RESISTING	OVERTURNING	RESTORING	OVERTURNING	RESTORING
VERTICAL LOADINGS								
DEAD LOAD		872979.79				36809666.62		20013193.92
ENTRAINED WATER								
- turbine		52000.86				1492424.68		1421344.32
- sluice channels		87801.83				3930955.35		3248858.04
HYDROST. UPLIFT	-592425.60				-22275202.56		-15311923.20	
HORIZONTAL LOADINGS								
HYDROST. LOADS			-151904.00	59337.50			-1012693.33	247239.58
EARTH PRESSURE			-2686.00	53245.20			-8456.90	170371.87
FRICTION				210178.44				
	-592425.60	1012782.48	-154590.00	322761.14	-22275202.56	42233046.65	-16324616.53	24930635.86
	TOTAL	420356.88		168171.14		19957844.09		8606019.33
FACTORS OF SAFETY	Flotation	1.71	Sliding	2.09	Overturning	1.90	Overturning	1.53
DESIGN VALUES	STABLE	1.40	STABLE	1.70	STABLE	1.40	STABLE	1.40

BEARING PRESSURES

y / x	.00	24.00	48.00
.00	73.65	22.31	-29.03
37.60	167.80	116.46	65.11
75.20	261.94	210.60	159.26

LOAD CASE : 2A ACCIDENTAL RAPID SHUTDOWN : AT START OF GENERATION

	WATERLEVEL (m)	CLAPOTIS SET UP (m)	WAVE FORCE (kN)	WAVE MOMENT (kNm)	WATER DENS. (kN/m^3)
BASIN	6.00	.00	.00	.00	10.10
SEA	-3.00	.00	.00	.00	10.10

	PRESSURE (kN/m^2)	FORCE (kN)	CENTROID OF FORCE (m) y	z	MOMENTS (kNm) My	Mz
BASIN	227.25	-192253.50	37.60	7.50	-1441901.25	-7228731.60
SEA	136.35	69211.26	37.60	4.50	311450.67	2602343.38
	TOTALS	-123042.24	37.60	9.19	-1130450.58	-4626388.22

RESULTANT FORCES LOAD CASE : 2A ACCIDENTAL RAPID SHUTDOWN : AT START OF GENERATION

DESCRIPTION	FORCE (kN)				MOMENTS (kNm)			
	VERTICAL		HORIZONTAL		Mx		My	
	UPWARD	DOWNWARD	DRIVING	RESISTING	OVERTURNING	RESTORING	OVERTURNING	RESTORING
VERTICAL LOADINGS								
DEAD LOAD		872979.79				36809666.62		20013193.92
ENTRAINED WATER								
- turbine		52000.86				1492424.68		1421344.32
- sluice channels		134934.99				5764702.26		4608376.84
HYDROST. UPLIFT	-656225.28				-24674070.53		-17061857.28	
HORIZONTAL LOADINGS								
HYDROST. LOADS			-192253.50	69211.26			-1441901.25	311450.67
EARTH PRESSURE			-2686.00	53245.20			-8456.90	170371.87
FRICTION				201845.18				
	-656225.28	1059915.64	-194939.50	324301.64	-24674070.53	44066793.56	-18503758.53	26354365.75
	TOTAL	403690.36		129362.14		19392723.03		7850607.22
FACTORS OF SAFETY	Flotation	1.62	Sliding	1.66	Overturning	1.79	Overturning	1.42
DESIGN VALUES	STABLE	1.20	STABLE	1.30	STABLE	1.20	STABLE	1.20

BEARING PRESSURES

y / x	.00	24.00	48.00
.00	80.05	16.40	-47.25
37.60	175.49	111.84	48.19
75.20	270.92	207.27	143.63

LOAD CASE : 2B ACCIDENTAL RAPID SHUTDOWN : DURING GENERATION

	WATERLEVEL (m)	CLAPOTIS SET UP (m)	WAVE FORCE (kN)	WAVE MOMENT (kNm)	WATER DENS. (kN/m^3)
BASIN	4.50	.00	.00	.00	10.10
SEA	-5.00	.00	.00	.00	10.10

	PRESSURE (kN/m^2)	FORCE (kN)	CENTROID OF FORCE (m) y	z	MOMENTS (kNm) My	Mz
BASIN	212.10	-167474.16	37.60	7.00	-1172319.12	-6297028.42
SEA	116.15	50223.26	37.60	3.83	192522.50	1888394.58
TOTALS		-117250.90	37.60	8.36	-979796.62	-4408633.84

RESULTANT FORCES LOAD CASE : 2B ACCIDENTAL RAPID SHUTDOWN : DURING GENERATION

DESCRIPTION	FORCE (kN)				MOMENTS (kNm)			
	VERTICAL		HORIZONTAL		Mx		My	
	UPWARD	DOWNWARD	DRIVING	RESISTING	OVERTURNING	RESTORING	OVERTURNING	RESTORING
VERTICAL LOADINGS								
DEAD LOAD		872979.79				36809666.62		20013193.92
ENTRAINED WATER								
- turbine		52000.86				1492424.68		1421344.32
- sluice channels		90692.45				4043416.83		3622663.38
HYDROST. UPLIFT	-592425.60				-22275202.56		-15603578.88	
HORIZONTAL LOADINGS								
HYDROST. LOADS			-167474.16	50223.26			-1172319.12	192522.50
EARTH PRESSURE			-2686.00	53245.20			-8456.90	170371.87
FRICTION				211623.75				
	-592425.60	1015673.10	-170160.16	315092.21	-22275202.56	42345508.13	-16775898.00	25249724.12
	TOTAL	423247.50		144932.05		20070305.57		8473826.12
FACTORS OF SAFETY	Flotation	1.71	Sliding	1.85	Overturning	1.90	Overturning	1.51
DESIGN VALUES	STABLE	1.20	STABLE	1.30	STABLE	1.20	STABLE	1.20

BEARING PRESSURES

y / x	.00	24.00	48.00
.00	81.34	23.02	-35.30
37.60	175.58	117.26	58.94
75.20	269.82	211.49	153.17

LOAD CASE : 2C POWER FAILURE

	WATERLEVEL (m)	CLAPOTIS SET UP (m)	WAVE FORCE (kN)	WAVE MOMENT (kNm)	WATER DENS. (kN/m^3)
BASIN	5.00	.00	.00	.00	10.10
SEA	-4.00	.00	.00	.00	10.10

	PRESSURE (kN/m^2)	FORCE (kN)	CENTROID OF FORCE (m) y	z	MOMENTS My	(kNm) Mz
BASIN	217.15	-175544.06	37.60	7.17	-1258065.76	-6600456.66
SEA	126.25	59337.50	37.60	4.17	247239.58	2231090.00
	TOTALS	-116206.56	37.60	8.70	-1010826.18	-4369366.66

RESULTANT FORCES LOAD CASE : 2C POWER FAILURE

DESCRIPTION	FORCE (kN)				MOMENTS (kNm)			
	VERTICAL		HORIZONTAL		Mx		My	
	UPWARD	DOWNWARD	DRIVING	RESISTING	OVERTURNING	RESTORING	OVERTURNING	RESTORING
VERTICAL LOADINGS								
DEAD LOAD		872979.79				36809666.62		20013193.92
ENTRAINED WATER								
- turbine		52000.86				1492424.68		1421344.32
- sluice channels		109240.59				4765044.66		3991711.24
HYDROST. UPLIFT	-619768.32				-23303288.83		-16186890.24	
HORIZONTAL LOADINGS								
HYDROST. LOADS			-175544.06	59337.50			-1258065.76	247239.58
EARTH PRESSURE			-2686.00	53245.20			-8456.90	170371.87
FRICTION				207226.46				
	-619768.32	1034221.24	-178230.06	319809.16	-23303288.83	43067135.96	-17444956.00	25673489.07
	TOTAL	414452.92		141579.10		19763847.13		8228533.06
FACTORS OF SAFETY	Flotation	1.67	Sliding	1.79	Overturning	1.85	Overturning	1.47
DESIGN VALUES	STABLE	1.20	STABLE	1.30	STABLE	1.20	STABLE	1.20

BEARING PRESSURES

y / x	.00	24.00	48.00
.00	79.59	20.08	-39.42
37.60	174.33	114.82	55.31
75.20	269.06	209.56	150.05

LOAD CASE : 3 EXTREME FLOOD

	WATERLEVEL (m)	CLAPOTIS SET UP (m)	WAVE FORCE (kN)	WAVE MOMENT (kNm)	WATER DENS. (kN/m^3)
BASIN	5.00	.00	.00	.00	10.10
SEA	6.70	.19	22484.00	331974.00	10.10

	PRESSURE (kN/m^2)	FORCE (kN)	CENTROID OF FORCE (m) y	z	MOMENTS My	(kNm) Mz
BASIN	217.15	-175544.06	37.60	7.17	-1258065.76	-6600456.66
SEA	234.32	226886.02	37.60	8.43	1912682.97	8530914.44
	TOTALS	51341.96	37.60	12.75	654617.21	1930457.79

RESULTANT FORCES LOAD CASE : 3 EXTREME FLOOD

DESCRIPTION	FORCE (kN)				MOMENTS (kNm)			
	VERTICAL		HORIZONTAL		Mx		My	
	UPWARD	DOWNWARD	DRIVING	RESISTING	OVERTURNING	RESTORING	OVERTURNING	RESTORING
VERTICAL LOADINGS								
DEAD LOAD		872979.79				36809666.62		-21889836.20
ENTRAINED WATER								
- turbine		52000.86				1492424.68		-1074696.96
- sluice channels		233407.17				9595827.53		-5889458.92
HYDROST. UPLIFT	-876789.89				-32967299.79		21290864.64	
HORIZONTAL LOADINGS								
HYDROST. LOADS			226886.02	-175544.06			1912682.97	-1258065.76
EARTH PRESSURE			2686.00	-53245.20			8456.90	-170371.87
FRICTION				-140798.97				
	-876789.89	1158387.83	229572.02	-369588.23	-32967299.79	47897918.83	23203547.61	-30112057.85
	TOTAL	281597.94		-140016.21		14930619.05		-6908510.23
FACTORS OF SAFETY	Flotation	1.32	Sliding	1.61	Overturning	1.45	Overturning	1.30
DESIGN VALUES	STABLE	1.30	STABLE	1.40	STABLE	1.30	UNSTABLE	1.30

BEARING PRESSURES

y / x	.00	24.00	48.00
.00	-14.54	-19.74	-24.94
37.60	83.21	78.01	72.81
75.20	180.96	175.76	170.56

APPENDIX 6 : CLOSURE MODEL DESCRIPTION

The main requirement for the model was to be applicable in two stages :

* When the first caisson is in place and a 75 m wide gap remains between the first caisson and the cofferdam (Stage I)

* When the second caisson is floating above its cill and is sunk down (Stage III-IV)

During the stages in between the flows are 2 - or 3 - Dimensional and too complex to handle with a simple model.

In a first attempt the barrage was modelled as a channel between the sea and the barrage. The aim was to discover which losses are important in the two stages.

The basic model equations are :

$$\frac{dH}{dx} = \frac{1}{gA} * \frac{dQ}{dt} + \frac{|Q|*Q}{C^2A^2R} + \frac{1}{gAs} * \frac{d}{dx}(Q^2/A) \qquad (1)$$

$$Q = \frac{dHb}{dt} * As \qquad (2)$$

If we neglect the last term of (1) (and check this later) and linearise the friction term we get :

$$Hb - Hs + M * Q + W * \frac{dQ}{dt} = 0 \qquad (3)$$

$$Q = \frac{dHb}{dt} * As \qquad (4)$$

in which : - Hb = Basin Level

- Hs = Sea Level

- Q = Discharge through Gap

- As = Surface Area of the Basin

- M = Inertia Term = $1/gA$

- W = Linear Friction Term = $8/3\pi * Qa/C^2A^2R$

- l = Length of Gap = 48 m

- g = Acceleration of Gravity = 9.81 m/s^2

- A = Flow Area of the Gap

- Qa = Aplitude of the Discharge

- C = Chezy factor

- R = Hydraulic Radius

For a constant As, M and W (2) may be substituted in (1) :

$$* \qquad Hb + MAs * \frac{dHb}{dt} + WAs * \frac{dHb^2}{dt^2} = Hs \qquad (5)$$

This equation is analytically solvable :

$$\text{if} \qquad Hs = R/2 * \cos(wt) \qquad (6)$$

then the harmonic response function for Hb is :

$$Hb = X * R/2 * \cos(wt+\Phi) \qquad (7)$$

in which : - $X = ((1-MAsw^2)^2 + (WAsw)^2)^{-1/2}$

- $\Phi = -\arctan(WAsw/(1-MAsw^2)$

However, this applies only for a constant As, M and W. Figure 6.? tells us that As varies with a factor of 10 during a spring tide, and Figure 6.? shows that the depth varies by a factor of 1.6 during a spring tide. To overcome this problem the variables As, M and W were kept constant during a small period, and (3) was solved. With the new values for Hb and Q (3) was solved again. Because starting values have to be met, a general solution has to be added to (5).

The reduced equation

$$* \qquad Hb + MAs * \frac{dHb}{dt} + WAs * \frac{dHb^2}{dt^2} = 0 \tag{8}$$

has a complete solution :

$$Hb = C * \exp(\mu t) \tag{9}$$

Equation (5) is substituted in (4) results with :

- a = WAs

- b = MAs

- c = 1

$$* \qquad a\mu^2 + b\mu + c = 0 \tag{10}$$

$$\text{Solution :} \quad \mu = \frac{-b \pm \surd\,(b^2 - 4ac)}{2a} \tag{11}$$

If $b^2 - 4ac > 0$ then the following family of solutions can be formed :

$$Hb = C1 * \exp(\mu_1 t) + C2 * \exp(\mu_2 t) \tag{12}$$

If $b^2 - 4ac < 0$ the complex solution is

$$\mu = \frac{-b \pm i \surd -(b^2 - 4ac)}{2a} \tag{13}$$

If we suppose that $p = -b/2a$ and $q = \surd -(b^2 - 4ac)$

then $\mu_1 = p + iq$ and $\mu_2 = p - iq$ and

$$Hb = \exp(pt) * (C1*\exp(iqt) + C2 * \exp(-iqt)) \tag{14a}$$

$$\text{or} \quad Hb = \exp(pt) * ((C1+C2)*\cos(qt) + i*(C1-C2)*\sin(qt)) \tag{14b}$$

By defining two new variables

A = C1 + C2 and B = i*(C1-C2)

the complete solution becomes

$$Hb = \exp(pt) * (A*\cos(qt) + B*\sin(qt)) \qquad (15)$$

The variables C1, C2, A and B are dependant from the starting values of Hb and Q.

If we add (13) to (5), we have the solution to (5). This equation, among other equations to solve the variables C1 and C2, or A and B, was put into a spreadsheet model. The model was run for a spring tide (range = 8.2 m) during a tidal cycle with one caisson in place (Figure A6.1) and during a closure situation (Figure A6.1). The graphics show apart from the levels and velocity also the influence of the inertia and friction term (the second and third term of (5)).

Although inlet and oulet losses have not been taken into account, it is possible to estimate what they would have been :

- Inlet losses : $dH = Ks * V^2/2g$ with Ks varying between 0.3 and 0.5

- Outlet losses : $dH = V^2/2g$; all velocity height lost at outlet

The estimated losses are listed in Table A6.1.

Losses (m)	Stage I	Stage III-IV
Inertia	0.002	0.012
Friction	0.008	0.210
Inlet	0.204	0.080
Outlet	0.068	0.040

Table A6.1 : Head Losses in Gap

Apparently the inertia losses are small compared to the other losses, and can therefore be neglected.

This gives us : $$Hb + W * |Q|Q + \frac{|Q|Q}{A^2 2g} * (1+Ks) = Hs \qquad (16)$$

or $$Hs - Hb = (W + (1+Ks)/A^2 2g)*|Q|Q \qquad (17)$$

If we substitute $W = L/(CA)^2R$ we get :

$$Q = A * (1 + Ks + 2gL/C^2R)^{-1/2} * \sqrt{2g(Hs-Hb)} \qquad (18)$$

The numeric model contains the following equations :

On $t = t_0$

- $Hs = 0.3 + R/2 * \cos(wt_0)$
- Hb = Starting Value
- $R = Hb + 16.5$
- $C = 25 * (R/k)^{1/6}$ Strickler
- $V = (1 + Ks + 2gL/C^2R)^{-1/2} * \sqrt{2g(Hs-Hb)}$
- $Q = V * 75 * (Hb+16.5)$

On $t = t_1$

- $Hs = 0.3 + R/2 * \cos(wt_1)$
- $Hb = Hb(t=t_0) + Q(t=t_0)/As$
- etc.